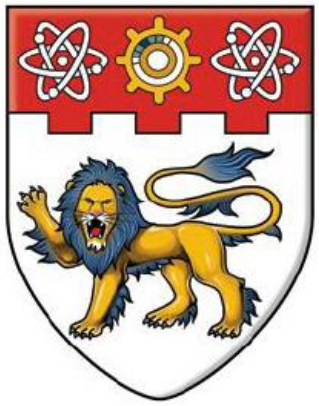

NANYANG TECHNOLOGICAL UNIVERSITY

ANTIMICROBIAL PEPTIDES ENGINEERING AND THEIR IMMOBILIZATION STUDIES FOR CATHETER COATING DEVELOPMENT

LIM KAIYANG

School of Chemical and Biomedical Engineering

2015

Acknowledgement

First, I would like to express my thanks to my supervisor, Associate Professor Kunn Hadinoto Ong and Associate Professor Susanna Leong Su Jan, for their precious guidance and consistent supports in my Ph.D. study.

Thanks to all my previous and present colleagues, Dr. Paul Tambyah, Dr Ho Bow, Dr Ray Chua Rong Yuan, Dr. Rathi Saravanan, Dr. Anindya Basu, Dr Mishra Biswajit, Dr. Foo Jee Loon and Dr. Li Peng.

Thanks to my dear friends in School of Chemical and Biomedical Engineering of Nanyang Technological University for all their friendship and supports.

Warmest thanks to my family for their understanding and support to my choices all the time.

Thank you all!

Table of Content

List of Publications

Mishra B., Basu A., Saravanan R., Li X., **Lim K.Y.**, Leong S.S.J., 2013, “Lasioglossin-III: Antimicrobial characterization and feasibility study for immobilization applications” RSC Advances 3:9534-9543.

Lim K.Y., Chua R.R.Y., Saravanan R., Basu A., Mishra B., Tambyah P.A., Ho B., Leong S.S.J., 2013, “Immobilization studies of an engineered arginine-tryptophan rich peptide on a silicone surface with antimicrobial and anti-biofilm activity” ACS Applied Materials and Interfaces 5; 13: 6412–6422.

Saravanan R., Li X., **Lim K.Y.**, Mohanram H., Li P., Mishra B., Basu, A., Lee J.M., Bhattacharyya S., Leong S.S.J., 2013, “Design of short membrane selective antimicrobial peptides containing tryptophan and arginine residues for improved activity, salt-resistance and biocompatibility” Biotechnology and Bioengineering; 111:37-49.

Lim K.Y., Chua RRY, Ho B, Tambyah PA, Hadinoto K, Leong SSJ., 2015, “Development of a catheter functionalized by a polydopamine peptide coating with antimicrobial and antibiofilm properties” Acta Biomaterialia;15:127-38.

Chuah Y.J., Koh Y.T., **Lim K.Y.**, Menon N.S., Wu Y.N., Kang Y.J., 2015, “Simple surface engineering of polydimethylsiloxane with polydopamine for stabilized mesenchymal stem cell adhesion and multipotency” Scientific Reports; Accepted.

Lim K.Y., Chua R.R.Y., Ho B., Tambyah P.A., Chang M.W., Leong S.S.J., 2015, “Dual layer coating for controlled release of antimicrobial peptides for prevention of CAUTI” Biomaterials; Submitted.

List of abbreviations

NPN	1-N-phenylnapthylamine
POPC	1-palmitoyl-2-oleoyl-sn-glycero-3-phosphocholine
TFE	2,2,2-trifluoroethanol
AGE	Allyl glycidyl ether
AMP	Antimicrobial peptides
AFM	Atomic force microscopy
ATR-FTIR	Attenuated total reflectance - fourier transform infrared
CAUTI	Catheter associated urinary tract infection
CD	Circular dichroism
CFU	Colony forming unit
EDS	Energy dispersive X-ray spectroscopy
FESEM	Field emission scanning electron microscopy
hRBC	Human red blood cell
LB	Luria broth
MRSA	Methicillin resistant Staphylococcus aureus
MTT	Methy tetrazolium

MIC	Minimum inhibitiory concentration
MH	Mueller Hinton
NMR	Nuclear magnetic resonance
P/L	Peptide to lipid ratio
PBS	Phosphate buffer saline
PDMS	Polydimethylsiloxane
PD	Polydopamine
PEG	Polyethylene glycol
PCL	Poly-ε-caprolactone
PI	Propidium iodide
SEM	Scanning electron microscopy
SMC	Smooth muscle cell
SDS	Sodium dodecyl sulfate
UV	Ultraviolet
UTI	Urinary tract infection
XPS	X-ray photoelectron spectroscopy

List of Figures

List of Tables

Abstract

With rapid rise in the frequency of nosocomial infections, there is an increasing demand for biomedical devices with good antimicrobial properties. Antimicrobial peptides (AMPs), which possess excellent bactericidal potency and biocompatibility properties, are promising antimicrobial coating agents for immobilization onto biomedical device relevant surfaces. The AMP's membrane-permeabilizing mechanism of action renders it more difficult for pathogens to develop resistance. In the first part of this Ph.D. research project, an arginine-, tryptophan-rich synthetic peptide (CWR11) with potent broad-spectrum antimicrobial activity and salt resistance properties was engineered to be used as a model AMP candidate for subsequent antimicrobial surface functionalization studies. To investigate if immobilization compromises the AMP's stability and antimicrobial property, two immobilization platforms were developed to graft CWR11 onto model polymethylsiloxane (PDMS) surface. The first platform utilizes an allyl glycidyl ether (AGE) polymer brush-based tethering chemistry while the later platform focuses on the use of a polydopamine (PD)-based surface functionalization strategy. A variety of surface characterization assays confirmed the successful grafting of AMPs onto the functionalized PDMS surface via both immobilization strategies. Surface antimicrobial assay and cytotoxic investigation confirmed that the CWR11-immobilized surfaces, from both immobilization platforms, have bactericidal and anti-biofim properties, and are also non-cytotoxic to mammalian cells. The simple immobilization strategy, enhanced peptide grafting efficacy and gentler treatment conditions makes the PD-based immobilization platform a more attractive choice for subsequent translational studies onto commercial silicone catheters. AMP-immobilized catheters, using the PD-based immobilzation platform, illustrated similar antimicrobial potency, as well as good long term stability retaining their

biocidal potency when exposed to a variety of solvent conditions and prolonged soft cleaning condition.

Contact active catheters developed in the first section, however, are ineffective in targeting planktonic bacteria, which can proliferate in the surrounding environment, eventually overcoming the immobilized AMP rendering them ineffective. To address this challenge, a subsequent study was initiated to formulate a controlled release polymeric coating that can provide localized, sustained AMP delivery to the target site. A dual-layered assembly (PCL(P)-POPC(P)) consisting of an AMP-impregnated basal PCL matrix layered with a thin POPC film to modulate release, was developed. This coating exhibited excellent sustained peptide release up to 30 days. Peptide characterization assays demonstrated conservation of the encapsulated AMP's (HHC36) structural integrity and antimicrobial functionality. PCL(P)-POPC(P)-coated catheters demonstrated potent antimicrobial and anti-biofilm activity against multiple UTI-relevant bacterial strains. The controlled and sustained release of AMP also prolonged bactericidal properties, retaining good antibacterial properties when subjected to multiple bacteria exposures.

In conclusion, this thesis presents proof-of-concept studies of the application of short AMPs as antimicrobial coating agents on urinary catheter. The successful engineering a potent, broad spectrum synthetic AMP and its successful application in the respective catheter antimicrobial coating development demonstrates the feasibility and potential of an AMP-based antimicrobial urinary catheter in treating or preventing CAUTI. The outcomes of this thesis now opens the way for further optimization of AMP-impregnated devices that can effectively prevent and/or treat bacterial infection while minimizing the risks of evoking pathogen resistance.

Chapter 1 Introduction

1.1. Introduction

Nosocomial infections have been one of the main causes of patient mortality and morbidity worldwide [1]. Annually, more than 1 million cases of nosocomial infections are reported in the United States and Europe [2, 3], with urinary tract infections (UTI) being the most common hospital acquired infection, of which, 80% are associated with indwelling urinary catheters [4]. While serving as a useful conduit to drain urine from the bladder into an attached bag, the catheter also provides an ideal surface for planktonic bacteria in the urine as well as from the atmosphere to adhere, colonize and develop into resistant biofilms [5]. It has been reported that 1500 times higher concentration of antibiotics is required to treat biofilm, as compared to planktonic bacteria [6]. With time, the bacterial infection can spread to the kidneys, leading to serious consequences such as acute or chronic pyelonephritis [7].

Since the discovery of penicillin in the 1940s, antibiotics have been the gold standard therapy against bacterial infections. Systemic administration of antibiotics is often applied in the treatment of nosocomial infections, especially catheter associated urinary tract infections (CAUTI). However, this method is often limited by the inefficacy of drug delivery to the target sites as well as the risks of potential systemic toxicity [8]. Moreover, with the increased occurrence of antibiotic resistant bacterial strains such as methicillin-resistant *Staphylococcus aureus* (MRSA), reliance on antibiotics is no longer viable [9]. Confronted by these challenges, it is important that extensive research efforts are focused on devising strategies to prevent and treat CAUTI, which forms the basis of this thesis.

The development of an antimicrobial coating on urinary catheters that can effectively kill invading uropathogens and efficiently prevent subsequent surface bacterial adherence merits further studies. Various antimicrobial coating approaches had been previously investigated, including impregnating the catheter with antibacterial compounds such as silver [6, 10-13] or antibiotics (e.g., gentamicin, vancomycin) [14, 15]. Although these catheters showed good antimicrobial activity *in vitro*, drawbacks such as high cytotoxicity, short-lived drug release rate and development of bacteria resistance limit their long-term usage [16, 17]. The need to find a potent, broad spectrum antimicrobial compound intensifies with the exponential increase in the development of antibiotic resistance in microbes. A promising alternative to antibiotics is antimicrobial peptides (AMPs) [18]. Natural AMPs form the first line of defence in an organism's immune system to combat microbial infection. These peptides are produced endogenously and display excellent anti-bacteria, anti-fungal [19, 20] and even anti-viral [21] traits. These antimicrobial properties, coupled with the peptide's immunomodulatory action [22] and membrane targeting mode of action [23], make AMPs a superior class of antimicrobial agents.

With an intensifying need for a safe and efficacious antimicrobial catheter coating and continual development of AMPs, this thesis seeks to investigate the use of AMPs as antimicrobial coating agents on silicone urinary catheters for treatment and/or prevention of CAUTI. However, to develop an effective AMP-based antimicrobial coating, there are a few challenges that need to be addressed. First, to serve as effective coating agents, the AMPs must meet several pre-requisites including broad-spectrum antimicrobial activity, biocompatibility and salt resistant properties. Many naturally occurring peptides, however, lack the ability to retain all these properties simultaneously. In particular, there are indeed very few AMPs that exhibit broad spectrum antimicrobial activity and salt resistance at the same time. Second, there is a dearth of research that focuses on the development of a

robust and readily scalable peptide immobilization platform. To date, most of the reported AMP tethering platforms require complex chemical treatment and processing steps, limiting their translatability onto commercial catheters. Third, a sustainable antibacterial agent delivery system that ensures sustained, localized and effective antimicrobial compound release is touted as the preferred CAUTI treatment method [24]. However, to date, limited research efforts have been dedicated towards the development of such AMP releasing platform which can be adopted for localized CAUTI treatment. Resolving these hurdles would facilitate the development of effective AMP-based urinary catheters for prevention and/or therapy of CAUTI, which forms the main objectives of this thesis.

1.2. Aims and objectives

This Ph.D. research has an overall aim which is to develop an AMP-based antimicrobial urinary catheters for prophylactic and/or therapeutic purposes against CAUTI. In order to achieve this, there are three specific objectives that should be met. The first objective is to systematically engineer a synthetic AMP which is resistant to physiological salt condition and possesses potent, broad spectrum antimicrobial activity. The synthetic peptide will serve as the model coating agent for tethering on silicone model platforms and subsequently, silicone urinary catheters. The second objective is to develop a robust AMP immobilization platform for proof-of-concept studies to investigate the impact of surface immobilization on AMPs' antimicrobial activity. The third objective is to study the translatability of the AMP immobilization platform onto silicone urinary catheters. These platforms will be characterized with respect to AMP immobilization efficacy, antimicrobial performance and biocompatibility. To achieve these overall objectives, specific studies with focused aims were performed as follow:

- Peptide engineering studies to develop a potent, salt-resistant, and broad spectrum synthetic AMP, followed by molecular characterization studies of candidate peptide's antimicrobial activity, conformational property and bactericidal mode of action.
- Development of a peptide immobilization platform to covalently and non-covalently immobilize AMPs onto silicone urinary catheter surfaces.
- Development of an AMP-based controlled release coating on urinary catheters for the treatment and prevention of CAUTI in longer term (two weeks to one month) catheterization.

1.3. Motivation

The motivation of this research is as follow:

- The AMP engineering studies will contribute to new knowledge in rational strategies for designing potent, broad spectrum, and salt resistant synthetic peptides, which could serve as useful guide in the future design of AMPs for similar applications.
- The development of AMP-functionalized urinary catheters is targeted to achieve a contact active surface which will facilitate the killing of microbes within surface proximity, and hence minimize or prevent bacterial adherence and subsequent biofilm development. The rational design of such a platform will open the way for potential development of AMP-based contact active coating for biomedical devices.
- The development of an AMP controlled release coating platform which can be used on urinary catheters will provide an effective approach to combat CAUTI, which will facilitate the sustained release of AMPs for implant site sterilization and prophylactic measures against subsequent infection. The pioneering work on

controlled AMP release will open the way for the development of localized peptide delivery system for CAUTI therapy, which is particularly essential in long term (two weeks to one month) catheterization.

1.4. Thesis organization

This thesis comprises six chapters. Chapter 1 presents the background, objectives and motivation of this research project. Chapter 2 presents a literature review on the structure and function of AMP, and discusses the factors to consider when employing AMPs as antimicrobial coating agents. The challenges of existing antimicrobial agents employed in medical devices are also discussed. Chapter 3 details the systematic engineering design of a *de novo* synthetic AMP with potent, salt resistant bactericidal action, followed by the development of a polymer brush surface immobilization platform for immobilization of the synthetic peptide on a model polydimethylsiloxane (PDMS) surface. Chapter 4 focuses on simplifying AMP immobilization procedures by utilizing a mussel-inspired polydopamine (PD)-based surface functionalization technique for AMP tethering on both PDMS and silicone urinary catheter surfaces. Chapter 5 reports the development of a localized AMP controlled release polymer coating for treatment and prevention of CAUTI in long term catheterized patients, who are subjected to catherization of two weeks to a month. Chapter 6 presents the conclusions of this thesis and future directions of this work.

Chapter 2 Literature Review

The discovery and development of antimicrobial peptides (AMPs) have revolutionized conventional microbial infection treatment. These short peptides are considered excellent alternative for resistance inducing antibiotics in treating nosocomial infections, especially for catheter associated urinary tract infection (CAUTI), which accounts for majority of these hospital acquired microbial problems. Although AMPs and CAUTI are extensively covered in numerous research studies and literature reviews, this chapter will mainly focus on three major areas; (i) CAUTI pathogenesis and clinical treatment methodologies, (ii) antimicrobial properties and therapeutic potential of AMPs for CAUTI therapy, and (iii) current development of AMP-based antimicrobial coating for urinary catheters and critical factors mitigating its efficacy. This chapter presents a comprehensive literature review for the application of AMPs in combating CAUTI.

2.1. Catheter Associated Urinary Tract Infection (CAUTI)

Urinary catheters are widely used in hospital and nursing home settings to help patients relieve potential urinary retention and urinary incontinence problems [25]. Catheterization can either be short term, less than 30 days, or long term, spanning up to few months. The duration of urinary catheterization is often dependent on the medical needs of the patients. Generally, indwelling catheters used in acute care facilities, such as hospitals, are usually short term, while chronic catheterizations are most common for residents of long term care facilities [26].

Foley indwelling urethral catheters, usually made of silicone or latex [27], represent one of the most commonly used urinary catheters in clinical settings. It is a closed sterile system comprising a flexible tube inserted through the urethral and held in place by an intra-bladder balloon (Figure 2.1). Urine within the bladder is directed and drained out through the catheter lumen into a connecting collection bag.

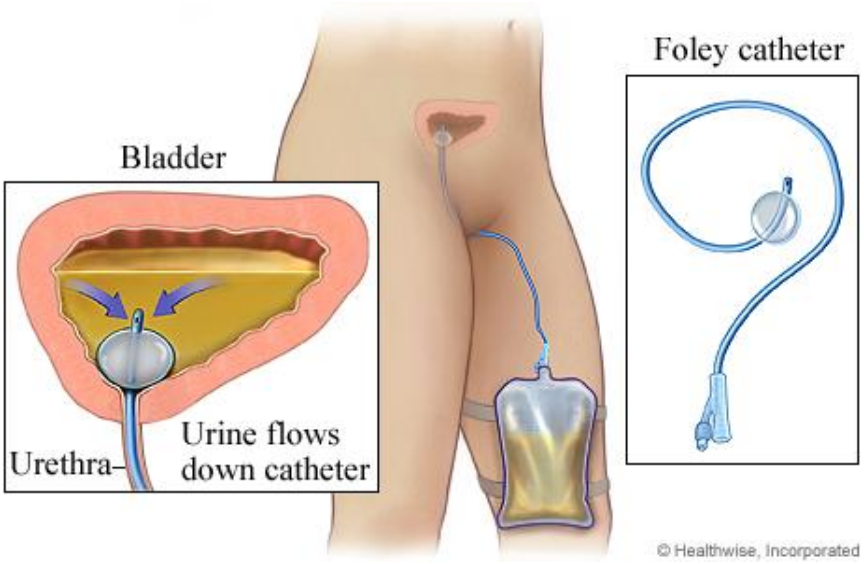

Figure 2.1. Foley indwelling urinary catheter (Reprinted from reference [28]).

Very often, the excessive use of indwelling catheters has resulted in patients being at risk for urinary tract nosocomial infections. Such infections can be avoided if the use of indwelling catheters is properly regulated. Surveys indicated a significant reduction in nosocomial infection rates if catheter usage is minimized [3, 29]. Despite that, the use of urinary catheters in some situations is unavoidable and the development of related infections has become part and parcel of the treatment procedure. CAUTI is significant due to its high occurrence and elevated economic cost, as well as adverse effects on patients' health. CAUTI is the commonest nosocomial infection worldwide, accounting for more than

1 million cases in United States and Europe annually [3], and poses a huge financial burden of approximately more than $1.6 billion [30]. CAUTI can have grave consequences on patients' health, ranging from mild (fever, urethritis and cystitis) to severe (acute pyelonephritis, renal scaring, calculus formation and bacteremia). If left untreated, these infections can lead to urosepsis and even death [26].

2.1.1. Pathogenesis of CAUTI

Despite of the protection from the innate immune system, physiological mechanical safeguards and different environmental conditions, specific uropathogens are still capable of colonizing the urinary tract. Virulence factors (e.g. adhesion, aerobatin system, hemolysin and K capsule) are crucial to the pathogenesis of these microbes within the urinary tract [31, 32]. The insertion of an indwelling catheter into the urinary tract compromises the closed urinary system and increases susceptibility to such uropathogens. These microbes invade the urinary tract mainly *via* three main routes (Figure 2.2). (1) Uropathogens colonizing the distal urethra may get picked up at the tip of catheter and pushed into urinary tract or bladder during the insertion process. (2) The second means for uropathogen to enter the urinary system is *via* the extraluminal route. Organisms dwelling in the distal urethra ascend along the catheter-uretheral interface into the urinary tract. (3) Microbes can also enter the urinary system by intraluminal means, where bacteria present in the collection bag climb up the device intraluminal surface and into the bladder [29]. A survey by *Tambyah* et al. on the route of infection indicated that the extraluminal route is the most probable mechanism of infection, accounting for 48% of the 253 CAUTI cases surveyed. Intraluminal means and catheter insertion are responsible for 34% and 18% of all the CAUTI induced, respectively [29, 33]. A separate *in vivo* study also

highlighted the prevalence of the extraluminal route for bacterial infection and colonization in catheterized animal model [34].

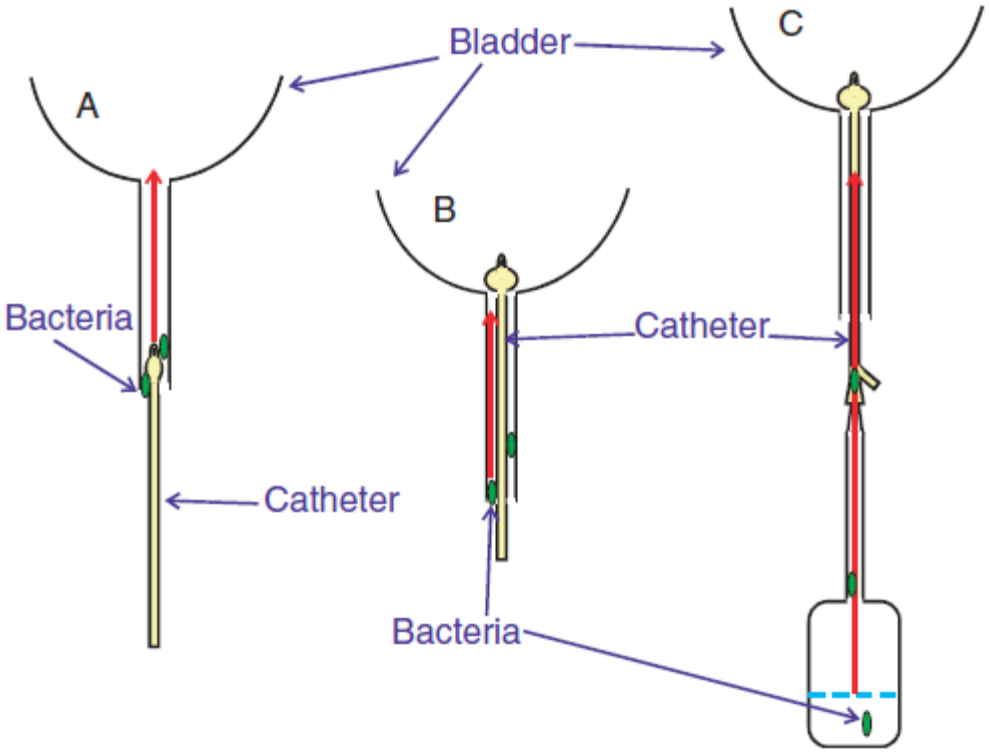

Figure 2.2. Three main routes for uropathogen entry into catheterized urinary tract. (A) Microbes dwelling around the distal urethra are being pushed in during the catheter insertion process. (B) Microbes attach to the catheter extraluminal surface and ascend into the urinary tract. (C) Microbes colonizing the collection bag migrate up the intraluminal surface of the catheter into the bladder. (Reprinted from reference [29]).

Upon gaining entry into the urinary system, uropathogens start attaching and colonizing the catheter surface and surrounding periurethral tissue. These microbes possess specialized bacterial adhesins that will ensure strong attachment onto target uroepithelial cell receptors and catheter surfaces [35]. Once firmly anchored onto target surfaces, the bacteria start to alter themselves phenotypically, expressing various virulence factors to fight against the harsh environmental stress imposed by the urinary system, such as high

osmolality and denaturing urea [36]. At the same time, these uropathogens produce exopolysaccharides that entrap the bacteria, serving as a robust protection against any antibiotic or host immune attack. These attached uropathogens then replicate and form microcolonies that eventually develop into massive biofilms. The shedding of daughter cells from actively growing cells and shearing of biofilm aggregates from the mature biofilm seed other sections, eventually colonizing the whole catheter or urinary tract [25].

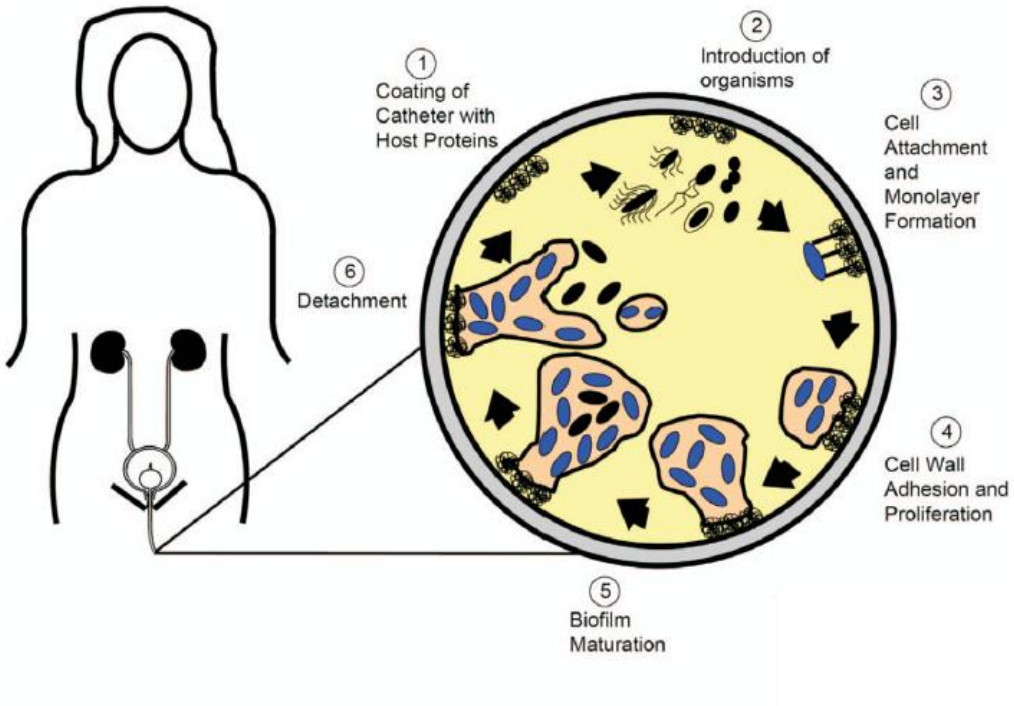

Figure 2.3. Pathogenesis of uropathogen attachment and biofilm development during CAUTI. (Reprinted from reference [25])

2.1.2. Microbiology of CAUTI

A diverse variety of microbes, both gram-negative and gram-positive, are found to be associated with CAUTI (Figure 2.4). Makeup of the bacteria community depends hugely on the patient population and prior antibiotic exposure [37]. *Escherichia coli* (*E. coli*) is the

more representative CAUTI pathogen [26]. A recent study on the diversity of bacteria isolated from long- and short-term catheterized patients exhibited that *E. coli* is the predominant microbe in CAUTI patients, making up 35% of the total bacteria population [38]. Other common CAUTI-linked gram negative bacteria species include *Pseudomonas aeruginosa* (*P. aeruginosa*), *Enterobacter cloacae* (*E. cloacae*) and *Klebsiella pneumonia* (*K. pneumonia*). Gram-positive microbes such as *Staphylococcus aureus* (*S. aureus*) and *Enterococcus faecalis* (*E. faecalis*) are also frequently associated with CAUTI. Yeast such as *Candida albican* (*C. albican*) are also found to be present in small quantities.

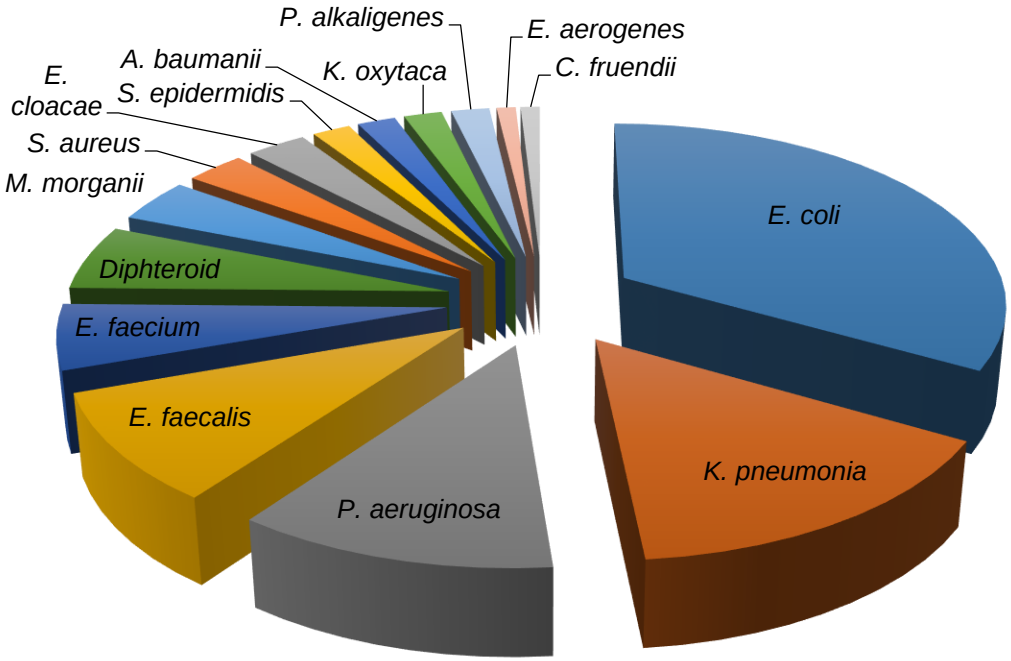

Figure 2.4. Distribution map of bacteria isolated from catheterized patients.

2.2. Therapy and Prevention against CAUTI

The occurrence of CAUTI can be managed by a dual-pronged approach, i.e., prevention and therapy. The prevention approach focuses on ways to reduce and/or avoid occurrence of CAUTI. In the unfortunate case when usage of catheter is necessary and CAUTI has been diagnosed, the therapy approach provides clinicians with treatment recommendations and/or guidelines.

2.2.1. Prevention

The occurrence of CAUTI can be reduced significantly if proper prevention measures were put in place. Studies reveal that 69% of CAUTI cases can be avoided with appropriate prevention strategies [3, 39]. The ideal and most effective method to reduce CAUTI is to avoid catheter usage, if possible. A study demonstrated that catheterization is unnecessary and can be avoided in 31% of the surveyed hospitalized patients. More stringent measures should be enforced to regulate and reduce the usage of indwelling urinary catheters. Reminder systems, if properly put in place, can help to alleviate the problem of unnecessary catheterization in healthcare settings. Physical reminders, such as face-to-face notification, paper-based notices, have proved to significantly improve appropriate use of catheter and reduce CAUTI rate [40-42]. Virtual reminders involve installation of software or electronic devices to prompt doctors and nurses of timely catheter removal. A study by *Blodgett* et al. demonstrated a significant reduction in CAUTI rates with an efficient virtual reminder system in place [43].

In the case when catheterization is required for measurement of urinary output or relieving obstructive uropathy, alternatives can be used to replace indwelling urethral catheterization. Percutaneous suprapubic urinary catheterization has been recommended

as a better alternative to urinary tract catheterization, with a higher level of comfort and lower incidence of CAUTI [3, 44, 45]. Intermittent catheterization, a procedure commonly used for patients with neurogenic bladder disorder, is another potential alternative to indwelling catheterization. In contrast to indwelling transurethral catheterization, intermittent catheterization exhibited a lower risk of CAUTI (12% in intermittent catheterization versus 39% in transurethral catheterization) [46]. Other potential substitutes, such as condom catheters [47], have also shown to effectively reduce risk of CAUTI. Proper catheter care is another essential prerequisite in preventing CAUTI. Aseptic condition during the initial insertion step and subsequent handling process can significantly lower the occurrence of CAUTI [48].

In the case where long term indwelling catheterization is unavoidable, the selection of an antimicrobial catheter can help lower the possibility of developing CAUTI. Silver, antibiotics and AMPs have been suggested as bactericidal compounds that can confer antimicrobial property onto catheters to minimize infection risks. A detailed discussion on the efficacy and challenges of using these compounds are presented in Section 2.3.

2.2.2. Therapy

For patients with CAUTI, it is important to initiate treatment as soon as possible to prevent further complications which can negatively impact the patients' health. In CAUTI patients where long term indwelling urinary catheter is deemed absolutely necessary, it is important to first remove any old infected catheters, and replace with a new one before initiating antibiotic or other treatment regiments [49, 50]. This will aid in accelerating the resolution of symptoms and lower risk of subsequent CAUTI episodes [50].

Urine analysis should follow to help guide the selection, dosage and duration of antibiotics regiment [51].

Table 2.1. Antibiotics and action of mechanism against respective bacteria strains

Bacteria strains	Recommended antibiotic	Action of mechanism
Gram-negative bacteria	moxifloxacin [52], ampicillin [53], chloramphenicol [54], nalidixic acid [55]	Permeabilize the protective outer and inner membrane, to inhibit and/or disrupt normal cellular functions
Gram-positive bacteria	vancomycin [56, 57], teicoplanin [56, 58], daptomycin [56, 57]	Penetrating the thick peptidoglycan layer of the cell wall, targeting cytoplasmic materials and signaling pathways

Each antibiotic has a different working mechanism, hence careful selection of drugs, based on bacteria population, is crucial to reduce any likelihood of antibiotic resistance development in bacteria (Table 2.1). Duration of antimicrobial therapy is another important factor that clinicians should take into account when handling CAUTI. Guidelines published by Infectious Diseases Society of America (IDSA) state that a seven-day antibiotic course should be prescribed to general CAUTI patients. In the case that patients show delayed response to the treatment, a prolonged fourteen-day antibiotic regiment should be implemented [49, 50].

Since the discovery of penicillin almost 90 years ago, antibiotics has been the gold standard and sole remedy in the treatment of bacterial infections. However, with the abusive use of antibiotics in the last decade, the medical community has seen a drastic increase in development of bacterial resistance towards antibiotics due to rapid bacteria evolution, chromosomal changes and exchange of genetic material [59, 60]. The prominence of such antibiotic resistant bacteria has prompted an urgent search for new alternative treatments and control strategies for infectious diseases. Silver compounds and nanoparticles have been gaining recognition from scientific society as a replacement for antibiotics [61, 62]. These silver compounds are reported to demonstrate potent

antimicrobial activity against both gram-positive and gram-negative bacteria strains [10]. However, studies have suggested that administering silver compounds can also post adverse cytotoxic effect to living beings [63]. Another alternative to antibiotics is AMPs. These short peptide chains possess broad spectra activity against most microorganism including gram-positive and gram-negative bacteria, viruses and fungi. Their membrane perforating action of mechanism ensures a relatively low chance for resistance development. These peptides possess superb biocompatibility with eukaryotic cells due to the lack of electrostatic interaction between them. Development and utilization of AMPs as an alternative to conventional antibiotics will be elaborated further in Section 2.4.

2.3. Antimicrobial coating on biomedical device

For patients who require long term catheterization, other than careful management to maintain sterility of the indwelling catheter, another strategy to prevent occurrence of CAUTI will be the use of antimicrobial urinary catheters. Two commercially available antimicrobial catheters are the silver alloy coated latex and nitrofurazone impregnated silicone ones.

2.3.1. Silver catheters

Exploitation of silver as an antibacterial agent for developing antimicrobial catheters is well justified due to its excellent activities against a broad spectrum of microbes [64], including antibiotic resistant *S. aureus* [65], many prevalent gram negative uropathogens [10, 66] and the opportunistic yeast *Candida albican* [67]. The development of resistance against these metallic compounds also reportedly requires extensive mutational change in the bacterial genome, which is extremely rare [68]. Silver compounds, such as silver oxide, silver citrate and various silver alloy, have thus been developed as coatings for urinary

catheters in the hope of preventing and/or delaying the onset of CAUTI occurrence. Early studies demonstrated the efficacy of silver catheter in reducing the incidence of CAUTI [69-72]. However, inconsistency in clinical potency, especially in patients requiring long term catheterization [73, 74], along with potential risk of argyrism [16] will limit its use in the medical settings.

The first silver catheter was developed by coating catheter surface with a thin layer of silicone elastomer loaded with micronized silver oxide. A large scale survey by *Riley* et al., however, reported that the silver catheter, had not only failed to prevent CAUTI, but had resulted in a significant increase in the occurrence of bacteriuria [75]. With further research and development, Bard Medical developed the Bardex I.C. infection control foley catheter. The latex catheter is incorporated with silver alloy which is chemically attached to its surface, followed by a subsequent gold/palladium coating that acts as barrier to allow sustained release of the silver ions from both intraluminal and extraluminal surface [76]. An additional hydrogel is coated on top of the silver/gold coating to enhance its lubricity. There is a wide disparity in the clinical effectiveness of these silver-impregnated catheters. A review by *Brosnahan* et al. illustrated that these silver alloy catheters dramatically reduced the incidence of asymptomatic bacteriuria in catheterized patient [77]. On the other hand, a separate study showed that 14.29% of the 1165 patients with silver catheter developed CAUTI. Compared with the 16.15% CAUTI rate for patient with basic silicone catheters, no significant difference in CAUTI rate was observed for patients with silver catheters [78]. While there is a wide disparity in the results between various clinical trials, the general consensus is that the effectiveness of the silver catheter dwindles with increasing duration of catheterization. The balance of evidence highlights that silver catheters are more therapeutic in short term catheterized patients.

Alternative coatings, exploiting characteristics of silver, have been researched upon in the hope of developing a truly efficient silver-based antimicrobial catheter. *Guggenbichler* et al. developed a novel technology enabling homogeneous distribution of nanosilver particles throughout a polyurethane matrix. Release profile suggested that the silver-loaded material exhibited a moderate, sustainable release kinetics for up to a year [79]. *Kumon* et al. also introduced an antimicrobial coating, consisting of a mix of lecithin, silver citrate and liquid silicone. The coating produced a hydrophilic surface with controlled released of silver ions. *In vitro* antimicrobial and anti-biofilm assay demonstrated potent resistance against microbe adhesion [80]. Although clinical trials of these silver loaded coatings have not been reported, these novel materials hold great potential to be translated for future development as antimicrobial catheters, if the cytotoxic challenge associated with silver catheters can be addressed.

2.3.2. Antibiotic catheters

In 1997, *Darouiche* et al. loaded a mix of antibiotics (minocycline and rifampicin) into urinary catheter material. The antibiotic-infused urinary catheter displayed significantly lower rates of infection for both *in vitro* and *in vivo* models. However, bactericidal efficacy of these antibiotic catheters deteriorated with extended catheterization [81, 82]. The lowered efficacy could be due to inadequacy of these antibiotics against gram-negative bacteria. With prolonged catheterization, gram-negative bacterial contamination is normally the predominant uropathogen population. These catheters were not optimized further due to the lack of long term efficiency.

Nitrofurazone is a potent antibiotic, possessing a broad spectrum of bactericidal activities against both gram-positive and gram-negative bacteria. The superb antimicrobial activity and chemical resilient property makes it an ideal coating agent for urinary catheters.

Throughout the years, various types of nitrofurazone-impregnated urinary catheters have also been developed. These antibiotic-coated catheters have been illustrated to successfully prevent or delay the onset of CAUTI [83]. Rochester Medical Corporation (Stewartville, USA) developed antimicrobial catheters exploiting these outstanding properties. Using a proprietary process, both intraluminal and extraluminal surfaces of silicone catheters are layered with nitrofurazone-impregnated silicone. A preliminary *in vitro* study indicated that the modified catheter was broadly active against common UTI pathogens, inhibiting 75% of the urinary bacterial isolates [84]. A study by *Maki* et al. highlighted the effectiveness of the nitrofurazone-impregnated catheters under clinical settings. The rate of CAUTI in catheterized patients was reported to be lower at 2.4% for patients receiving nitrofurazone catheters compared to 6.9% in patients with normal silicone catheters [85]. Further studies into the nitrofurazone catheters revealed that these antibiotics-impregnated devices are more potent and sustainable in contrast to silver catheters [86]. However, inconsistent antimicrobial results were obtained when these antibiotic-infused catheters were tested under different clinical settings, especially when catheterization period was lengthened [72, 74]. A separate survey illustrated insignificant differences (P=0.22) in CAUTI rates between control and nitrofurazone catheterized patients for up to 7 days [85, 87]. Such inconsistencies in clinical results could be associated with nitrofurazone's lack of bactericidal action against certain CAUTI-related bacterial strains, such as *Proteus mirabilis*, *P. aeruginosa, Enterobactor sp.* and *Serratia sp.* While the growth of other CAUTI-related bacteria was curbed by released nitrofurazone, these unaffected microbes continue to multiply and colonize, eventually compromising the indwelling antimicrobial catheter.

The search for antibiotics-laden antimicrobial catheters has not ceased due to inconsistencies in clinical result. In 2003, *Richard* et al. developed an alternative

antimicrobial catheter by adding antiseptic chlorhexidine digluconate (CHG) to silicone elastomer and subsequently molded these material to form a urinary catheter via high pressure compression. These CHG-loaded catheters displayed good resistance against bacteria adhesion and colonization for prolonged periods of time without evoking any cytotoxicity. More recently, *Fisher* et al. developed a simple strategy to impregnate commercially available silicone catheters with a variety of antibiotics (rifampicin, sparfloxacin and triclosan). *In vitro* flow experiments show that these antimicrobial catheters were effective for up to 7 weeks, preventing surface colonization by common uropathogens [88]. Despite these promising preliminary results, the long term sustainability of antibiotics-laden catheters poses a huge question on the effects of their use on propagating resistance development in pathogens.

2.3.3. AMP catheters

AMPs have been touted as the next generation antibiotics. These short peptides possess unique physical and biochemical properties including rapid and broad spectrum bactericidal action, high biocompatibility, and low susceptibility to bacterial resistance development due to its membrane-targeting mode of action [89]. These properties make AMPs excellent antimicrobial coating agents for biomedical devices. However, to effectively exploit AMPs as coating agents, it is important to immobilize these peptides on targeted surfaces without compromising their conformational and functional integrity. An introduction of AMPs, their bactericidal mechanism and the applicability of these peptides as antimicrobial coating agent for medical devices, especially urinary catheters, will be discussed in the following sections of this chapter.

Table 2.2. Competitive advantages of AMP-based urinary catheter over current CAUTI treatment methodologies.

Current CAUTI treatment	AMP-based urinary catheter
Resistance development	Minimal chance of resistance development
Unstainable antimicrobial performance	Sustainable prolonged performance
Bacteria specific	Broad spectrum antimicrobial action
Systemic cytotoxicity associated with systematic antibiotic therapy	Localized treatment

2.4. AMPs: functions and therapeutic potential

AMPs are endogenous peptides inherently present within multi-cellular organisms. Formerly, in the nineteenth century, before the categorization of AMPs, it was noticed that certain antimicrobial compounds were present in secretions, blood and various lymphatic tissues. These compounds exhibited bactericidal properties against both gram-positive and gram-negative bacteria [90]. Upon exposure to invading microorganisms, these antimicrobial compounds would be induced to kill or retard the growth of these microbes, supporting the action of natural and adaptive immunity [91]. Further research efforts and improved separation techniques led to the isolation of certain peptides, which are responsible for the extensive antimicrobial actions, and thus the discovery of AMPs and birth of AMP research. Cecropins, magainins and defensins were among the first few AMPs to be isolated and purified [92-94]. Subsequently, the field of AMP research

expanded vastly. Up till now, more than 1220 different AMPs had been discovered, with extensive functions ranging from antibacterial to anticancer [95].

2.5. Diversity of AMPs

AMPs can generally be categorized into 5 broad categories (Table 2.3), based on distinctive features such as amino acid sequence and secondary structure [96]. The first subgroup consists of peptides that are anionic. This group of peptides is generally present in pneumonary extracts and cells [97]. These short peptides are proven to exhibit broad-spectrum activities against both gram-positive and gram-negative bacteria [98, 99]. The second category of peptides is the cationic AMPs, which are generally short and deprived of cysteine residues. These peptides are unordered in aqueous solution, but adopt a distinctive alpha helical conformation in the presence of bacterial membrane mimicking sodium dodecyl sulphate (SDS) micelles [100]. Examples of such peptides include magainin [101] and LL-37 [102]. It has been hypothesized that the cationic charges enhance electrostatic interaction between the peptide and bacterial membrane, aiding its membrane targeted antimicrobial action. Another group consists of peptides that are rich in certain amino acids. Some examples include indolicidin, which is rich in tryptophan content [103], and prophenin, which contains high amounts of proline and phenylalanine [104]. Similar to the cationic peptides, these peptides lack cysteine residue. Depending on the inherent amino acid sequence and solvent environment, these peptides can adopt various conformations. The fourth subgroup of AMPs consists of peptides containing cysteine residues. These peptides form intra- or inter-chain disulfide bonds and generally adopt beta-sheet structure. A typical example of such peptides is the defensins [93, 105]. β-defensin represents one of the largest groups of AMP in human and animals. These peptides are generally 36 – 42 amino acids long with 6 cysteine residues, linked by 3

intramolecular disulfide bonds. These peptides exhibit good antimicrobial characteristics against a broad spectrum of microbes.

Table 2.3. Categorization of AMPs.

Classes of AMPs	Examples
Anionic peptides without cysteine residue	Maximin H5 [106]
Cationic peptides without cysteine residue	Cecropins [107], andropin [108], moricin [109], melittin [101], LL37 [102]
Cationic peptide without cysteine residue, but with high content of specific amino acids	Indolicidin [103], prophenin [104], PR-39 [110]
Peptides with cysteine residues	β-defensin [111], drosomycin [112]

2.6. Mechanism of action of AMPs

With the rapid discovery of new and more potent AMPs, extensive effort had also been directed to evaluate the killing kinetics and mode of action of these peptides. Such information is crucial for the design and development of more effective AMPs.

Killing kinetic assays were employed to estimate the speed of bactericidal action of the target peptide. Speed of AMP mediated killing can vary with peptides, which is presumably due to the different mechanisms of action. Some peptides initiate their antimicrobial action seconds within exposure. Novispirin G10, a synthetic peptide, kills bacteria within 2 minutes [113]. On the other hand, there exist peptides that mediate their cell killing at a relatively slower rate. Killing kinetic assay conducted on cecropin P1 demonstrated that it requires approximately 20 minutes to exert its bactericidal effect [114].

Despite the differences in microbe killing rate or specific antimicrobial action, all AMPs generally undergo similar steps to induce the required bactericidal effect (Figure 2.5). Prior to any antimicrobial action, the peptides must first be attracted to the bacteria membrane surface. A well-known mechanism for such attraction is *via* electrostatic interactions, where cationic peptides are attracted to oppositely charged phospholipids present in lipopolysaccharides of gram-negative bacteria, and teichoic acids on surface of gram-positive bacteria [91]. A study by *Ouhara* et al. reported that bacteria strains with higher net negative charge are more susceptible to peptide-mediated killing compared to counterparts which possessed a lower net negative charge [115]. This observation illustrates the importance of electrostatic interaction for initial interaction between peptide and its respective bacteria target. Hydrophobic interaction, between the hydrophobic regions of the AMP and zwitterionic phospholipids of the bacterial phospholipid bilayer, is also hypothesized to play an important role in the attachment and subsequent partitioning of AMP to bacterial membrane [116]. Such hydrophobic interaction is important for peptide attachment to bacterial membrane surface, especially for anionic or weakly cationic peptides. Regardless of the peptide genre, the hydrophobic interaction is crucial for subsequent permeabilization into and disruption of the bacterial phospholipid bilayer, as per hypothesized in the three models introduced in the next section.

Upon closing in and traversing through the capsular polysaccharides surrounding the respective bacterial species, the peptides subsequently interact with the outer membrane (in gram-negative bacteria) / cytoplasmic membrane (in gram-positive bacteria). These membranes are composed of phospholipids arranged in a bilayer conformation. In general, peptides bind to the lipid bilayer in 2 distinct states, S- and I-states [117]. At low peptide to lipid ratio (P/L), the peptides would be adsorbed into the lipid head group of the membrane phospholipid, stretching and thinning the lipid bilayer (S-state) [118]. With increasing

peptide attachment to surface, beyond a critical P/L, the peptide transit to the I-state, where the peptides align perpendicularly and permeabilize the lipid bilayer, disrupting the orderly arrangement of the phospholipids. Three different models have been proposed to simulate the mechanisms of membrane permeabilization, i.e. the barrel stave, carpet and torroidal pore models (Figure 2.5).

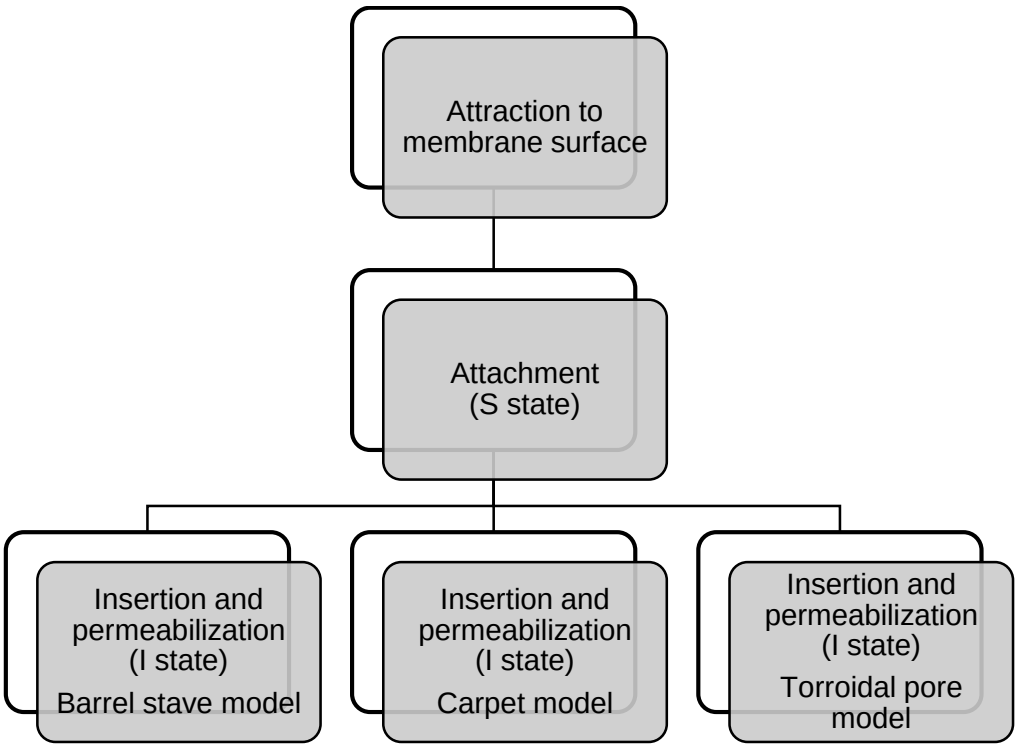

Figure 2.5. Mechanism of action of AMPs.

In the barrel stave model (Figure 2.6), peptides align vertically in a bundle within the phospholipid bilayer. In the middle of the bundle is a central lumen. It had been suggested that the central lumen provides the avenue for escape of cytoplasmic material, which eventually leads to killing of the microbe. One typical peptide that adopts the barrel stave model of membrane permeabilization is alamethicin [119-121]. In the alamethicin barrel stave model, the hydrophobic region of the peptides face the hydrophobic core of the lipid bilayer, while hydrophilic regions face the central lumen, forming a hydrophilic channel in the membrane phospholipid bilayer. Cytoplasmic contents were gradually leached out to the external environment, leading to death of the microbe.

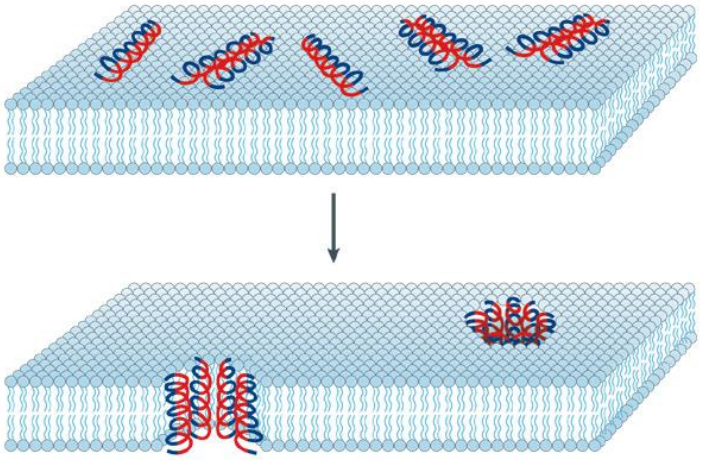

Figure 2.6. Barrel-stave model of AMP (Reprinted and adapted by permission from Macmillan Publishers Ltd: Nature Reviews Microbiology [91], copyright 2005).

Another model that is suggested for AMP mediated killing is the carpet model (Figure 2.7). In this model, the peptide is attracted to the oppositely charged membrane surface, *via* electrostatic interaction. These peptides cover the phospholipid bilayer surface at various sites. Upon reaching a critical concentration, the peptides would form transient holes in the membrane, disrupting the orderly lipid bilayer in a detergent-like manner. Subsequently, the membrane disintegrates into numerous micelles, killing the target microorganism [121, 122]. Some peptides that are hypothesized to adopt the carpet model mechanism include ovispirin [123], dermaseptin [124], cecropin [125] and LL-37 [126].

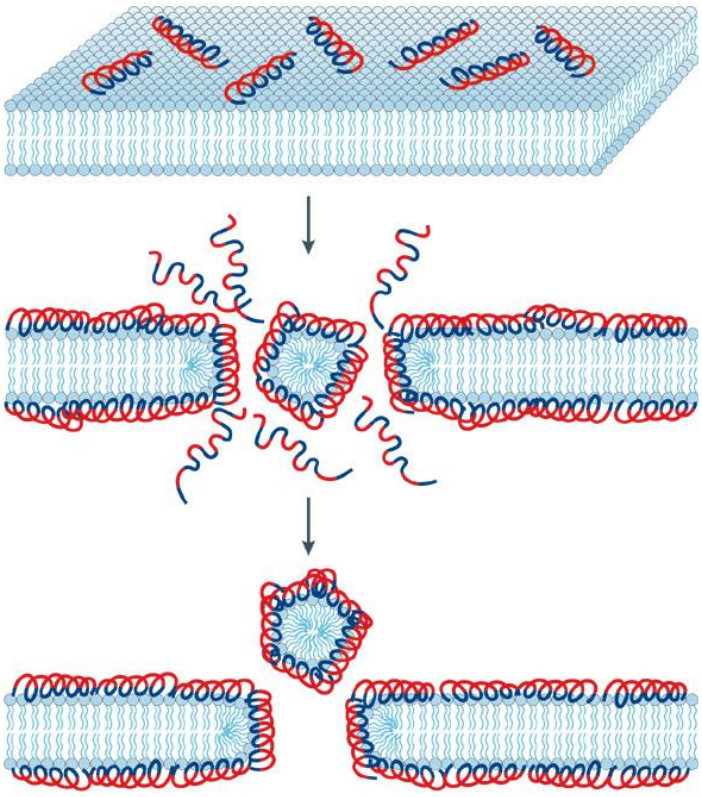

Figure 2.7. Carpet model of AMP (Reprinted and adapted by permission from Macmillan Publishers Ltd: Nature Reviews Microbiology [91], copyright 2005).

The last mechanism of action adopted by AMPs is the torroidal pore model (Figure 2.8). In this model, the peptides form helices and penetrate into the phospholipid bilayer. Peptide penetration causes the lipids to bend inwards, resulting in the formation of a water core to be present in the bilayer, lined by both the peptides and the polar head group of the phospholipid [91]. Osmotic pressure from external environment and leakage of cytoplasmic materials through the hydrophilic pore eventually kills the target bacteria. Magainin, an AMP isolated from African clawed frog *Xenopus laevis,* is well known to exhibit such torroidal pore membrane permeabilization mechanism [127].

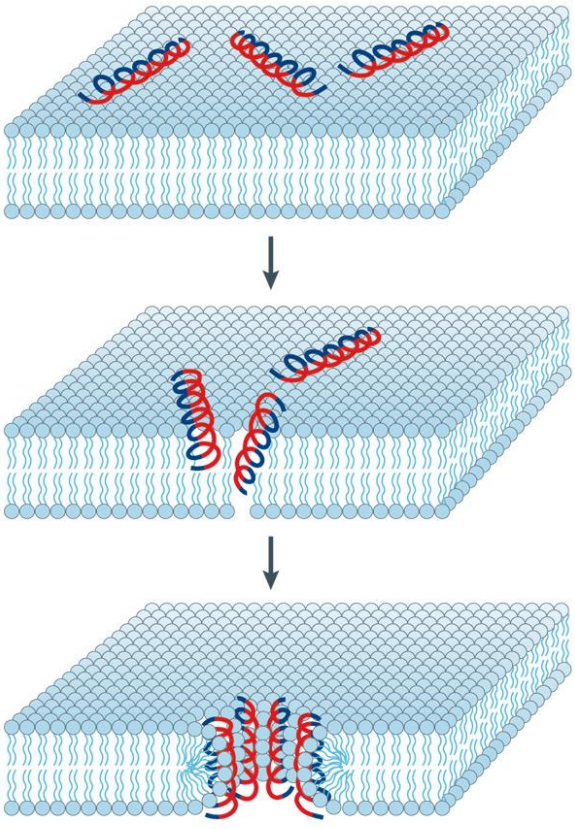

Figure 2.8. Torroidal pore model of AMP (Reprinted and adapted by permission from Macmillan Publishers Ltd: Nature Reviews Microbiology [91], copyright 2005).

The three models provide researchers with a general outlook to the action of mechanism of AMPs but detailed structure-function relationship of AMPs remains poorly understood and affects our ability to take full advantage of these potent peptides. Further and more in-depth research efforts have to be dedicated to understanding the peptide's mechanism of action along with development of analytical tools to guide structure-function studies. To aid in evaluating the mode of action of AMPs, various high resolution analytical techniques had been utilized including Nuclear magnetic resonance (NMR) spectroscopy, fluorescence and Circular Dichroism (CD) spectroscopy [91]. Solid state NMR-spectroscopy can provide molecular insights into the secondary conformation, alignment and insertion of the peptide with respect to the phospholipid bilayers. CD is commonly used to determine the secondary structure adopted by AMP under various solvent environments.

2.7. Engineering AMPs for improved functionality

Natural AMPs are often confronted with inherent limitations such as susceptibility to high physiological salt concentration (150 mM NaCl) which can adversely affect an AMP's antimicrobial potency due to charge shielding effect, degradation by protease and limited biocompatibility. Performance of these AMPs can be enhanced by synthetically engineering the original amino acid sequence to improve specific peptide properties. Some common modification strategies include N-terminal acetylation, C-terminal amidation, D-amino acids incorporation and cyclization [128].

2.7.1. N-terminal acetylation and C-terminal amidation

N-terminal acetylation and C-terminal amidation are two of the commonest chemical modifications in AMP engineering. While C-terminal amidation helps to increase overall net charge of the AMPs, enhancing electrostatic attraction to negative bacteria membrane [129,

130]; N-terminal acetylation acts to improve peptide stability, by preventing N-terminal degradation [131, 132]. *Strandberg* et al. investigated the influence of C-terminal amidation on antimicrobial activity of AMPs. Minimum inhibitory concentration (MIC) of candidate AMPs (PGLa, MSI-103 and MAP) reduced drastically upon amidation [129]. A structural study indicated that amidation stabilizes the amphiphilic helical conformation of AMP, hence enhancing association and partitioning of the peptides into the bacterial membrane, allowing a higher concentration of AMP attachment at the interface [133]. In a separate study by *Brinkenhoff* et al., stability of immunogenic peptide $Mart_{127-35}$ against degradative endo- and exopeptidase was markedly enhanced with N-terminal acetylation [132].

2.7.2. Hybridisation of AMPs

Through appropriate substitution and addition of certain moieties to the natural AMP sequence, a peptide's antimicrobial efficiency and biocompatibility can be significantly improved. Some examples of hybridized AMPs include CA(1-13)M(1-13) and Me-D. CA(1-13)M(1-13) is a synthetic AMP, derived from hydridisation of cecropin *A* and melittin. The variant peptide displayed better bactericidal potency and broader spectrum of activities, in contrast to both the parent peptides [134]. In a separate study, *Xu* et al. integrated the anti-biofilm amino acid sequence FV7 (FRIRVRV) into AMP RR16. The resultant R-F-V16 demonstrated superb antimicrobial action against both gram-positive and gram-negative bacteria as well as good anti-biofilm property [135]. It is shown that by integrating the active regions of various AMPs, the hybrid analogs possessed the combined benefits from each fragments.

2.7.3. Incorporation of unusual amino acids and/or amino acid sequences

Me-D, a melittin diastereomer comprising D-amino acids and leucine zipper moieties, displayed 8-fold lower hemolytic activity in contrast to melittin [136]. Another advantage of peptidomimetics is that these peptides are more resistant to proteolytic degradation. P113D, a derivative of histadine, was reported to be less susceptible to proteolysis by common enzymes, but retained similar antimicrobial potency as the parent peptide [137]. D-amino acid substitution has also been reported to improve AMP's bactericidal activity and biocompatibility [138, 139]. A systematic study of D-amino acid substitution on AMP revealed that replacement with these unusual amino acids induced certain localized change in chirality and/or secondary conformation, affecting its interaction with target bacterial membrane and serum protein [140]. Such structural alteration might be the underlying cause for the observed change in the modified peptide's performance.

2.7.4. Molecular dynamic simulations for rational peptide design

Molecular dynamic simulations has been commonly employed to elucidate an AMP's mode of antibacterial mechanism. However, it can also serve as an invaluable tool for peptide design and engineering. Upon better understanding the peptide template's interaction with bacterial and/or eukaryotic membrane, rationale engineering strategies can be taken to optimize subsequent variant's antimicrobial performance and/or cytotoxicity. In 2009, *Tsai* et al. utilized coupling molecular dynamic simulations to develop an indolicidin analogue, which possessed improved antimicrobial potency and enhanced biocompatibility, with cytoxicity against erythrocyte cells dropping to only 10% of the parent AMPs' [141].

2.7.5. Phage display library screening for identification of potent AMPs.

Other than specific engineering strategies that were mentioned earlier, it is also essential that extensive efforts are being diverted into developing strategies which are able to systematically and efficiently screen large library of random peptide sequences for potent synthetic AMPs. A powerful tool for such purpose phage display library screening [142, 143]. Briefly, phage library displaying random peptide sequences, being fused to its coat protein, was exposed to whole cells of *E. coli* that were immobilized to the bottom of 96 well plates. Unbound phages were removed and peptide sequences that illustrated enhanced bacterial binding capabilities were isolated. Multiple rounds of such biopanning process were conducted to narrow down and finally select the peptide sequence with the highest bacterial membrane binding efficacy. In a recent study, *Shilpakala* et al., using a 12-mer phage display library screening, to identify a novel AMP that demonstrated proficient bacterial binding capability [144]. Antimicrobial assay results show that the 12-mer peptide is bactericidal against Gram-negative organisms, with superior membrane interaction and permeabilization properties. The peptide has also been illustrated to be highly biocompatible, with negligible cytotoxicity against eukaryotic erythrocyte cells.

The above-mentioned engineering methods represent some of the more common strategies to modify AMPs, in a bid to improve antimicrobial potency, conformational stability and biocompatibility. Other ways include enhancing amphipathicity, increasing hydrophobicity and peptide cyclization. The list is non-exhaustive. With the abundance of such modification methodologies, numerous synthetic peptides, with superior physical and biochemical properties, are being developed. In this research project, some of these modification strategies will be adopted and optimized to synthesize a *de-novo* synthetic AMP as antimicrobial coating agent for biomedical devices.

2.8. Covalent Immobilization of AMPs

Covalent immobilization of AMPs onto biomedical device surfaces has been suggested as a possible strategy to tackle the problem of nosocomial infection. By tethering bactericidal AMP onto silicon surface, scientists hope to generate a contact active, antimicrobial surface where microbes will be killed upon interaction with the peptide-lined surface. Moreover, covalent immobilization of AMP has been shown to minimize peptide leaching, enhance bactericidal activity and provide long-term antimicrobial protection for the target surface [145, 146]. Various studies have been conducted in the past decade to develop an AMP-based antimicrobial surface (Table 2.4).

Table 2.4. Published AMP immobilization studies (Reprinted from reference [147], Acta Biomaterialia, 7, Costa F, Carvalho IF, Montelaro RC, Gomes P, Martins MCL., Covalent immobilization of antimicrobial peptides (AMPs) onto biomaterial surfaces, 1431-40, Copyright 2011, with permission from Elsevier.)

	AMP	**Substrate**	**AMP immobilization strategy**	**Microorganism assessed**
[148]	Magainin II and related synthetic amphiphilic peptides	Polyamide resin (pepsin K)	Directly synthesized on polyamide resin, after immobilization through their C-terminal amino acids. •AMP orientation was controlled. •Short spacer with 2- or 6-carbon chains was used. •Stability to heat was studied. •No AMP release was observed.	*E. coli*, *S. aureus*, *K. pneumoniae*, *B. subtilis*, *C. albicans*, *A. niger* and *P. aeruginosa*
[149]	Magainin I	Non-fouling copolymer brushes based on different percentages of:2-(2-methoxyethoxy)ethyl methacrylate (MEO2MA)/hydroxyl-terminated oligo(ethylene glycol) methacrylate (HOEGMA)	Peptide immobilized by its C-terminal amino acid. The process consisted of a previous incorporation of a cysteine residue on the C-terminal of magainin, to be reacted with the polymeric brushes via PMPI (N-(p-maleimidophenyl)isocyanate). •AMP orientation was controlled. •Brushes were used as spacers. •Different AMPs densities was tested.	*L. ivanovii* and *B. cereus*
[150]	Magainin I	Mixed OH/COOH-terminated self-assembled monolayers (SAMs)	Immobilization by the free AMP amines after activation of the COOH groups of the SAM with NHS/EDC •AMP orientation was not controlled. •No spacers. •No AMP release was observed.	*L. ivanovii*, *Enterococcus faecalis* and *S. aureus*
[145]	Magainin-derived MK5E and KLAL	PEGylated TentaGel S, HypoGel 400 and HypoGel 200 resin beads	C-terminally immobilized peptides were achieved by standard solid-phase peptide synthesis and Fmoc (9-fluorenylmethoxycarbonyl)-chemistryN-terminal and side-chain immobilization were achieved by thioalkylation and oxime formation.	*E. coli* and *B. subtilis*

			•AMP orientation was controlled. •Different AMPs densities were tested. •Effect of PEGylated spacers was tested. •The hemolytic effect was assayed.	
[151]	Melimine	Commercial contact lenses (etafilcon A)	Immobilization by the free AMP amines using 1-ethyl-3-(3-dimethylaminopropyl)carbodiimide. •AMP orientation was not controlled. •No spacers.	*P. aeruginosa*, *S. aureus* and *S. pneumoniae*
[152]	Melimine	Glass coverslips	Immobilization through the free AMP amines using two different strategies. •Using EDC after previous activation of the OH groups of the glass surface with 4-azidobenzoic acid (ABA) and irradiation with UV-light (320 nm). •As above but using 4-fluoro-3-nitrophenyl azide (FNA) instead of ABA. •AMP orientation was not controlled. •No spacers. •Different AMP densities were tested.	*S. aureus* and *P. aeruginosa*
[153]	Cathelin LL37	Silanized titanium surfaces: Using glycidyloxypropyl triethoxysilane (epoxy silane)3-aminopropyl triethoxysilane(amino silane)	•N-maleimidopropionic acid succinimide ester. •R-N-hydroxysuccinimidyl-ö-maleimidyl-PEG. •Effect of AMP orientation was tested. •Effect of PEGylated spacers was tested. •Different AMPs densities were tested.	*E. coli*

A study published in 1995 by *Haynie* et al. represents one of the first few attempts to covalently graft AMPs onto target surface [148]. Naturally occurring Magainin II and several

synthetic AMPs were covalently grafted onto polyamide resin surfaces. These AMP-immobilized resins displayed good antimicrobial activity against all tested microbes. The result from the study verified the possibility of an AMP-based antimicrobial coating, and initiated a new wave of research for a more efficient peptide immobilization platform. Numerous studies started to surface, promoting various efficient strategies for peptide grafting. In 2008, *Wilcox* et al. successfully translated these immobilization strategies onto biomedical devices for clinical applications [151]. In that study, melimine, a synthetic AMP, was covalently immobilized onto contact lens surfaces. The peptides were tethered onto 1-ethyl-3-(3-dimethylaminopropyl)carbodiimide activated contact lens surface *via* covalent coupling with free peptide amines. The AMP-linked lens showed significant bactericidal property, with >70% inhibition in bacterial growth. More recently, SESB2V was immobilized onto titanium artificial cornea skirt [154]. Both *in vitro* and *in vivo* antimicrobial assays showed promising results, with lower incidence and lesser extent of infection on AMP-grafted implants than untreated controls. These studies demonstrated the viability and clinical potential of an AMP-based antimicrobial coating for preventing nosocomial infections.

Along with the platform development, various investigational studies were also conducted to examine important factors mitigating the efficiency of peptide immobilization. Based on the result from the respective studies, several crucial activity modulating parameters that directly affect the efficacy of peptide tethering and immobilized peptide functionality can be identified. Some of these factors include chemical coupling strategies, spacer specificities, immobilized AMP density and peptide orientation upon tethering.

2.8.1. AMP chemical coupling strategies

Peptide immobilization strategies can differ with various external factors such as amino acid sequence, AMP orientation, presence of spacer and spacer specificities. Immobilization can be carried out in a random manner or through specific means.

Random peptide immobilization normally involves reacting free amine groups along the peptide length with exposed surface carboxyls (or vice versa, i.e. reacting carboxyls from peptide with surface amines) to form strong amide bonds. The presence of multiple free amine (or carboxyl) groups along the peptide length meant that the AMP can be attached onto the carboxyl (or amine) functionalized surface at any point, hence the lack of specificity. The antimicrobial potency of these randomly immobilized AMPs are usually compromised. In an early study to investigate the effect of immobilization specificity on tethered AMP antimicrobial potency, LL37 was grafted onto titanium surface *via* random and specific strategies [153]. In contrast to specifically grafted AMPs which demonstrated strong microbe inhibition, randomly immobilized LL37 lost its antimicrobial activity with no significant killing observed.

Alternatively and ideally, peptide immobilization can be conducted in a specific manner. Specifically bounded AMPs are preferred over random immobilization as the former tethering platform can be designed to ensure maintenance of peptide structural motifs known to be relevant for activity, and to allow better exposure and flexibility that can closely mimic behavior of the AMP in soluble state [147].

A straightforward way to ensure specific immobilization of peptides is to synthesize them directly onto the targeted surface. Briefly, the surface is functionalized with an initiator from which selectively protected amino acids can be incorporated in a stepwise manner, *via* Fmoc/Bu strategy. Upon assembling the desired amino acid sequence, de-protection

treatment is eventually performed to activate the peptide. In a 2009 study by *Bagheri* et al., AMPs (KLAL and MK5E) were constructed directly on PEG functionalized resin bead surfaces [145]. Resin-bound peptides exhibited good bactericidal functionality, with strong antimicrobial activity against both gram-positive and gram-negative bacteria. Several other studies using similar peptide immobilization method also showed promising results [148, 155]. Despite the optimistic outcome, such immobilization method suffers from several drawbacks such as process complexity, limited application and discounted antimicrobial efficiency.

A promising alternative to building the peptide directly onto the surface is to covalently attach AMPs onto the target surface. In order to achieve this, the peptides have to be incorporated with a specific functional group at a selected position. This peptide can then be chemoselectively tethered onto the appropriately functionalized compatible surface.

(a) Aldehyde surface

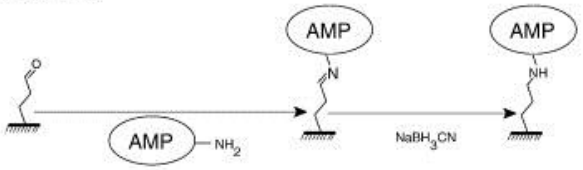

(b) Carboxylic acid surface

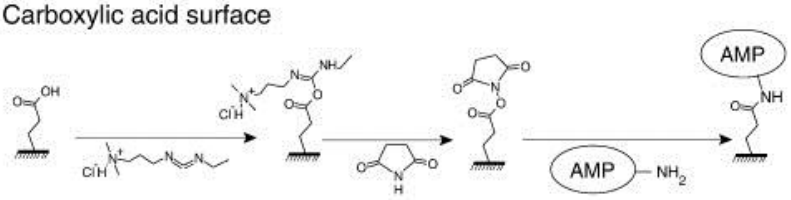

(c) Epoxide surface (X is NH for lysine or S for cysteine)

(d) Maleimide surface

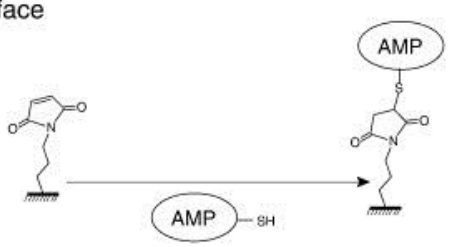

(e) Amine surface

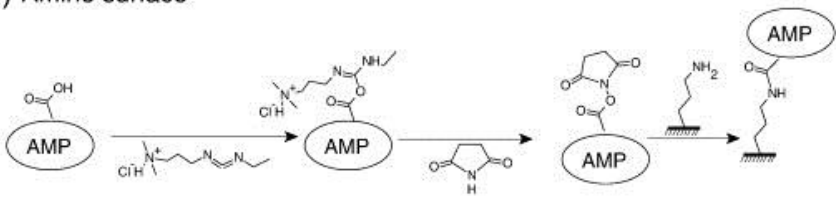

(f) Isothiocyanate

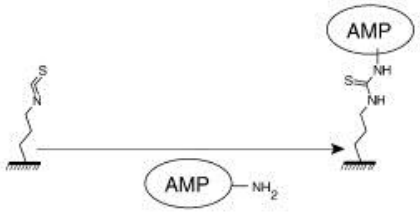

(g) Thiol Surface

Figure 2.9 illustrates various chemical coupling strategies for controlled covalent grafting of peptides onto respective functionalized surfaces.

An easy and commonly used site-specific AMP coupling strategy involves developing self-assembly monolayer (SAM) of reactive compounds on suitable surface. The free end of the SAM film is normally functionalized with certain reactive chemical groups (e.g. maleimide, aldehyde and isothiocynate) for subsequent peptide coupling. *Humblot* et al. reported a novel method to functionalize gold surface with mixed thiolated SAMs, on which Magainin I was covalently grafted on through sulfhydryl chemistry. The Magainin I-immobilized surface demonstrated significant antibacterial activity against tested gram-positive bacteria [150]. In a separate study, cysteine-terminated cecropin P1 was chemically immobilized onto a silane-EG4-maleimide SAM. These cecropin-immobilized surfaces showed potent killing efficiency against *E. coli* [156].

In recent years, the use of polymer brushes for covalent AMP-surface grafting has gained significant attention. Polymer brushes consist of ultrathin assemblies of multiple polymer chains that have one end tethered to the respective substrate surface. The free ends of these polymer chains are usually functionalized with a specific chemical group (e.g. epoxide and thiols), to which peptides can bind *via* specific chemical bonding such as sulfhydryl chemistry. These polymer brushes can be easily fabricated on different surfaces [157]. Polymer brush properties, such as high mechanical robustness, negligible cytotoxicity, increased immobilization sites and potent anti-biofilm functionalities, play a vital role in ascertaining their potential application in surface AMP attachment. In a recently published study, synthetic peptides RK1 and RK2 were grafted onto the allyl glycidyl ether (AGE) polymer brush [158]. The immobilization platform was applied to both model PDMS and silicone catheter surfaces. These peptide-coated surfaces demonstrated excellent bactericidal activities against both bacteria and fungi.

Polydopamine (PD)-based coating represents another attractive approach that can be easily adopted for AMP grafting. Since being reported in 2007, the use of PD has revolutionized the way surface functionalization was done [159]. Instead of the conventional cumbersome and complicated process of activation and functionalization, substrate surfaces, both organic and inorganic can be easily, easily functionalized with active amine and/or catechol group through a simple immersion step [159, 160]. The functionalized surface can then be used for grafting with various chemical compounds or biological moieties with complementary active groups. *Lee* et al. successfully immobilized cell-adhesive RGD-containing peptides and basic fibroblast growth factor onto polydopamine deposited poly(lactic acid-co-ε-caprolactone) [161]. The immobilization of respective bioactive molecules synergistically accelerated adhesion, migration, proliferation and differentiation of human umbilical vein endothelial cells. In a separate experiment, *Yang* et al. reported the immobilization of ECM-derived adhesion peptides and neurotrophic growth factors onto PD-functionalized polystyrene and poly(lactic-co-glycolic acid) substrates. The growth factor or peptide-immobilized substrates demonstrated excellent efficacy in enhancing differentiation and proliferation of human neural stem cells [160]. Results from these studies demonstrate that bioactive molecules, such as peptides and proteins, can be efficiently grafted onto PD-functionalized surface and such immobilization does not affect the functionality of the respective molecules. However, no similar studies have been conducted to attach AMPs onto PD-functionalized surface. The plausibility for the use of PD-functionalized surface for AMP attachment will be further explored in Chapter 4 of the thesis.

Various other coupling strategies, such as click-chemistry based approaches, have been investigated for covalent AMP immobilization. However, the various drawbacks associated with these alternate approaches limited their application for AMP tethering.

SAM and polymer brush remain the two mainstream methodologies for covalent AMP attachment.

(a) Aldehyde surface

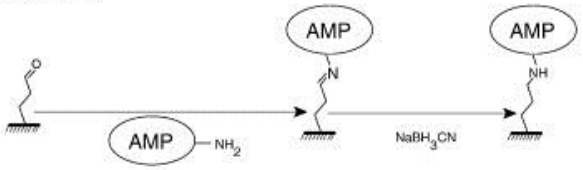

(b) Carboxylic acid surface

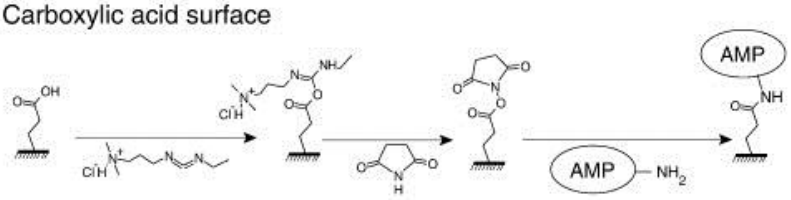

(c) Epoxide surface (X is NH for lysine or S for cysteine)

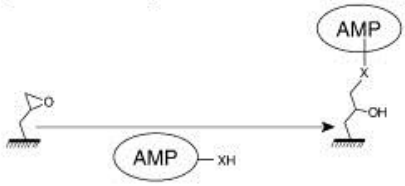

(d) Maleimide surface

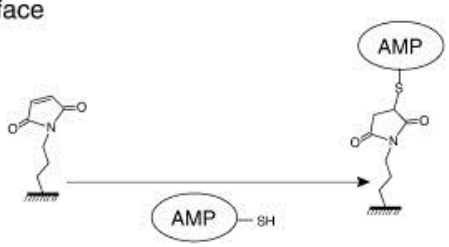

(e) Amine surface

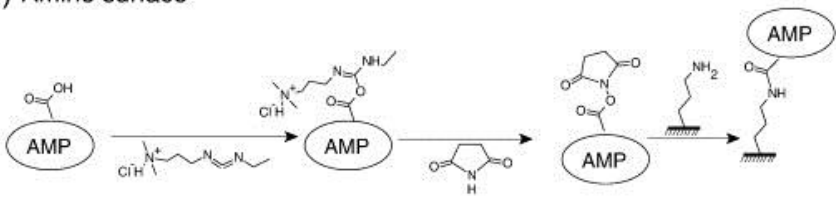

(f) Isothiocyanate

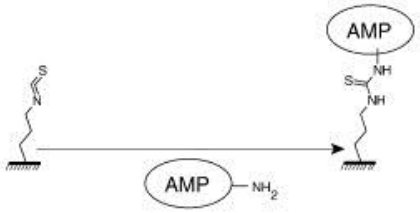

(g) Thiol Surface

Figure 2.9. Chemical coupling strategies for covalent AMP attachment (Reprinted from reference [89], Biotechnology Advances, 29, Onaizi SA, Leong SSJ., Tethering antimicrobial peptides: Current status and potential challenges, 67-74, Copyright 2011, with permission from Elsevier).

2.8.2. Effect of spacer

The inclusion of a spacer as part of the peptide coupling strategy has been the subject of much discussion. To date, most of the AMP immobilization platforms published were incorporated with a spacer [145, 148, 149, 153, 155, 162]. In most cases, the spacer is a polyethylene glycol (PEG) molecule, size averaging around 4000 Da. The use of a PEG spacer boasts many benefits such as improved anti-biofilm properties [6], enhanced peptide conformational functionality with reduced surface steric hindrance and better peptide penetrability due to increased reach with a long spacer. In fact, various studies examining the effect of PEG spacer demonstrated that inclusion of spacer is pivotal to preservation of immobilized AMP's bactericidal potency [145, 153, 155, 162]. For example, it was reported that 'PEG spacer'-bound LL37 demonstrated good antimicrobial activities against inoculated *E. coli* [153]. On the other hand, LL37 that was directly attached to the titanium surface showed negligible bacteria killing. It was suggested that the long flexible PEG spacer provided the AMP with the necessary lateral mobility for it to permeate bacterial membrane. In a separate study, *Bagheri* et al. [145] varied PEG chain length in an attempt to investigate the effect of spacer length on bactericidal activity of KLAL and MK5E peptides. The result showed a proportionate improvement in antimicrobial potency of the immobilized peptide with increased spacer length. This result further confirmed the importance of a long, flexible spacer on immobilized peptides' antimicrobial action.

There is also an opposing school of thought, proposing the redundancy of spacers and the disadvantage of an additional spacer incorporation step, which is detrimental to the

efficiency of peptide immobilization, resulting in a lower concentration of AMP covalently grafted onto the surface. In 1995, *Haynie* et al. [148] observed no difference in antimicrobial activity when AMPs were separately conjugated to resin surfaces via two- and six-carbon chain linker. In a more recent study, *Li* et al. [158] reported direct immobilization of an arginine-, tryptophan-rich peptide onto polymer brush ends without spacer. The immobilized AMP retained its potent and broad spectrum activity. The density of immobilized peptide is thought to be the determining factor in antimicrobial performance of immobilized peptides in these studies.

Comparing and drawing a definite conclusion from these studies, is nonetheless difficult due to difference in the AMP sequences and hence structure-activity relationship, substrate materials and immobilization chemistries, which may have an influence on the role of spacers.

2.8.3. Immobilized peptide concentration

The importance of immobilized peptide density on surface bactericidal property is also an important area of study. Peptide surface concentration is usually reliant on the accessibility of AMP's reactive groups and the type of chemical coupling strategies used. Despite concrete evidence suggesting the importance of immobilized peptide density, various reports showed that it may not be the most critical parameter in dictating surface antimicrobial potency. In studies by *Gabriel* et al. [153] and *Glinel* et al. [149], surface biocidal activity was observed to be independent of the amount of peptide grafted. *Bagheri* et al. [145] conducted a study to evaluate the effect of varying peptide density and spacer span on immobilized AMP's bactericidal property. Results from the study demonstrated that peptide density is second fiddle in impacting antimicrobial activity. The study indicated

that an increase in peptide loading was insufficient to compensate for the loss in activity due to shrinkage in spacer length and distortion in peptide conformation [145].

Albeit these studies disputing the influence of peptide loading on dictating immobilized AMP antimicrobial activity, other reports had provided evidence that the effect of peptide density should not be marginalized. *Chen* et al. [152] investigated the effect of immobilized melimine concentration on bactericidal activity when immobilized *via* two different coupling strategies. The result demonstrated a proportional relationship between immobilized peptide density and AMP's antibacterial property. This is especially true for the 4-azidobenzoic acid tethering platform, where a more profound bactericidal activity can be observed with higher concentration of grafted peptide [152]. *Hilpert* et al. [163] developed an alternative peptide immobilization platform, tethering biotinylated peptides onto streptavidin-coated surfaces. Antimicrobial activity of the AMP grafted surface was found to be concentration dependent, with an increase in microbe killing observed with increasing tethered peptide concentration. In a recent effort by *Basu* et al. [164], Polybia-MPI was immobilized onto silicone substrate using allyl glycidyl ether (AGE) based polymerization chemistry. The Polybia-MPI tethered surface displayed concentration dependent antimicrobial activity, where surface bactericidal potency improved as a function of increasing immobilized peptide concentration.

The difference in these reported results makes it hard to draw a clear-cut conclusion on the significance of immobilized peptide concentration on antimicrobial activity. Despite inconsistencies between the studies' finding, it can be concluded that immobilized peptide density is one of few key factors in determining antimicrobial potency, especially when the grafted AMP concentration is low, below a certain critical threshold value.

2.8.4. Immobilized peptide orientation

AMPs kill bacteria by first attaching to the microbe membrane through electrostatic interaction, followed by disruption of the phospholipid layers through various penetrative and/or lysis modes. Peptide structural studies have exhibited that AMPs generally change and adopt a more structured conformation (i.e., α-helical or β-sheet) upon interaction with bacterial membrane [165, 166]. It is well-established that such conformational changes are crucial to the peptides' antimicrobial action [167]. In the case of immobilized AMPs, it is essential to maintain the conformational integrity and flexibility of these peptides.

AMPs can be immobilized onto substrate surfaces at various position (i.e. at C-terminal, N-terminal or along the peptide chain length), depending on the coupling strategy and location of functional group along the peptide length. Common positions for surface attachment include N-, C-terminal and/or N-side chain. Variation in grafting positions has been shown to bear significant impact on the peptide's orientation and flexibility, hence affecting its antimicrobial activity [145, 153, 162, 168]. Reports by *Gabriel* et al. [153] and *Steven* et al. [162] compare the differences in antimicrobial efficiency of peptides grafted *via* N-terminally and N-side chain. Results from both studies demonstrated consensus results, with only N-terminally attached peptides retaining their antimicrobial activity. N-terminal conjugation offers the peptide extra mobility and flexibility for structural alterations, which is critical for bacteria membrane interaction and subsequent pore formation [153]. On the other hand, Lys ε-amino group tethering seemed to have a deleterious effect on the AMP's bactericidal activity, probably due to the active site being occupied for surface immobilization, hindering the formation of intramolecular bonds and preventing proper assembly of necessary peptide configuration. In a separate study, *Bagheri* et al. [145] compared the antimicrobial properties of C-terminal, N-terminal and N-side-chain

immobilized peptides. N-terminally grafted AMPs were the most potent, followed by N-side-chain tethering. C-terminally attached peptides have the highest MIC values. *Li* et al. [168] conducted a comprehensive study to investigate the difference in orientation between C- and N-terminally immobilized peptides. Analysis with sum frequency generation vibrational spectroscopy and molecular simulation illustrated that AMP immobilized through the N-terminus was perpendicularly oriented with respect to substrate surface, while C-terminally grafted peptide adopted a parallel orientation. It was suggested that the “standing up” orientation of N-terminally grafted AMP offered lesser steric hindrance for peptide folding and higher exposure for bacterial interaction, hence a quicker and more potent antimicrobial action [168].

Other than the position of peptide immobilization, other factors such as amino acid sequence and coupling strategies, are also crucial in determining immobilized peptide structure.

2.9. AMP controlled release coating

AMPs can also be immobilized onto solid surfaces through physical means. It normally involves physically loading these peptides into polymeric and/or matrix systems, which upon implanting, gradually release the AMPs into the surrounding environment for sterilization of implanted site and as prophylactic measurement against subsequent bacterial infection. Table 2.5 illustrates some of the commonly applied peptide encapsulation strategies and the different modes of release [169]. However, there is no one ideal encapsulation system or release mechanism. More often than not, the choice of encapsulation system is largely dependent on the targeted application and release mechanism. Conventional controlled release platforms often rely on a combination of several mechanisms. An ideal AMP release profile should exhibit high initial release rate

within 24 h upon implantation, for initial site sterilization while the immune system is compromised. This should be followed with a slow, sustained release as prophylactic measurement against possible subsequent bacterial infection [170].

Table 2.5. Peptide encapsulation methodology and subsequent release mechanism [169].

Peptide encapsulation methodology	**Peptide release mechanism**
Emulsion polymerization	Bulk and surface erosion
Interfacial polymerization	Diffusion mechanism
Solvent evaporation	Osmotic pressure
Salting out	
Coacervation	
Layer-by-layer technology	
Solvent displacement	

Shukla et al. incorporated an AMP, ponericin G1, into polyelectrolyte multilayer matrices, composed of poly(β-amino ester), alginic acid, chondroitin sulfate and dextran sulfate [171]. Peptide release profiling indicated sustained release of the peptide up to 10 days, accompanied by effective inhibition of *S. aureus* growth during the period of release. On top of that, the peptide-rich coating demonstrated potent anti-biofilm property, resisting possible bacterial attachment. In a separate study, Nisin, a common food preservative, was loaded into a polyethylene polymer film. The AMP loaded film demonstrated prolonged

bactericidal activity, successfully curbing *Brochothrix thermosphacta* growth for up to 21 days [172]. Recently, *Kazemzadeh-Narbat* et al. reported the use of a calcium phosphate-POPC dual layer assembly to achieve prolonged AMP release on titanium implant. The dual layer system illustrated sustained AMP release up to 7 days. The released peptide retained superb, broad-spectrum antimicrobial activity, effectively inhibiting both *S. aureus* and *P. aeruginosa* growth [170].

Despite achieving sustained peptide release profile and superb antimicrobial potency, there are several drawbacks that are often associated with the current controlled release platforms. For example, AMPs encapsulated deeper within the matrix system normally lack direct contact with the surrounding bulk and might not be effectively released at significant concentration [89]. To address this problem, manipulation to factors such as diffusion pathway tortuosity [173] and assembly thickness [174], are needed to ease the release of these deeply encapsulated AMPs. However, such changes are often complex and hard to implement. There is also the problem of short term release, in which AMP release is non-sustainable. This could be due to binding of bacteria onto the superficial layer of the assembly, blocking subsequent diffusion of peptides from within the matrix [89]. Moreover, the long term stability and biocompatibility of such polymeric and/or matrix assembly remain to be better understood. There have been studies reporting the release of cytotoxic by-products upon biodegradation of some polymers. For example, poly(lactic-co-glycolic acid) (PLGA) produces acidic by-products upon degradation [175]. In order to better design an optimal, sustainable and controlled AMP release platform for antimicrobial coating, the aforementioned considerations would have to be carefully taken into account.

2.10. Current challenges in AMP functionalization of urinary catheters: a summary

The regular usage of indwelling medical devices in hospital settings has seen a steep rise in the frequency of nosocomial infection occurrence, of which, CAUTI accounts for the majority. Currently, the only treatment option involves systemic administration of antibiotics. However, due to the large extent of uncontrolled antibiotics use and constant evolution of multi-resistant bacteria strains, CAUTI has become increasingly difficult to treat. There is an urgent need for the development of an alternative antimicrobial compound that possess potent, broad-spectrum bactericidal action with good biocompatibility and minimum risk of evoking resistance development.

A proposed method to effectively prevent the development of CAUTI would be to develop an antimicrobial coating for urinary catheter surfaces which can provide efficient and broad-spectrum protection against possible uropathogen colonization. This forms the basis of this Ph.D. thesis. Many different antimicrobial coatings have been developed including those of antibiotics and metallic compounds. As reviewed in this chapter, these coatings still suffer from drawbacks such as risk of bacterial resistance development, low biocompatibility and short term efficiency. Generally, two different types of antimicrobial coatings are recommended. The first type of coating can be achieved by covalently attaching AMPs onto urinary catheter material to create a contact active surface. The biocidal surface is designed to kill any microbes in close proximity, preventing bacterial adherence and subsequent biofilm development. Despite the emergence of numerous grafting platforms, there has yet to be a simple, efficient and robust platform that can be easily translated onto biomedical devices.

The second type of antimicrobial coating can be designed to facilitate peptide release. Upon implantation, this coating is expected to release the encapsulated antibacterial compound in a controlled and sustained manner, inhibiting growth of planktonic bacteria and simultaneously providing a prophylactic measurement against subsequent bacterial infection. There is an apparent dearth in the development of an efficient controlled release platform for alternative antimicrobial compounds other than silver and antibiotics, which have been associated with argyrosis and antibiotic resistance development, respectively. Moreover, literature also suggests that many of the existing release platforms do not satisfy the ideal release profile. An ideal delivery system should display high initial release during post-implantation period (~24 h) which is critical for site sterilization, followed by sustained and significant release for at least 14 days to render it effective for use in long term catheterization. Most of the suggested delivery system release the loaded antimicrobial compound within a short time period.

This thesis aims to develop an AMP-based antimicrobial coating for urinary catheter which is both contact active and able to release the peptides in a sustained manner for improved efficacy to treat CAUTI in long term catheterized patients.

Chapter 3 Engineering arginine-, tryptophan-rich peptide and its immobilization on a silicone surface to confer antimicrobial and anti-biofilm activity[1]

Confronted by the need to establish an antimicrobial therapy with minimum risk of antibiotic resistant bacteria development, this thesis focuses on utilizing AMPs as the candidate antimicrobial agent. The use of AMPs is strongly justified by its membrane-penetrating antimicrobial action which is hypothesized to curtail possibility of bacteria mutation towards resistance development. However, in order for AMPs to serve as an effective therapeutic and coating agent, the peptides must satisfy certain pre-requisites including broad spectrum bactericidal activity, excellent biocompatibility and stability under physiological condition. To date, most naturally occurring AMPs lack the ability to retain all these properties simultaneously [176, 177], and peptide engineering to improve these properties could be necessary. Moreover, to effectively utilize AMPs as an antimicrobial coating agent, an efficient and robust immobilization platform is necessary. Most of the immobilization platform presented in literature is either too complicated requiring numerous

[1]A version of Chapter 3 has been published. This chapter is adapted from "Lim K.Y., Chua R.R.Y., Saravanan R., Basu A., Mishra B., Tambyah P.A., Ho B., Leong S.S.J., 2013, Immobilization studies of an engineered arginine-tryptophan rich peptide on a silicone surface with antimicrobial and anti-biofilm activity, ACS Applied Materials and Interfaces 5; 13: 6412–6422". Copyright (2013) American Chemical Society.

complex chemical reactions or incompatible for application onto inert silicone materials, limiting translatability onto medical devices.

Royal Jelly, a yellowish-white, viscous secretion produced by the honeybees, serves as the principal food source for the queen honeybees. Despite it being a highly nutritious food source, the royal jelly is generally free of microbial contaminations that is commonly found in other related bee hive related products. An early study revealed the presence of a 51-mer antimicrobial polypeptide, royalisin, which can account for the antimicrobial properties of the royal jelly [178]. However, the modest concentration and narrow spectrum of antimicrobial action meant that this royalisin is unlikely to be the sole antimicrobial agent accounting for all the biocidal properties of royal jelly. It should be working in tandem with some other antimicrobial agents. In 2004, *Renato* et al. managed to isolate and characterise a family of short peptides, Jelleines, from the royal jelly [179]. Three out of the four Jelleine peptides demonstrated good, broad-spectrum bactericidal activities against both Gram-negative and Gram-positive bacteria, and also against yeasts. Out of which, Jelleine I exhibited the best antimicrobial potency with MICs kept below 20 μg/mL against a broad spectrum of bacteria. On top of that, the short peptide sequence (8 amino acids) and lack of cysteine residues within the intrinsic sequences aid to lower cost as well as synthesis process complexity. These intrinsic properties render Jelleine I a suitable AMP candidate template for further engineering.

This chapter reports a study conducted to develop a *de-novo* synthetic AMP through rational modification strategies from the candidate AMP template, Jelleine I. The final engineered arginine-, tryptophan-rich peptide (CWR11) exhibited potent antimicrobial activities against gram-negative and gram-positive uropathogen strains, and possessed excellent salt resistance properties. A tethering platform was developed in a subsequent study to covalently graft CWR11 onto polymethylsiloxane (PDMS), creating a contact

active antimicrobial surface on the model silicone platform. Various surface characterization techniques were performed to verify and elucidate coating properties. Antimicrobial activity and anti-biofilm property of the AMP-grafted surface was evaluated against prevalent uropathogens, i.e., *Escherichia coli*, *Staphylococcus aureus* and *Pseudomonas aeruginosa*. Biocompatibility of the coating was investigated against human aorta smooth muscle cells. The results of this chapter have been published [180].

3.1. Materials and methods

3.1.1. Materials

Wild type Jelleine I and engineered peptide variants were chemically synthesized by GL Biochem (Shanghai, China) at a purity of >90%. Chemicals were procured from Sigma Aldrich, unless otherwise specified. Bacterial strains used in this study were *Escherichia coli* (ATCC 8739 and UTI 89) (*E. coli*), *Staphylococcus aureus* (ATCC 6538) (*S. aureus*) and green fluorescence protein-expressing *Pseudomonas aeruginosa* (PAO1) (GFP-*P. aeruginosa*).

3.1.2. Peptide concentration determination

Peptide was dissolved in distilled water and the peptide concentration was quantified by absorbance using the *Beer-Lambert* law. Molar absorption coefficient (ε) of the peptide was determined based on an empirical formula developed by *Pace* et al [181].

$$\varepsilon\,(280nm) = 5500\,(\#\,Trp) + 1490\,(\#Tyr) + 125\,(\#Cys) \quad \text{[Equation 3.1]}$$

Absorbance measurements of the peptide solutions were performed using a UV/Vis spectrophotometer (Boeco S-22, Germany).

3.1.3. Minimum Inhibitory Concentration (MIC) assay

MICs of CWR11 were performed against *E. coli*, *S. aureus* and GFP-*P. aeruginosa* by using a standard broth microdilution assay [182]. Briefly, wells of a 96 well microplate were filled with 50.0 µL CWR11 peptide at different concentrations (1.6 µg/mL to 50.0 µg/mL). 50.0 µL of 10^6 CFU/mL bacterial suspension were then added to each well to obtain a final bacterial concentration of 5 x 10^5 CFU/mL. The microplate was incubated at 37.0^{o}C for 16 h. 5.0 µL of the cell suspension from each well was plated on Mueller Hinton (MH) agar plate. MIC was determined to be the peptide concentration at which no colony could be observed on the agar plate.

3.1.4. Circular Dichroism (CD) spectroscopy

CD analysis of the peptides was performed using the Chirascan Circular Dichroism Spectrometer (Applied Photophysics Limited, UK). Briefly, the CD spectra of CWR11 were generated in three environments, (i) deionized water, (ii) phosphate buffered saline (PBS) solution, and (iii) 20 mM sodium dodecyl sulfate (SDS) solution. Each spectrum was obtained over a wavelength range from 190 to 260 nm with an interval of 0.5 nm, at 1.0 nm s^{-1} speed and 1.0 nm bandwidth. Three scans were conducted and averaged to obtain each spectrum, which was presented in terms of molar ellipticity (degrees·cm^2·mol^{-1}). Baseline scans were obtained for the respective buffer and micelle solutions only, and subtracted from the respective CD spectra generated in the presence of the peptide. All spectra were recorded at a fixed peptide concentration of 300 µM. Peptide secondary structure compositions under different physicochemical environments were determined by spectra deconvolution using the CDNN software.

3.1.5. Membrane permeabilisation studies

3.1.5.1. Field Emission Scanning Electron Microscopy (FESEM)

The peptide, at pre-determined MIC concentration, was incubated with *E. coli*, *S. aureus* and GFP-*P. aeruginosa* for 1 h at 37.0ºC. After incubation, the bacteria cells were fixed with 2.5% glutaraldehyde and incubated for 16 h in 10 mM sodium phosphate buffer (pH 7.0) on glass sides (24 × 50 mm). The glass slides were rinsed with 10 mM phosphate buffer (pH 7.0) and dehydrated through a graded ethanol series (25 – 100%). The slides were dried under constant airflow for 15 min, and sputtered with platinum for 100 s at 10 mA. The bacterial membrane morphologies were imaged with FESEM (JEOL field electron microscope, Jsm-6700F, Japan).

3.1.5.2. 1-N-phenylnapthylamine (NPN) uptake assay

The extent of peptide-induced outer membrane permeabilisation was determined by the NPN uptake assay [183]. Briefly, *E. coli* strains were grown overnight, re-inoculated and grown to an optical density at 600 nm (OD_{600}) of 0.5. Bacterial cells were washed thrice with 10 mM PBS solution (pH 7.0), before re-suspension in the same buffer to attain an OD_{600} of 0.5. 1.0 mL of the bacterial suspension was added to various concentrations of peptide (0-14 μM), followed by 20.0 μL of 0.5 mM NPN solution to attain a final NPN concentration of 10 μM. Florescence measurements of the samples were performed using a fluorescence spectrophotometer (Perkin Elmer LS5, USA) at an excitation wavelength of 350 nm, emission wavelength of 420 nm, and slit width of 5.0 nm. Fluorescence measurements were taken in triplicates and averaged.

3.1.5.3. Propidium iodide (PI) fluorescence assay

The membrane permeabilization ability of the peptide CWR11 was investigated by fluorescence measurements of DNA-binding PI. *E. coli* cells were grown overnight in Mueller Hinton (MH) medium and sub-cultured in fresh medium to an OD_{600} of 0.5. Cells were harvested and subjected to 3 times washing with 10 mM PBS (pH 7.0). Washed bacterial cells were re-suspended in 10 mM PBS (pH 7.0) to obtain a final concentration of 1 x 10^8 CFU/mL. 1.0 mL of the *E. coli* cells was withdrawn and mixed with 20.0 µL of PI (1.0 µg/mL). The bacterial suspension was then added with sequential peptide concentrations ranging from 1/8 to 1X MIC. Fluorescence measurements were measured using a fluorescence spectrophotometer (Perkin Elmer LS5, USA) with excitation and emission wavelength set at 520 nm and 620 nm, respectively.

3.1.6. CWR11 immobilization on polydimethylsiloxane (PDMS) slides

3.1.6.1. Synthesis of PDMS slides

PDMS polymer was synthesized using a kit (184 elastomer kit, Dow Corning, US), according to the manual's instructions in 90 mm petri dishes and subsequently cut into 1.0 × 1.0 cm slides for peptide immobilization studies.

3.1.6.2. Plasma and Ultraviolet (UV) polymerization of PDMS slides with allyl glycidyl ether (AGE)

AGE brush polymerization on PDMS slides was performed using continuous surface plasma activation, followed by UV radiation with AGE monomer. Briefly, 1 cm^2 PDMS slides were rinsed with acetone to remove any impurities on the surfaces, and subjected to argon plasma treatment for surface activation. Plasma activation was conducted using the March

PX-500 Plasma treatment system (Nordson, USA). Continuous plasma was performed at 300 W for 10 min in the presence of inert argon gas. The activated PDMS slides were successively immersed in 100% (v/v) AGE, and subjected to UV radiation for 60 min. The AGE-tethered slides (PDMS-AGE) were washed with distilled water (3 times, 5 min each time with 5.0 mL distilled water).

3.1.6.3. Attachment of PEG spacer to PDMS-AGE slide

Maleimide-PEG-Amine heterobifunctional polyethylene glycol (PEG)spacer (NH_2-PEG-Mal) (3.4kDa) was purchased from Nanocs (USA). NH_2-PEG-Mal was dissolved in deionized water to a final concentration of 5.0 mg/mL. The activated surface of PDMS-AGE slides were covered with the PEG solution and incubated at 25.0^{o}C for 16 h. The PEG-grafted PDMS slides (PDMS-AGE-PEG) were then washed in deionized water (3 times, 5 min each time with 5.0 mL deionized water) to remove unattached PEG linker.

3.1.6.4. Crosslinking of CWR11 to chemically modified PDMS surface *via* sulfhydryl chemistry

Peptide crosslinking was performed using the sulfhydryl chemistry between the peptide's thiol moiety and maleimide group derived from the PEG-functionalized PDMS slides based on a reported protocol [184]. Briefly, the PDMS-AGE-PEG slides were immersed in 2.0 mg/mL peptide solution and the reaction was allowed to occur at 25.0^{o}C for 16 h. After incubation, the peptide-tethered PDMS slides (PDMS-AGE-PEG-CWR11) were rinsed thoroughly with 10 mM PBS (5 times, 5 min each time with 5.0 mL of 10 mM PBS), followed by deionised water (5 times, 5 min each time with 5.0 mL deionized water) to remove any unbound peptides. The slides were dried in a nitrogen stream and stored at -20.0^{o}C for future use.

3.1.7. Surface characterization of CWR11-immobilized PDMS slides

3.1.7.1. Contact angle measurement

Static water contact angle measurements of the respective PDMS samples (PDMS, PDMS-AGE, PDMS-AGE-PEG and PDMS-AGE-PEG-CWR11) were performed with a dynamic contact angle analyzer (Fta 200, Fta, U.K.). 5.0 µL water droplet was introduced onto the respective PDMS surfaces and digital images were taken with high magnification imaging lens (Navitar, USA). Contact angle quantitation was performed using the Fta32 software.

3.1.7.2. X-ray photoelectron spectroscopy (XPS)

XPS analysis was performed to determine the elemental atomic percentage on the peptide-immobilized PDMS slide surface. High-resolution spectra of carbon, nitrogen, oxygen and silicon elements were obtained individually using an X-ray photoelectron spectrometer (Axis-ULTRA, Kratos) installed with A1 Kα source (10.0 mA, 15.0 kV), and analyzed to determine the respective elemental ratio.

3.1.7.3. Energy Dispersive X-ray Spectroscopy (EDS)

Attachment and distribution of peptides immobilized on the PDMS surface was analyzed using EDS (FESEM, JEOL field electron microscope, Jsm-6700F, Japan). The elemental content was quantified using the Analysis Station software.

3.1.7.4. Attenuated Total Reflectance – Fourier Transform Infrared (ATR-FTIR) spectroscopy

Peptide-immobilized PDMS samples were subjected to ATR-FTIR analysis to verify the presence of amide bonds on the surface. The spectrum was recorded on a Thermo Nicolet 5700 FT-IR spectrometer (Thermo Fisher Scientific, USA) equipped with a Diamond ATR accessory unit on which PDMS-AGE-PEG-CWR11 and PDMS-AGE-PEG slides were placed upon. Each spectrum was recorded at 25.0^{o}C from 400 cm^{-1} to 4000 cm^{-1} over 32 scans.

3.1.7.5. Peptide concentration determination by sulfosuccinimidyl-4-o-(4,4-dimethoxytrityl) butyrate (sulfo-SDTB) spectrophotometric assay

Immobilized peptide concentration was determined using the Sulfo-SDTB spectrophotometric assay (Bioworld, USA) according to the suppliers' instruction manual. Briefly, 3.0 mg of Sulfo-SDTB was dissolved in 1.0 mL of dimethylformamide (DMF), and topped up to 50.0 mL with sodium bicarbonate solution (pH 8.5). To the peptide-immobilized samples, 1.0 mL of the Sulfo-SDTB solution and 1.0 mL of sodium bicarbonate was added, and incubated for an hour at 25^{o}C. The samples were subsequently washed twice in 5.0 mL of distilled water, and immersed in 2.0 mL of perchloric acid for 30 min. Upon incubation, 500 µL of the perchloric acid was removed and absorbance at 498 nm was measured. The amount of amine groups on the surface of each sample was quantified using *Beer-Lambert* law (Equation 3.1) with an extinction coefficient of 70 000 $M^{-1}cm^{-1}$. The amount of peptides immobilized on each sample was calculated by calibration against the predicted number of amines per peptide.

3.1.8. CWR11-immobilized PDMS slide surface antimicrobial assay

The surface antimicrobial activity of the PDMS-AGE-PEG-CWR11 slides was determined using an adapted ISO protocol 22196 [185]. Briefly, *E. coli* bacterial strains were cultivated in MH medium, 16 h at 37.0^{o}C. The overnight bacterial suspension was then sub-cultured in fresh medium and grown to OD_{600} 0.5 (mid-log phase), then further diluted to a final concentration of 1 x 10^6 CFU/mL. 50.0 µL of the bacterial suspension was then spread over each PDMS-AGE-PEG-CWR11 slide. The inoculated slides were incubated at 37.0^{o}C for 3 h, under 70 rpm shaking conditions. 5.0 µL of the inoculum was withdrawn from each PDMS slide and plated for colony counts. The same PDMS slide, with the remaining inoculum, was then immersed in 2.0 mL of fresh MH medium and incubated at 37.0 ^{o}C, 250 rpm for 18 h to verify the antimicrobial activity of the slides. The protocol was repeated in triplicate for *E. coli*, *S. aureus* and GFP-*P. aeruginosa*.

3.1.9. Stability determination of immobilized peptides

To determine the stability of the PDMS-immobilized peptides, a leaching assay was conducted using a reported protocol [184]. Peptide-immobilized PDMS slides were immersed in distilled H_2O for 1 to 3 days. Peptide stability was investigated by surface antibacterial assay as described in Section 3.1.8.

3.1.10. Anti-biofilm activity of peptide-immobilized PDMS slides

3.1.10.1. Gram crystal violet viability assay

Each PDMS slide was rinsed with 70% ethanol (v/v) and dried. The PDMS-AGE-PEG-CWR11 slides were secured to the bottom of the wells, in a 24-well plate. 1 × 10^8 CFU GFP-*P*. *aeruginosa*, in 1 mL of biofilm promoting medium (BPM). was added to each well.

BPM with no bacteria was used as control. After 24 h at 37°C incubation, planktonic bacteria were removed and the wells together with the PMDS–AGE-PEG-CWR11 slides were washed 5 times with deionized water. 1.2 mL of 0.1% crystal violet stain was added to the wells and incubated for 15 min at 25.0°C, followed by washing with distilled water. The wells and PDMS slides were dried in a 37.0°C incubator. The crystal violet stain on PDMS slides were solubilized in 200 µL 30% acetic acid (v/v) for 15 min. 100 µL of solubilized crystal violet was added to 100 µL of 30% acetic acid in wells of 96-well plate, and the amount of solubilized crystal violet was measured by their absorbance at 550 nm.

3.1.10.2. Live/dead biofilm staining

Overnight *E. coli* culture was diluted in MH broth to a final concentration of 1×10^8 CFU/mL. PDMS-AGE-PEG-CWR11, PDMS-AGE-PEG and PDMS slides were immersed in 2.0 mL bacteria suspension for 5 days to ensure complete biofilm formation. After 5 days, planktonic bacteria were removed by briefly rinsing the respective slides with PBS. The slides were then dried and stained with a LIVE/DEAD kit (Invitrogen Molecular Probes, USA) according to the manufacturer's instructions. The samples were examined with a LSM710 META confocal microscope (Carl Zeiss, Germany). For detection of SYTO 9 (green channel), the excitation wavelength was set at 488 nm. For PI detection (red channel), the 561 nm excitation wavelength was utilized. Images at both excitation wavelengths were captured, and processed using the Zen 2009 software.

3.1.11. Cytotoxicity assay

3.1.11.1. Hemolytic assay

The hemolytic activities of the immobilized peptides against human erythrocyte cells were studied using a method adapted from *Shai* et al [186]. Fresh human red blood cells

(hRBC) were rinsed and washed thrice with PBS, centrifuged for 10 min at 900 g and re-suspended in PBS to a final erythrocyte concentration of 5.0% (v/v). The peptide-immobilized and untreated PDMS slides were each immersed in 2.0 mL hRBC solution and incubated for 1 h at 37.0^{o}C, with agitation at 100 rpm. Upon incubation, the samples were centrifuged at 1500 g for 5 min. Hemoglobin release was measured by absorbance measurement of the supernatant at 540 nm. Controls for 0% hemolysis and 100% hemolysis were obtained by suspending hRBC in PBS and 1% Triton X respectively.

3.1.11.2. Cell viability assay

Methyl tetrazolium (MTT) assay was also performed to determine cell viability and proliferation capability of human aorta smooth muscle cells (SMCs), CC-2571 (Lonza, USA) on the peptide-immobilized slides. The PDMS-AGE-PEG-CWR11 slides were cut into 5 mm diameter disks and placed in 70% ethanol for 24 h for sterilization, followed by incubation in PBS for 16 h in 96-wells culture plate. Smooth muscle cells (0.5×10^5 cells/cm^2) and culture medium were then added to the respective wells containing the slides. The cells were allowed to grow for 7 days, coupled with culture medium change every 2 days. On day 1, 2 and 7, mammalian cell culture from the wells containing peptide-treated and untreated PDMS slides were withdrawn and placed in a 96 well tissue culture polystyrene plate. MTT solution (5 mg/ml, 100 µL) was incubated with the respective mammalian cell culture at 37°C for 4 h, followed by addition of 200 µL dimethyl sulfoxide (DMSO) addition and shaking for 30 min. Absorbance measurement at 490 nm was conducted using a microplate spectrophotometer (Bio-Rad, USA). Viability of smooth muscle cells upon 7 days of incubation with peptide-immobilized and control PDMS slides, was examined with the LIVE/DEAD Assay. Cells were stained with LIVE/DEAD Assay reagent (Invitrogen,

USA) and incubated at 25°C for 45 min. Morphology of the cells was observed with an inverted optical microscope (Zeiss, Germany).

3.1.12. Statistical analysis

All experiments were conducted in triplicates [except crystal violet staining of biofilm (duplicates)]. Mean and standard deviations, as indicated by respective error bars, were calculated for all repeated measurements. Statistical analysis was performed with SPSS for Mac software version 21.

3.2. Results and discussion

The first study involved identifying a naturally occurring peptide that shows good potential to serve as a template for peptide modification. Jelleine I, an AMP naturally present in royal jelly of honeybees, *Apis mellifera*, was chosen as the candidate peptide for engineering studies because of its short peptide sequence, which is advantageous in easing synthesis, as well as relatively low MIC values against both gram-positive and gram-negative bacteria. Jelleine I does not contain any cysteine residues within its amino acid sequence which also simplifies chemical synthesis [187]. These intrinsic properties render Jelleine I a suitable candidate template for further engineering.

3.2.1. Jelleine I engineering studies for improved antimicrobial potency

Jelleine I was first engineered to systematically vary hydrophobicity, charge and amphipathicity properties (Table 3.1).

Table 3.1. Variant peptides from first round of peptide modification.

Peptide	Sequence	Net Charge	Hydrophilicity	Modification
Jelleine I, J0	PFKISIHL	1.1	-0.6	-
J1	PFKIISHL	1.1	-0.6	Positional change of amino acids
J2	IFKIISHL	1.1	-0.9	Positional change and substitution of amino acids
J3	PFKRISHL	2.1	0	Positional change and substitution of amino acids
J4	WFKIISHL	1.1	-1.1	Positional change and substitution of amino acids
J5	PFKIWSHL	1.1	-0.8	Positional change and substitution of amino acids
J6	PFKWWSHL	1.1	-1	Positional change and substitution of amino acids
J7	PFKWWSHW	1.1	-1.2	Positional change and substitution of amino acids
J8	PFKIIRHL	2.1	-0.3	Positional change and substitution of amino acids
J9	PFIKILHR	2.1	-0.3	Positional change and substitution of amino acids
J10	PFRKILHR	3.1	0.3	Positional change and substitution of amino acids
J11	WFWKWWRR	3	-0.9	Positional change and substitution of amino acids
J12	IFIKIIRR	0.3	-0.1	Positional change and substitution of amino acids
J13	RFWKWWRR	0.4	-0.1	Positional change and substitution of amino acids

Microbroth dilution assays were conducted on the variant peptides to determine MICs of the respective variant peptides against *E. coli* (data not shown). Out of 13 variants, J11 possessed the lowest MIC value, i.e. 14.3 ± 1.5 µg/mL. Based on the antimicrobial assay results, J11 was chosen as the candidate for next round of modification.

The second round of modification involved optimizing electrostatic charge of candidate peptide J11, by adding arginine residues at the C-terminal. Table 3.2 displays the peptide variants generated from modification of J11.

Table 3.2. Variant peptide from second round of peptide modification.

Peptide	Sequence	Net Charge	Hydrophilicity	Modification
J11a1	WFWKWWRRR	+4	-0.9	Amino acid addition
J11a2	WFWKWWRRRR	+5	-0.9	Amino acid addition
J11a3	WFWKWWRRRRR	+6	-0.9	Amino acid addition

Similarly, a round of MIC assay was conducted to determine the variant peptide with superior antimicrobial activity. The second round of MIC determination assay illustrated that J11a3 was the most bactericidal with a low MIC of 7.0 ± 1.6 µg/mL (data not shown). Based on this result, J11a3 was chosen as the candidate peptide for the next round of modification.

The third round of modification involved amidation of candidate peptide J11a3 at the C-terminal. The hydroxyl group (-OH) of the C-terminal carboxylic acid group (-COOH) was amidated to form a primary amine ($-NH_2$) group. The amidation reaction increased the net

charge of the peptide to +7, which is hypothesized to improve electrostatic interaction between the peptide and bacterial membrane.

Table 3.3. Variant peptide from third round of peptide modification.

Peptide	Sequence	Net Charge	Hydrophilicity	Modification
J11a31 (WR11)	WFWKWWRRRRR-$\underline{NH_2}$	+7	-0.9	Amidation at C-terminal

A third round of antimicrobial assay was conducted to investigate the effect of amidation on the bactericidal property of J11a3. Indeed, with enhanced electrostatic interaction, AMP is better able to initiate membrane attachment and hence improve antimicrobial action. MIC of J11a31 (WR11) for *E. coli* was further improved to 6.1 ± 1.1 μg/mL. The low MIC of J11a31 against *E. coli* makes it a potential candidate for structure-activity and immobilization studies. J11a31 will be referred to as WR11 from this point on, where WR signifies the tryptophan- and arginine-rich nature of the peptide and 11 represents the number of amino acid residues present in the peptide sequence.

Several cycles of systematic amino acid addition and/or substitution of arginine and tryptophan residues were performed on the wild type Jelleine-I peptide to generate a *de-novo* arginine-, tryptophan-rich peptide (WR11) with an optimal peptide charge to hydrophobic ratio, which is expected to lead to maximum antimicrobial potency. Tryptophan was chosen to modulate the peptide's hydrophobicity due to its preference for membrane-water interfacial region [188], which is likely to augment the insertion of peptide into the hydrophobic core of the phospholipid bilayer membrane. Substitution with arginine residues was aimed to enhance electrostatic interaction with the negatively charged bacterial membrane. In contrast to lysine, arginine side chains are able to form hydrogen

bonds with surrounding water molecules while engaged in cation-π interaction with tryptophan [189, 190]. This cation-π interaction with tryptophan, coupled with formation of multiple hydrogen bonds with water molecules makes the entry of arginine residues into the hydrophobic bilayer more energetically favourable. The most potent engineered variant, WR11, possessed a net charge of +7, which is contributed by the high arginine content and amidation of the C-terminal. WR11 exhibited significantly lower MIC toward three species of tested uropathogens compared to the parent peptide.

3.2.2. Antimicrobial activity and structural studies of soluble WR11

The MICs of WR11 against three target uropathogens were determined by performing standard broth microdilution assays [182]. Table 3.4 shows that the engineered peptide (WR11) possessed low MICs of 3.1 μM, 1.7 μM and 4.6 μM toward *E. coli*, *S. aureus* and GFP-*P. aeruginosa*, respectively. The peptide was particularly potent against gram-positive *S. aureus* with a MIC of 1.7 μM, a microbe prevalent in community- and hospital-acquired infections, possessing strong resistance against conventional antibiotics and even natural AMPs, such as defensin [191]. Such superior activity merits the use of WR11 for the development of an antimicrobial coating agent for biomedical devices.

With the aim to subsequently immobilize the peptide on a surface *via* specific sufhydryl coupling, cysteine was added to both the N- and C-terminals of WR11. WR11 engineered with an N-terminal cysteine (CWR11) displayed improved antimicrobial activities compared to cysteine engineered at the C-terminal (data not shown), and was selected as the candidate peptide for further immobilization studies. In comparison with WR11, CWR11 possessed a slightly higher MIC. Addition of 150 mM NaCl also slightly inhibited the antimicrobial activity of CWR11, as reflected by a slight increase in MIC values to 7.3 μM, 4.7 μM and 8.7 μM against the respective uropathogens, probably due to salt-induced

charge shielding effects (Figure S.1). However, CWR11 MIC values remained below 10.0 μM and demonstrated retained antimicrobial potency even in the presence of salt. These properties still render CWR11 superior in contrast to many AMPs, which lose antimicrobial activity in physiological salt concentration [102, 192, 193].

Table 3.4. MICs of wild type peptide, WR11, and CWR11 against three bacterial strains (*E. coli*, *S. aureus*, GFP-*P. aeruginosa*) [187].

	Minimum Inhibitory Concentration (μM)			
	Jelleine I	WR11	CWR11	
			No NaCl	150 mM NaCl
E. coli	2.6	3.1±0.6	5.2±0.5	7.3±0.0
S. aureus	10.5	1.7±0.0	2.5±0.0	4.7±0.9
GFP-*P. aeruginosa*	10.5	4.6±0.2	5.5±0.0	8.7±1.2

Secondary structure analysis of CWR11 by CD spectroscopy suggests that CWR11 adopts a mixed α-helix and β-sheet conformation in deionized water (Figure 3.1), with 2 weak trough and shouldering observed at 202 nm and 215 nm respectively, as well as a peak at 190 nm. In PBS, the troughs shifted to 205 nm and 222 nm, while in the presence of 20 mM SDS, a further shift of the trough and shouldering to 207 nm and 218 nm was observed, with increased intensity. Spectra deconvolution indicated an enhanced peptide helicity in the presence of PBS and membrane mimicking SDS, where an estimated increase in helicity from 40.9% (in deionized water) to 96.2% and 98.4% in PBS and 20 mM SDS, respectively, was attained. Secondary structure enhancement in the presence

of phospholipid mimicking molecules is commonly observed in most naturally occurring α-helical AMPs, which has been hypothesized to be attributed to increased electrostatic interaction between the peptide and micelle [167, 194, 195]. In the presence of PBS, CWR11 also showed high α-helicity. It is hypothesized that electrostatic repulsion between the positive charges is reduced in the presence of salt, leading to increased interchain hydrophobic interaction. As such, the high α-helicity observed could be attributed to the cumulative effect of helix formation due to interchain interactions. A study by *Enrique* et al. showed similar enhancement in ellipticity in the presence of 1.4 M salt [196].

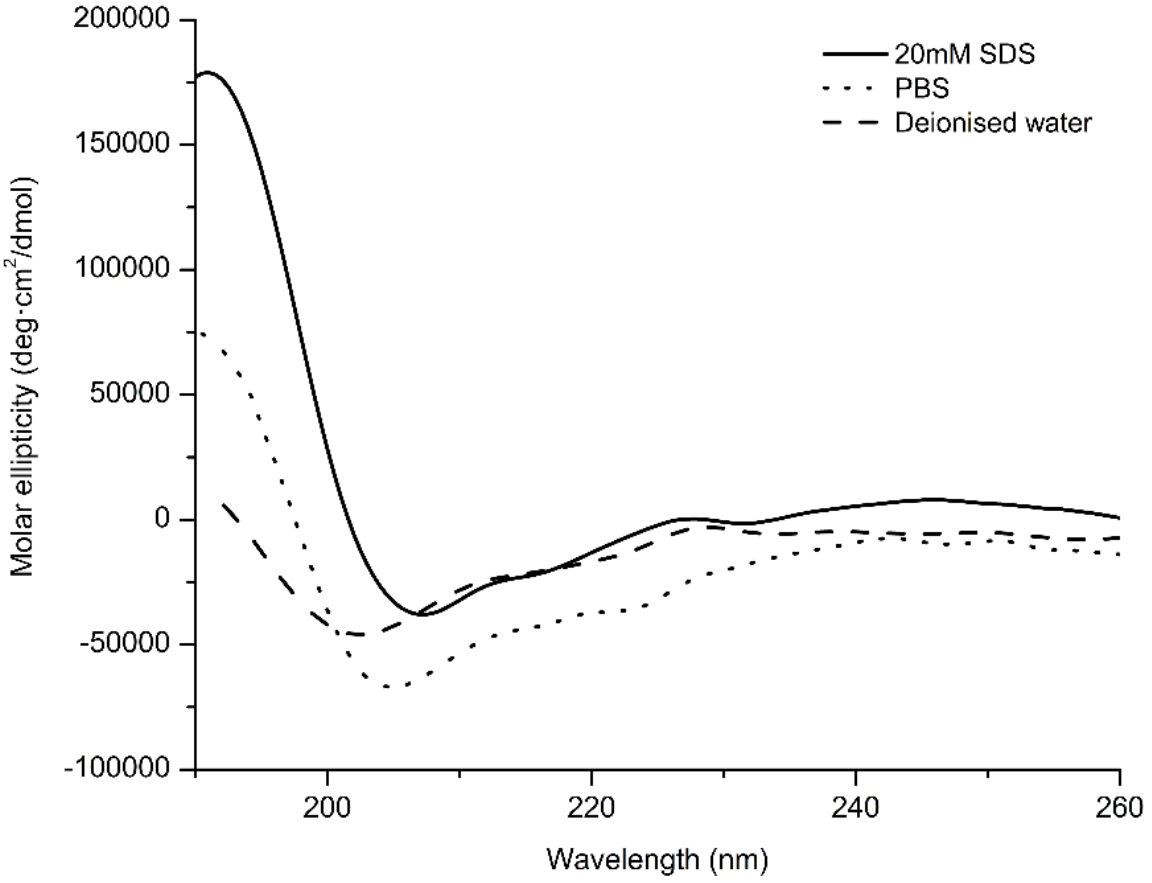

Figure 3.1. The CD spectra of CWR11 peptide in (- -) deionised water, (….) PBS buffer and (—) 20 mM SDS. Peptide concentrations are fixed at 300 μM.

3.2.3. Membrane permeabilisation studies

The effect of CWR11 on bacteria membrane morphological change was studied by field emission scanning electron microscopy (FESEM). Figure 3.2 shows the electron microscopy images of CWR11-treated and untreated bacteria cells. Heavily crinkled outer membrane coupled with formation of bulbous structures on the peptide-treated cells confirmed the membrane disruption ability of CWR11.

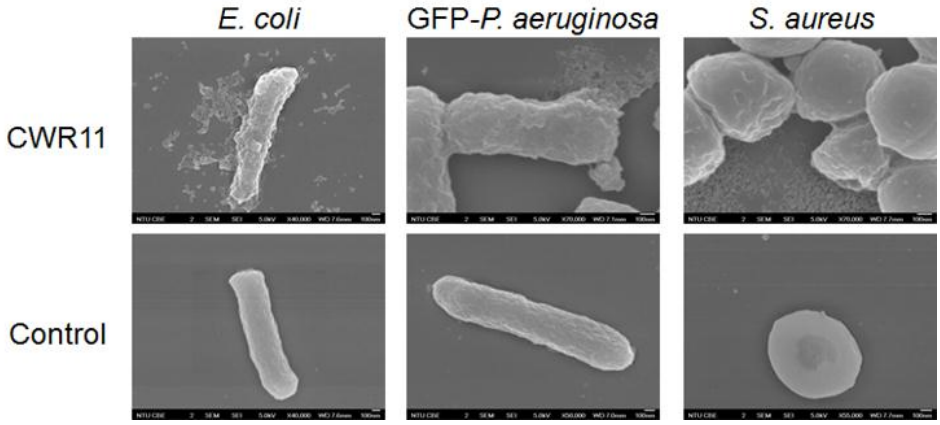

Figure 3.2. *In vitro* characterization of CWR11 membrane disruption potential. FESEM images of CWR11 induced disruption of *E. coli*, GFP-*P. aeruginosa* and *S. aureus* (top panels) and untreated controls (bottom panel).

The outer membrane perturbation ability of CWR11 was further confirmed by the NPN uptake assay. NPN is a chemical compound that fluoresces weakly in aqueous environment, but in the presence of hydrophobic condition, gives off a strong fluorescence with excitation at 350 nm [197]. Figure 3.3 shows an increase in NPN fluorescence with increasing CWR11 concentrations, when incubated with *E. coli*. At a peptide concentration above 10 μM, there was no increase in fluorescence with further increase in peptide concentration, indicating that all the available surface area of the cell membrane had been permeabilized by the peptide.

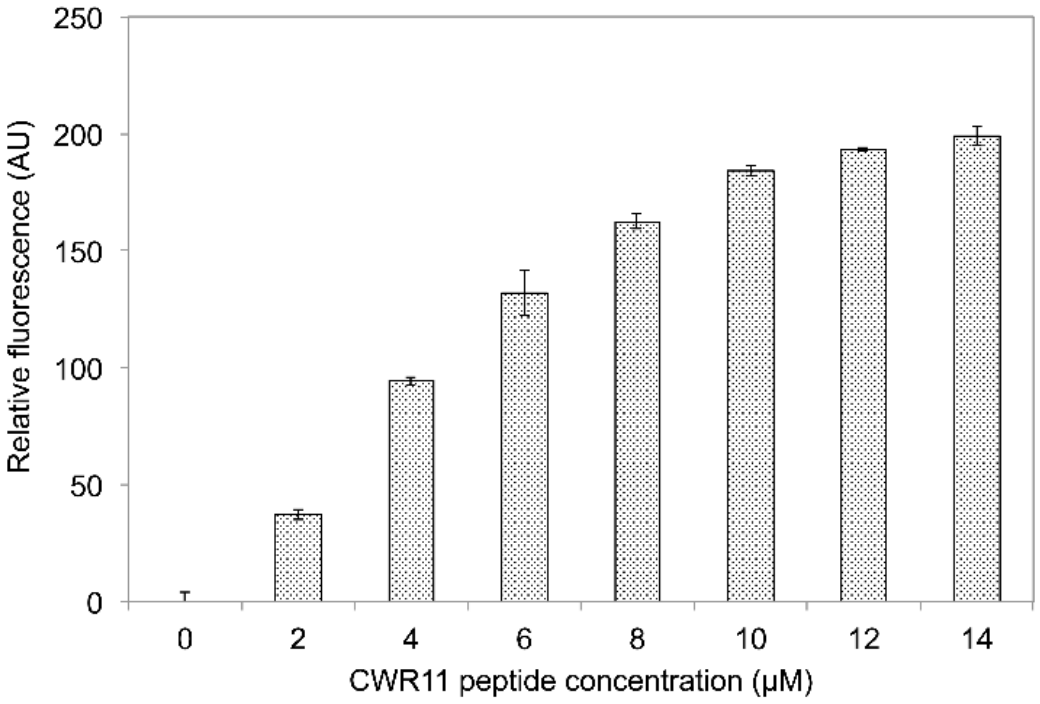

Figure 3.3. Outer membrane permeabilisation studies by NPN fluorescence assay.

The membrane permeabilisation ability of CWR11 was also assayed by studying DNA binding of PI [198]. Upon binding to DNA, PI fluoresces strongly at an excitation wavelength of 520 nm. Figure 3.4 shows that beyond ¼ MIC, the PI fluorescence reading increases with increasing peptide concentration, which indicates the cytoplasmic membrane disruption ability of CWR11, leading to diffusion of PI into the bacteria's cytoplasm, enabling interaction with the bacteria DNA.

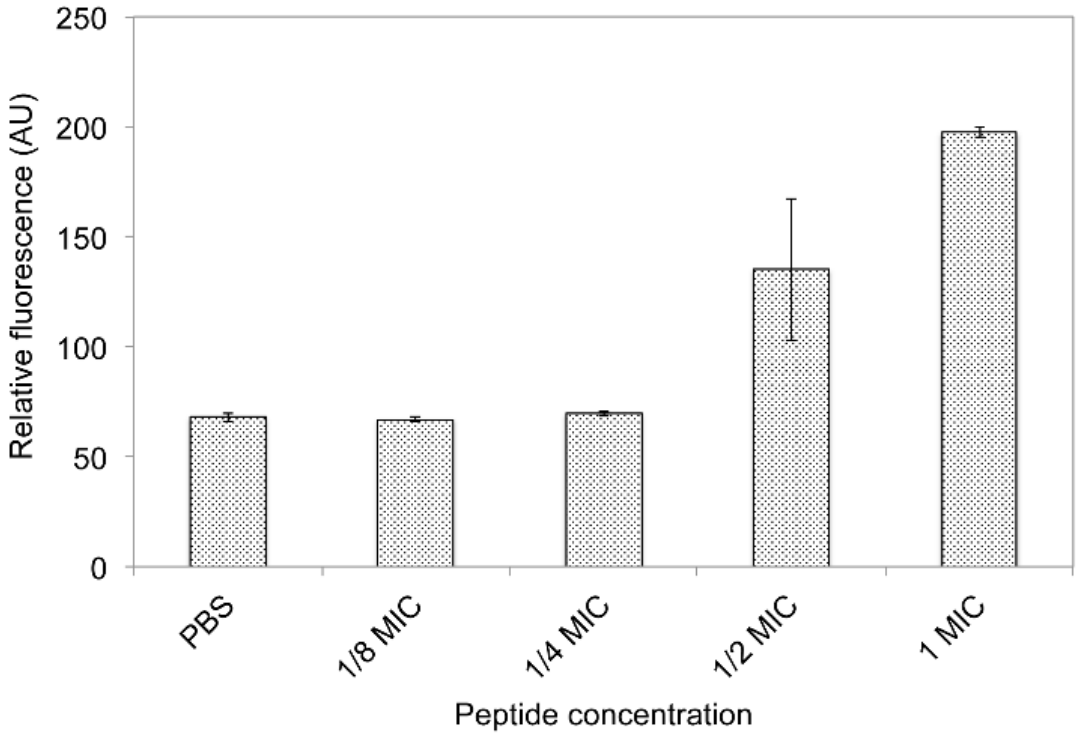

Figure 3.4. DNA intercalation with PI dye to study membrane permeabilisation effect of CWR11.

FESEM morphology analysis, coupled with results from the NPN uptake and PI leakage assay, suggest the potent membrane perturbing ability of CWR11. The membrane perturbing mechanism of action is commonly observed in many AMPs, for example cecropins, magainins, and melittins [199]. It is widely hypothesized that such membrane-targeting mode of action enhanced the broad-spectrum antimicrobial action of AMPs.

The excellent antimicrobial characteristics and salt-tolerant properties of CWR11 merit further studies to evaluate the peptide's potential as an antimicrobial coating agent on biomedical devices. Due to the high occurrence of nosocomial bacterial infection in various biomedical devices including stents and catheters [200, 201], there is an urgent need for the development of antimicrobial surfaces, which is both bactericidal and anti-biofilm. AMP

immobilization on biomedical device surfaces promises to improve antimicrobial functionalities of these devices, without easily evoking antibiotic resistance in pathogens, which forms the basis of our immobilization studies.

3.2.4. CWR11 immobilization on PDMS surface and surface characterization by contact angle, ATR-FTIR, EDS, XPS analyses and Sulfo-SDTB spectrophotometric assay

Most biomedical implantables are made of silicone polymeric materials [202], with PDMS being one of the most widely used material for permanent or short term implantation [203]. In view of this, an immobilization platform using PDMS was developed for the CWR11 immobilization studies.

Immobilization methods reported in the literature often involve multiple reaction steps, with extensive use of a variety of chemicals [145, 153, 204]. To circumvent problems associated with process complexity and specificity, we developed an immobilization platform comprising of plasma-based polymerization reaction, coupled with the use of a heterobifunctional PEG spacer (NH_2-PEG-Mal) (Figure 3.5). The maleimide group attached at the end of each PEG chain ensures specificity of peptide-derived cysteine attachment, and minimizes non-specific reactions between the peptide and polymer brush. Figure 3.5 illustrates the process of peptide immobilization. The first step of the immobilization process utilized continuous plasma to activate the PDMS surface with radicals that are highly reactive to specific chemical groups [205]. Following surface activation, the PDMS was immersed in 100% (v/v) AGE monomer solution, and exposed to UV to impart reactive epoxide groups onto the PDMS surface. This treatment yields extensive polymer brush formation on the PDMS surfaces, with epoxide groups exposed at the end of each chain, which were then reacted with the amine group from the

heterobifunctional PEG moiety (NH_2-PEG-Mal). The epoxide-amine addition reaction is fairly reactive, with a reported activation energy of ~ 63 KJ/mol [206]. Completion of this reaction would lead to formation of AGE polymer brushes with long PEG spacers, and maleimide groups exposed at the end of each chain (PDMS-AGE-PEG). The diffusional and conformational flexibility provided to the peptide by the relatively long PEG spacer (323 nm) [207], is expected to enhance peptide reach and improve peptide-bacterial interaction. Lastly, specific sulfhydryl coupling between maleimide groups of PEG spacer and cysteines of CWR11 facilitated the immobilization of CWR11 to the polymer brushes.

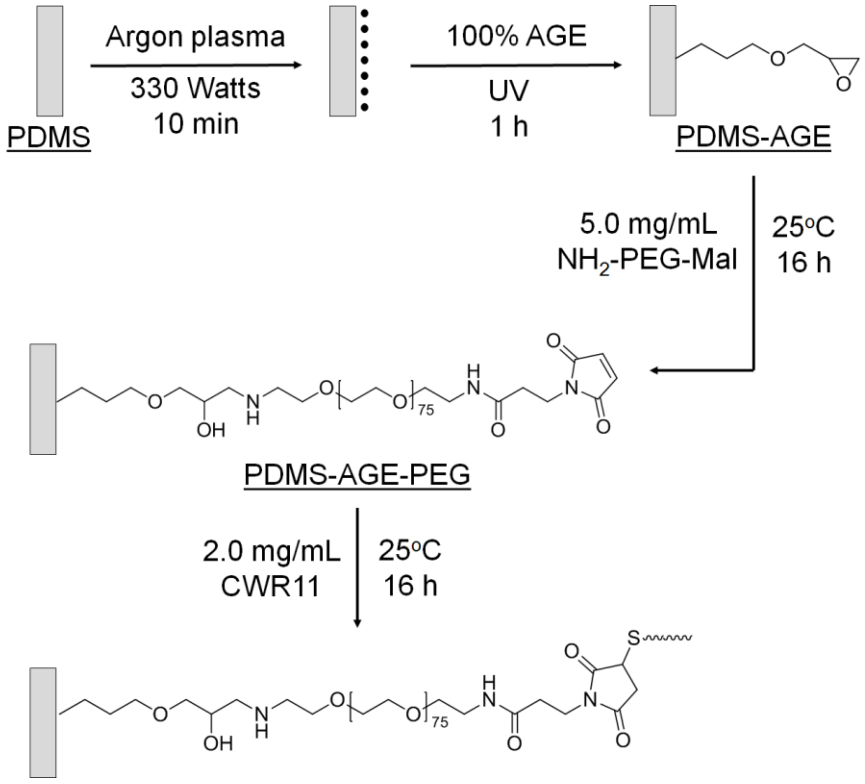

Figure 3.5. Tethering chemistry schematic of CWR11 peptide to PDMS surface.

Various assays were conducted to characterize the peptide-immobilized PDMS surface, and verified the successful tethering of CWR11 onto the polymer brush.

Contact angle measurements were performed to assess the change in surface hydrophilicity of the AMP-immobilized PDMS slides (Table 3.5). PDMS is inherently hydrophobic [208] as shown by a high contact angle of 106^{o}. Plasma activation and polymerization of AGE onto the PDMS surface drastically enhanced the hydrophilicity of the PDMS surface, as shown by a reduction in contact angle to 43^{o}. Subsequent attachment of PEG moieties and peptide slightly increased surface hydrophobicity, as indicated by an increase in contact angle by 8^{o} and 13^{o}, respectively, which is attributed to the hydrophobic carbon backbone of the PEG and peptide. This result is comparable to that reported by *Gao* et al [209], where a final contact angle of ~60^{o} was attained upon peptide immobilization.

Table 3.5. Contact angle measurement of deionised water on respective treated and untreated PDMS surfaces.

	Contact angle (^{o})
PDMS	105.76 ± 5.62
PDMS-AGE	42.96 ± 5.10
PDMS-AGE-PEG	54.20 ± 0.72
PDMS-AGE-PEG-CWR11	67.01 ± 0.98

Figure 3.6 shows the ATR-FTIR spectra obtained for PDMS-AGE-PEG-CWR11 and PDMS-AGE-PEG. For PDMS-AGE-PEG-CWR11, peaks were observed at 1653 cm^{-1} and 1558 cm^{-1} representative of amide I and amide II bands. These peaks were absent in the PDMS-AGE-PEG samples. The presence of these bands confirms successful peptide

immobilization on the slides. This agrees with previous studies on characterizing attachment of peptides onto activated surfaces. For example, covalent immobilization of laminin onto treated chitosan surfaces was also verified by the presence of absorption bands at 1665 cm^{-1} and 1543 cm^{-1} [210].

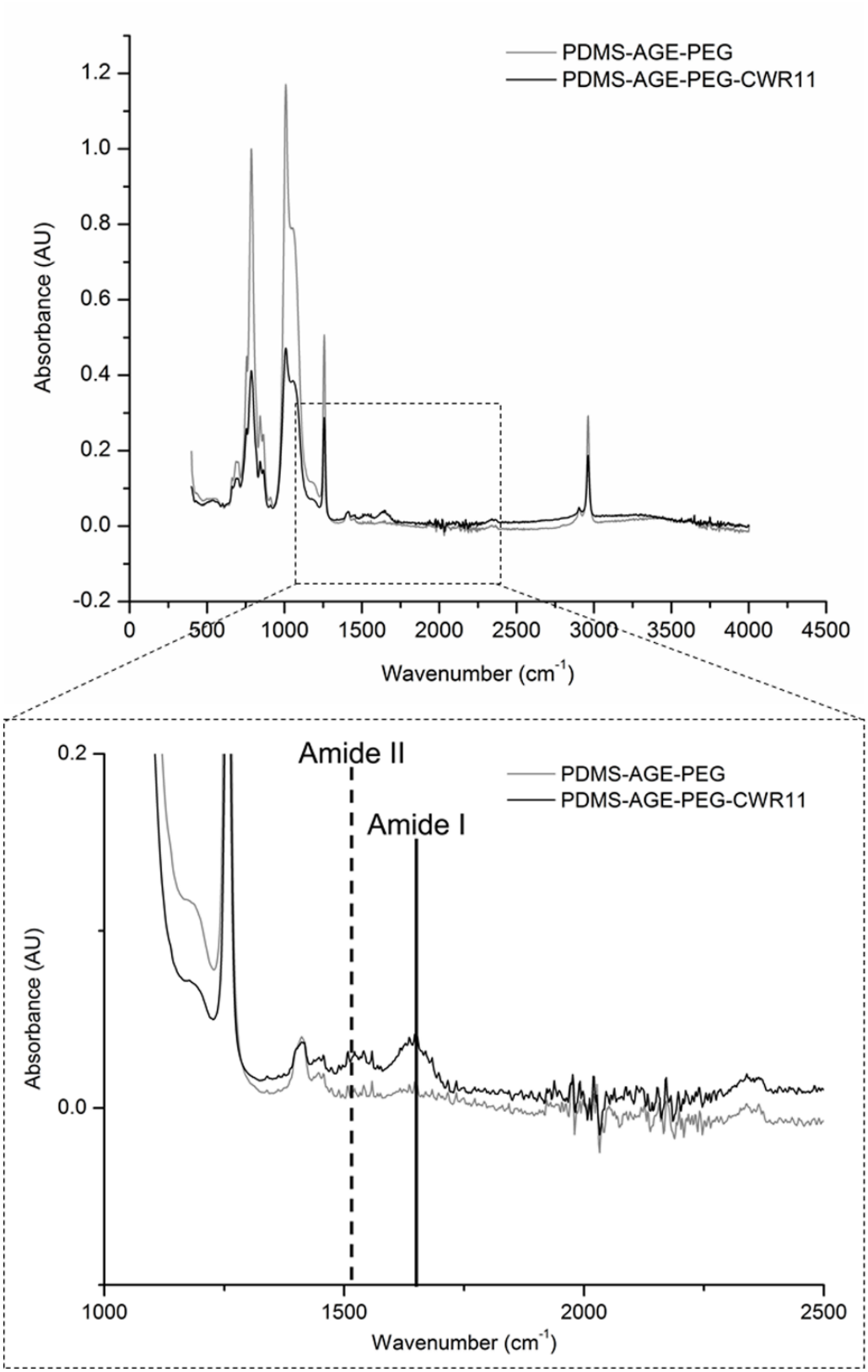

Figure 3.6. ATR-FTIR spectrum for determination of amide bonds in PDMS-AGE-PEG (grey) and PDMS-AGE-PEG-CWR11 (black) slides.

XPS analysis is a highly sensitive tool to determine atomic percentages of elements on surfaces [185]. Measurement of nitrogen atomic percentages could provide qualitative and quantitative indications of the success of PEG and peptide attachment to the PDMS surfaces. The XPS spectrum indicates the appearance of peaks at 400 eV (representative of nitrogen atoms) for both PDMS-AGE-PEG and PDMS-AGE-PEG-CWR11 samples (Figure 3.7), albeit at different intensity. The N1s peak for PDMS-AGE-PEG corresponded to 1.1% atomic N content while that in PDMS-AGE-PEG-CWR11 corresponded to 6.1%. XPS analysis of PDMS-AGE-PEG confirmed the presence of nitrogen, which originated from the amine derived from the PEG chain. Upon immobilization of CWR11, the nitrogen content increased due to the relatively higher amounts of the amine groups present in the peptide, contributed mainly by arginine residues.

(A)

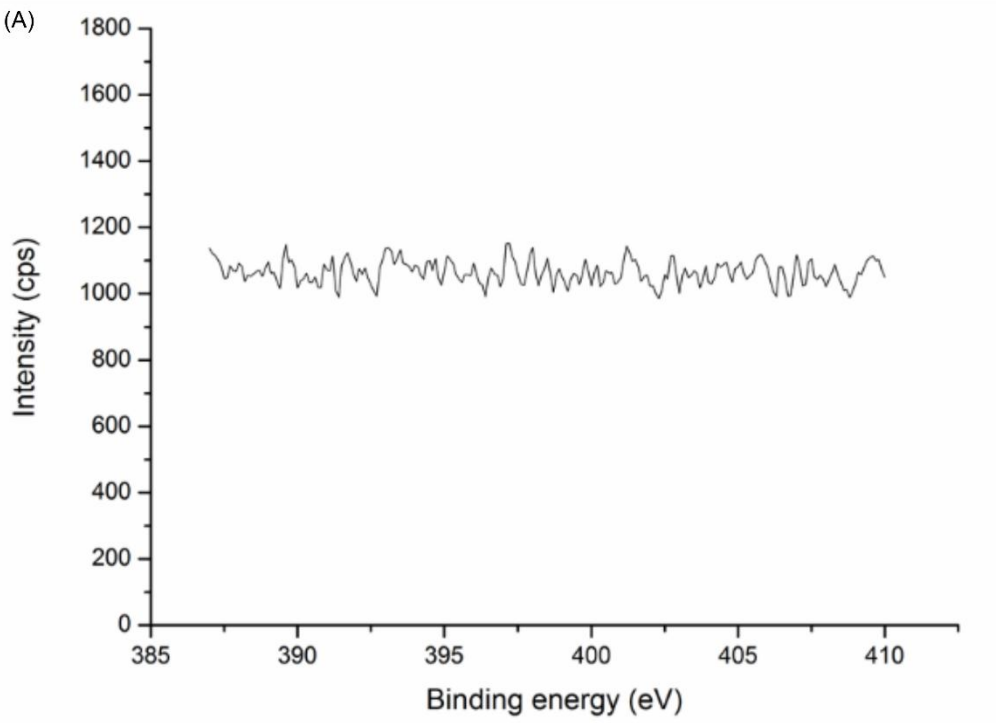
Intensity (cps)
1800
1600
1400
1200
1000
800
600
400
200
0
385
390
395
400
405
410
Binding energy (eV)

(B)

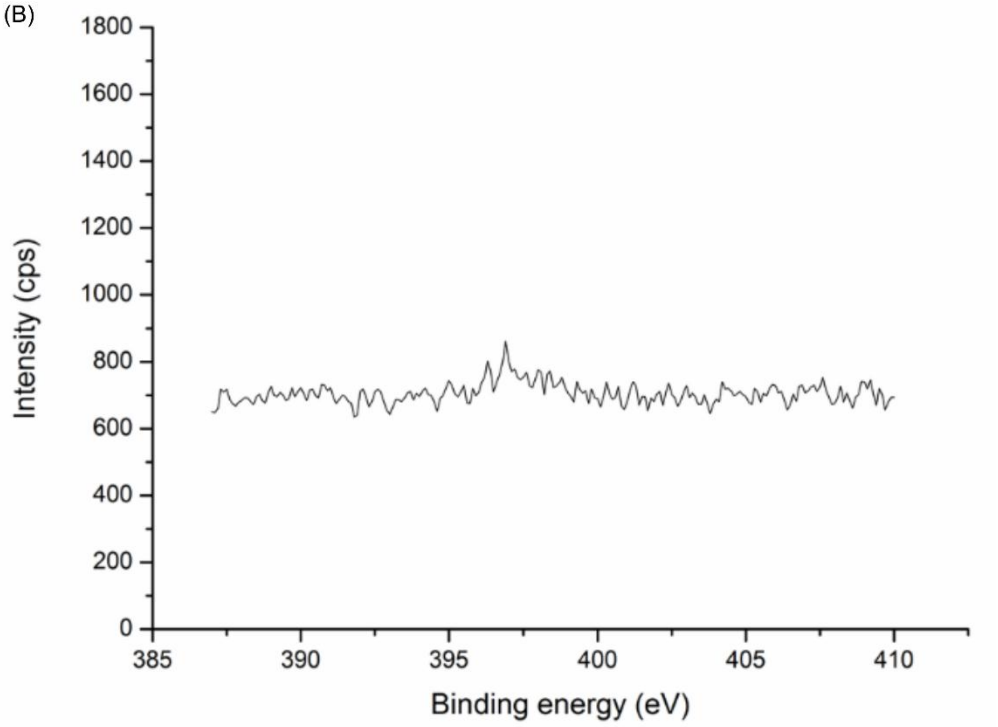
Intensity (cps)
1800
1600
1400
1200
1000
800
600
400
200
0
385
390
395
400
405
410
Binding energy (eV)

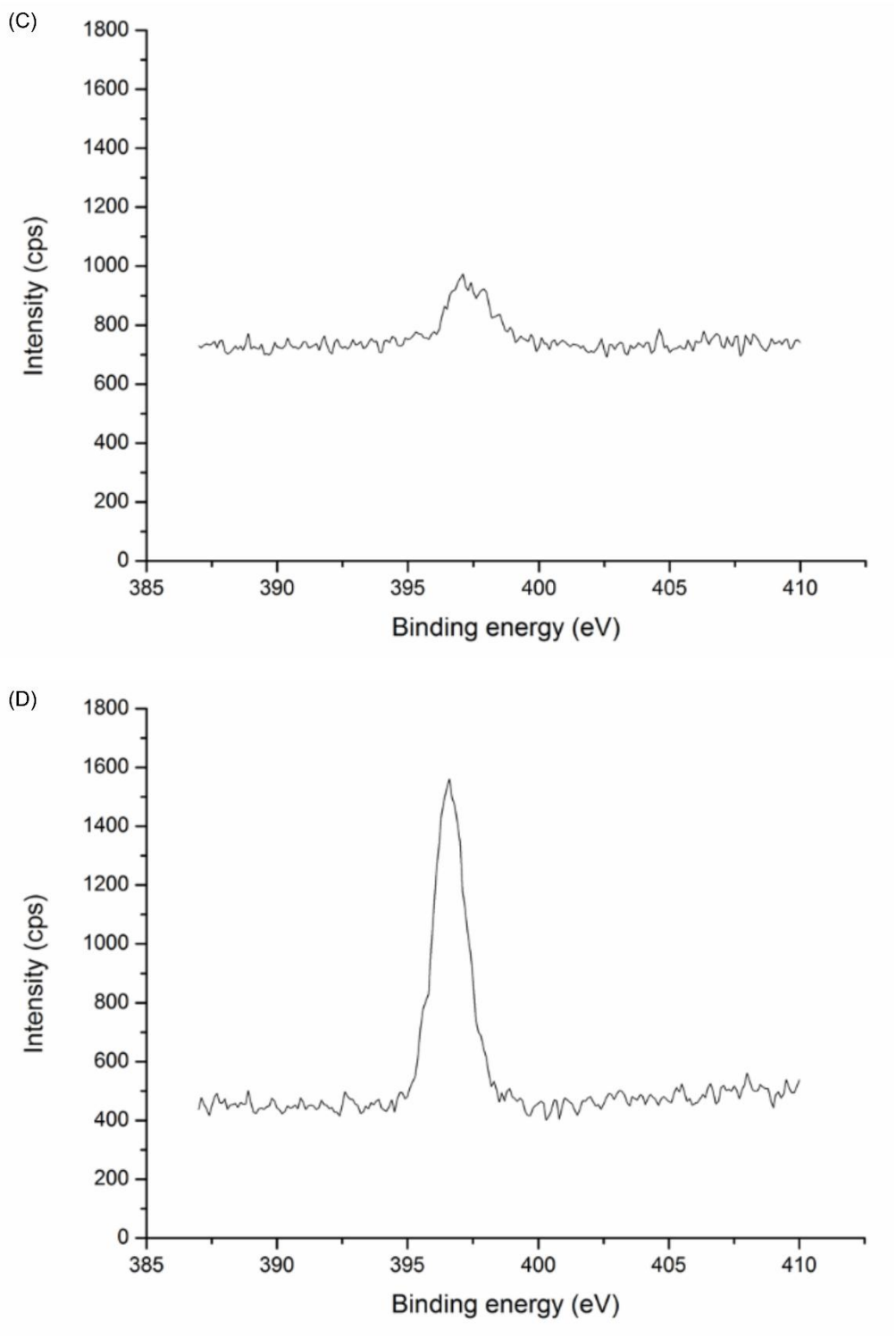

Figure 3.7. XPS analysis of PDMS samples at different tethering stages. High-resolution XPS spectra of N1s region for PDMS (A), PDMS-AGE (B), PDMS-AGE-PEG (C) and PDMS-AGE-PEG-CWR11 (D).

EDS was employed to further confirm peptide immobilization by sulfur content measurement. Based on the library from the Analysis Station software, a peak specific to sulfur was identified for the sample, which was absent for the other control samples, i.e. PDMS, PDMS-AGE and PDMS-AGE-PEG slides (data not shown). A quantification analysis of the sulfur atomic percentage indicates that ~1.1% of sulfur was present on PDMS-AGE-PEG-CWR11 (Table 3.6).

Table 3.6. EDX analysis of sulfur percentage on PDMS-AGE-PEG-CWR11 slides.

	Sulfur atomic composition (%)
PDMS	0.00 ± 0.00
PDMS-AGE	0.00 ± 0.00
PDMS-AGE-PEG	0.00 ± 0.00
PDMS-AGE-PEG-CWR11	1.05 ± 0.25

Sulfo-SDTB was used to quantify the amount of free amine groups on the peptide-immobilized PDMS surface. Under acidic condition, 4,4-o-dimethoxytrityl ions would be released from the surface-bound sulfo-SDTB, which is determined by absorbance measurement at 498 nm [211]. Using this method, an immobilized peptide concentration of 0.8 ± 0.2 μg of CWR11 per cm^2 of PDMS slides was verified. This concentration agrees well with other AMP immobilization studies reported using different coupling strategies [153, 212]. In comparison with conventional grafting methods, which requires large amount of different chemicals and complex reaction steps [204, 209], this platform provides a simpler avenue for site-specific immobilization of peptides that involves 3 simple reaction steps,

while yielding similar peptide grafting efficiency. With the use of a simple heterobifunctional PEG spacer, it enables the direct immobilization of cysteine-terminated peptides onto AGE polymer brushes, bypassing cumbersome chemical modification steps.

3.2.5. Antimicrobial activity determination of CWR11-immobilized PDMS

The antimicrobial property of the peptide-immobilized PDMS slides was quantitatively assessed *via* a protocol adapted from ISO 22961 [213]. Table 3.7 shows that no viable bacterial colony was observed on the agar plate, highlighting the bactericidal potency of peptide-immobilized PDMS slides. Absorbance measurement of the peptide-immobilized surface treated bacterial inoculum showed corresponding results. The CWR11-immobilized slides inhibited bacteria growth (99.9% inhibition) while the control (PDMS-AGE-PEG) slide supported bacteria growth (Figure 3.8). This confirms that the antimicrobial activity of the peptide was retained upon immobilization. This observation was consistent for all 3 bacterial strains, demonstrating broad spectrum action of the AMP coating.

Table 3.7. Antimicrobial activity of CWR11-immobilized PDMS slides against *E. coli*, *S. aureus* and GFP-*P. aeruginosa*. CFU counts after incubating 10^6 CFU/mL of respective bacterial suspension with PDMS-AGE-PEG-CWR11 slides.

E. coli		***S. aureus***		***P. aeruginosa***	
CFU count (CFU)	**Inhibition (%)**	**CFU Count (CFU)**	**Inhibition (%)**	**CFU Count (CFU)**	**Inhibition (%)**
0 ± 0	99.9 ± 0.0	0 ± 0	99.9 ± 0.0	0 ± 0	99.9 ± 0.0

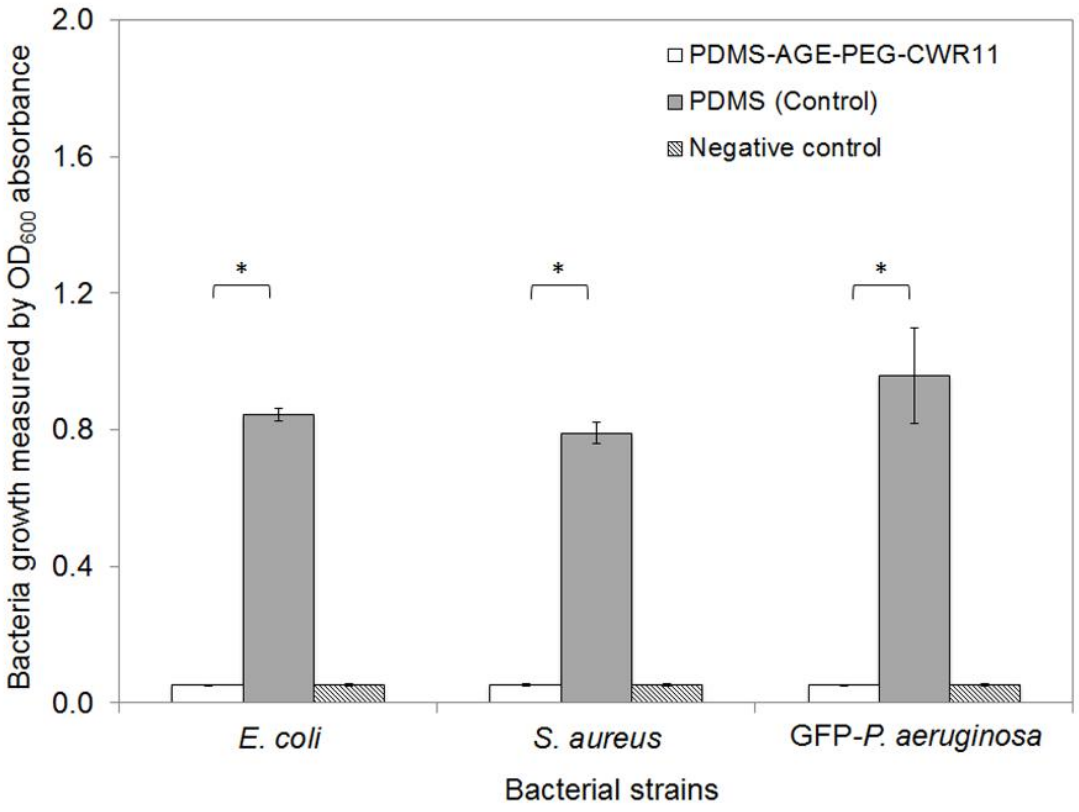

Figure 3.8. Antimicrobial activity of CWR11-immobilized PDMS slides against *E. coli*, *S. aureus* and *P. aeruginosa*. Optical density reading of fresh MH medium after overnight incubation with PDMS slides containing remaining bacterial suspension after performing CFU counts. * indicates $p<0.05$ in comparison to untreated PDMS controls.

3.2.6. Stability of CWR11-immobilized PDMS slides

To investigate the stability of immobilized CWR11, PDMS-AGE-PEG-CWR11 slides were subjected to soft cleaning condition (i.e. overnight immersion in water), followed by surface antimicrobial assay. Figure 3.9 shows the colony counts obtained after immersion of PDMS-AGE-PEG-CWR11 in distilled water, which indicated that the slides retained antimicrobial potency and completely inhibited *E. coli* growth up to at least 3 days. Such stability is crucial, especially if this platform is to be applied onto biomedical devices, used in long term implantation.

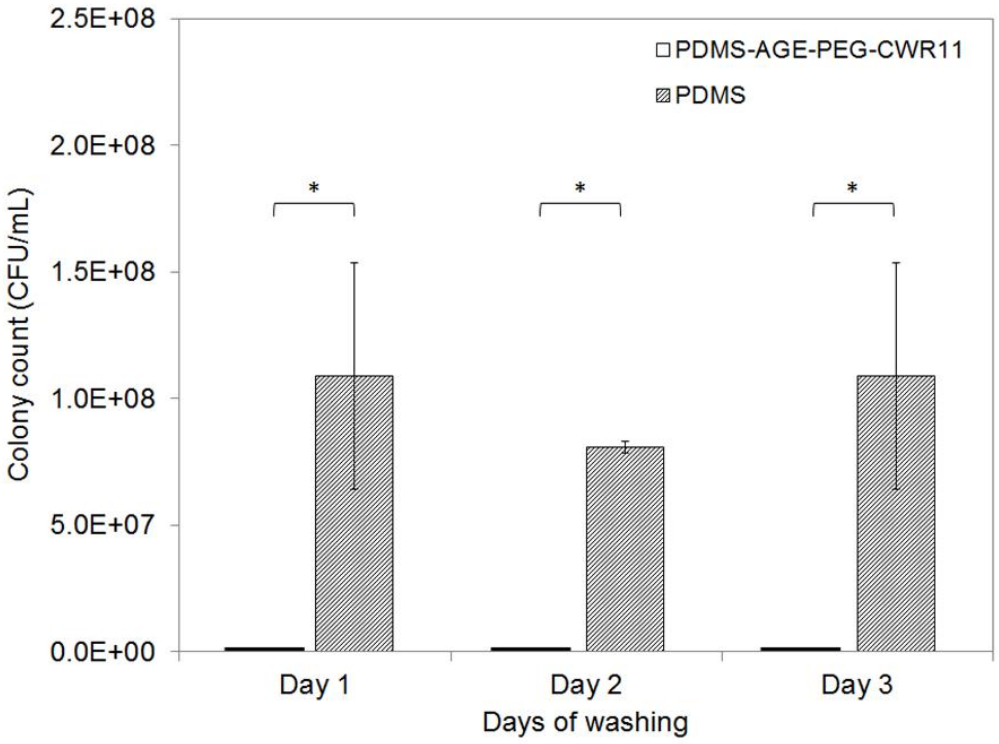

Figure 3.9. The antibacterial activity determination of PDMS-AGE-PEG-CWR11 after immersion in deionised water for 1 to 3 days by CFU count with the respective samples. * indicates $p<0.05$ in comparison to untreated PDMS controls.

3.2.7. Anti-biofilm determination of immobilized CWR11

Biofilm formation is another important aspect of nosocomial infection that needs to be addressed. It is well known that biofilms are difficult to eradicate and play a crucial role in bacteria resistance development [89]. Hence, it is essential that the peptide-immobilized surface should not only be antimicrobial but also anti-biofilm. Using crystal violet staining to determine biofilm formation on surfaces [214], it was observed that the PDMS-AGE-PEG-CWR11 slides showed a much lower crystal violet staining intensity in contrast to the negative control, PDMS (Figure 3.10). An optical density measurement of the crystal violet solution shows a significant reduction in biofilm formation on PDMS-AGE-PEG-CWR11

compared to the control slide (Figure 3.11), which suggests the potent anti-biofilm capability of the peptide-tethered surface.

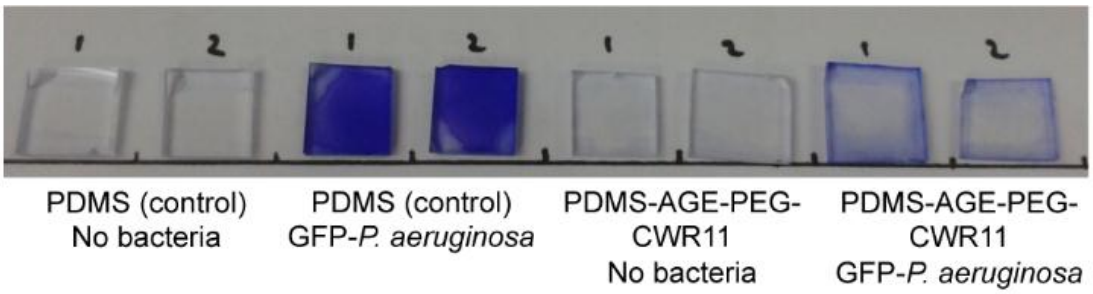

Figure 3.10. Assessment of biofilm formation *via* crystal violet staining. Treated and untreated PDMS samples and controls stained with crystal violet upon incubation with GFP-*P. aeruginosa* for 24 h, to allow substantial biofilm formation.

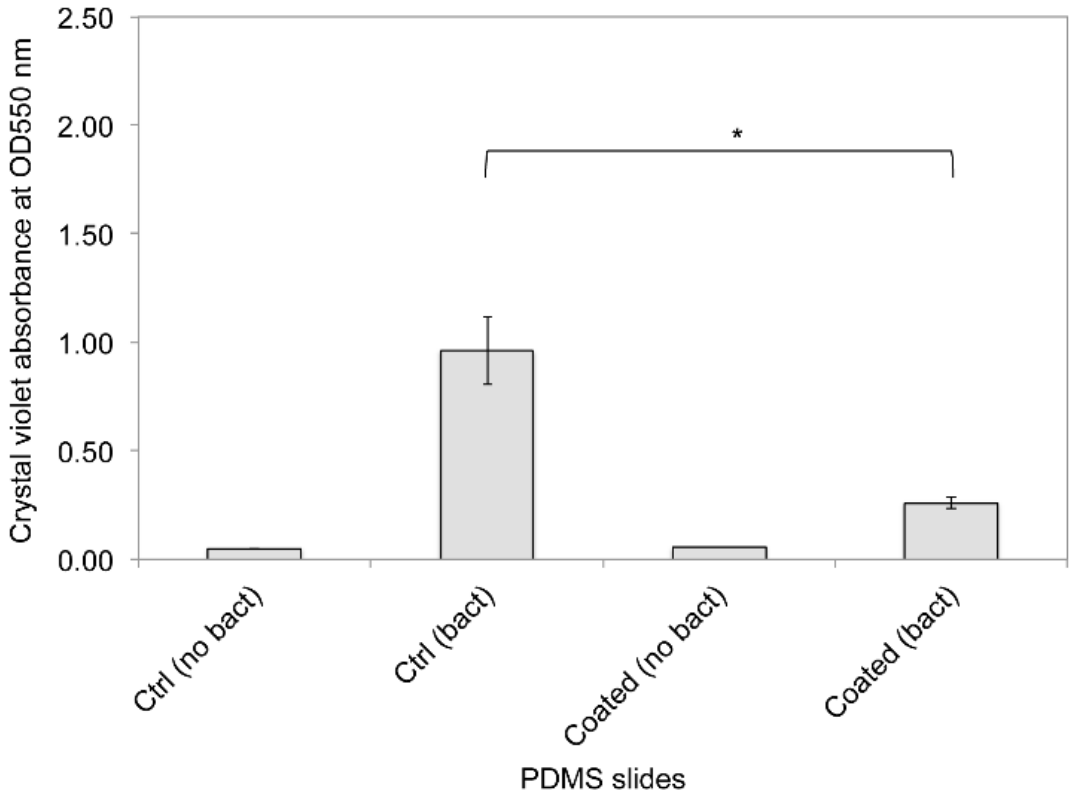

Figure 3.11. Assessment of biofilm formation *via* crystal violet staining. Optical density measurement of the crystal violet solution. * indicates $p<0.05$ in comparison to untreated PDMS controls.

Figure 3.12 shows the confocal microscopy image of *E. coli* biofilm, stained with LIVE/DEAD dyes. The high fluorescence observed on the unmodified PDMS slides indicated that a large number of cells attached on the slide surface. Corresponding PI staining showed that most of the cells are viable, indicating the presence of extensive biofilm on the untreated PDMS surface. Reduced cell attachment was observed for the PDMS-AGE-PEG slides, which is expected, given the anti-adhesion properties of PEG [6]. The PDMS-AGE-PEG-CWR11 slides almost completely eradicated cell attachment, where hardly neither viable nor dead cells could be observed on the slide surface.

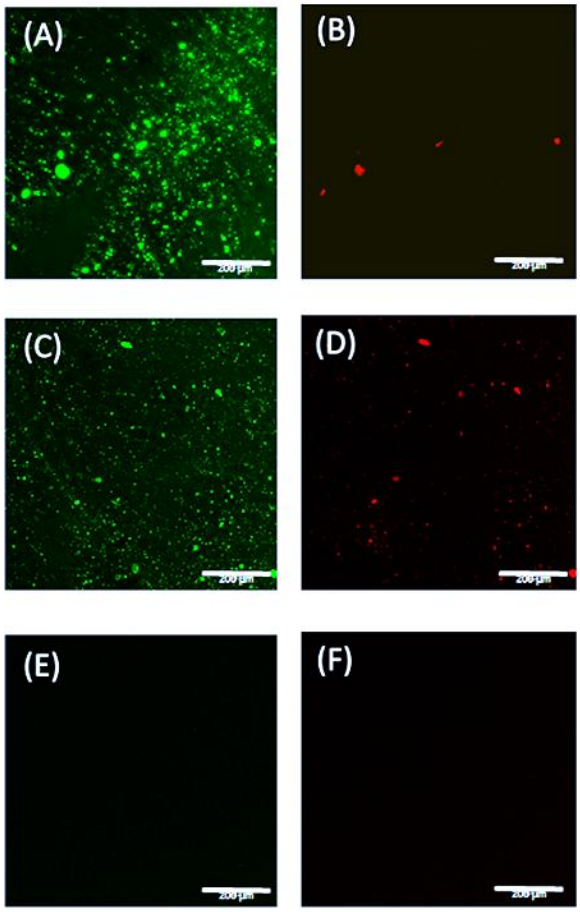

Figure 3.12. *E. coli* biofilm formation after 5 days of growth on CWR11-immobilized and untreated PDMS slides. The biofilms were stained with LIVE/DEAD assay and imaged with confocal laser scanning microscopy. Staining of untreated PDMS slides with Syto 9 (A) and PI (B), PDMS-AGE-PEG slides with Syto 9 (C) and PI (D), and PDMS-AGE-PEG-CWR11 with Syto 9 (E) and PI (F).

Both crystal violet staining and LIVE/DEAD staining results demonstrate that the CWR11-immobilized PDMS slide surfaces did not support bacterial cell attachment, and hence prevented the formation of biofilm. The increase in surface hydrophilicity upon modification of the PDMS surface with PEG spacers and peptides is believed to contribute to the observed anti-biofilm property. Such anti-biofilm property makes the peptide-loaded surface a superior choice compared to other antibiotic loading techniques, which is not

only relatively ineffective in overcoming bacteria biofilm formation [215], but has a high tendency to promote antibiotic resistance development.

3.2.8. Cytotoxicity assay of immobilized CWR11

Cytotoxicity is of utmost importance for biomedical implants. Conventional antimicrobial materials such as silver ions are not widely utilized for surface coating despite its potent bactericidal property, due to its high cytotoxicity at moderate concentration [216]. To determine the cytotoxicity of the peptide-immobilized surface, PDMS-AGE-PEG-CWR11 samples were subjected to hemolytic and MTT assays.

PDMS-AGE-PEG-CWR11 slides incubated in 2.0 mL 5.0% erythrocyte solution showed no statistical difference in hemolytic activity compared to the untreated PDMS control (Figure 3.13). No significant hemolytic activity (~3.0%) was detected from the immobilized peptides after an hour of incubation with red blood cells, which indicated that the amount of peptide impregnated on the PDMS slides were not toxic to red blood cells. This result is comparable to that reported by other biocompatible antimicrobial surfaces [145, 163].

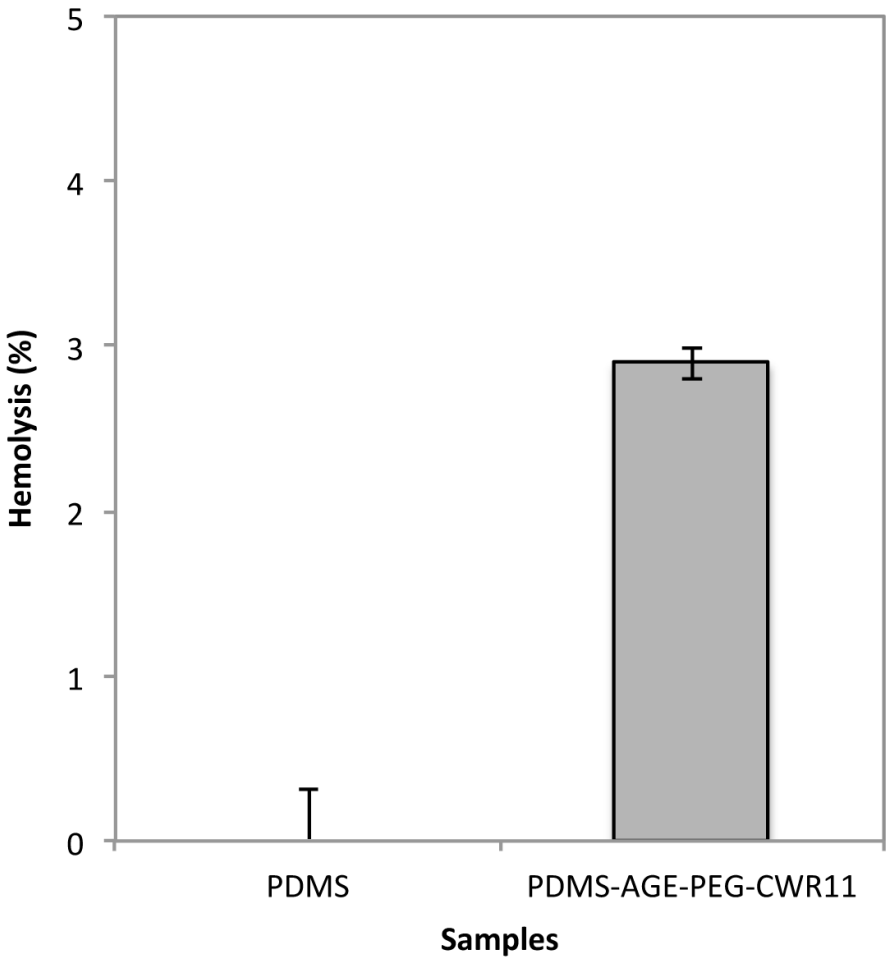

Figure 3.13. Cytotoxicity assay for CWR11-immobilized PDMS slides against hRBCs.

The cytotoxicity of PDMS-AGE-PEG-CWR11 slides against mammalian SMCs was determined using the MTT assay. The peptide-immobilized PDMS slide displayed negligible toxicity to mammalian cells. On incubation with PDMS-AGE-PEG-CWR11 slide, the SMCs continued to grow, as indicated by an increase in MTT absorbance from day 1 to day 7 (Figure 3.14). LIVE/DEAD assay of the mammalian cells exposed to PDMS-AGE-PEG-CWR11 showed that majority of the mammalian cells remained viable up to 7 days of incubation with the slide (Figure 3.15). No statistical difference in MTT absorbance was observed between the untreated PDMS control and the peptide-immobilized slides.

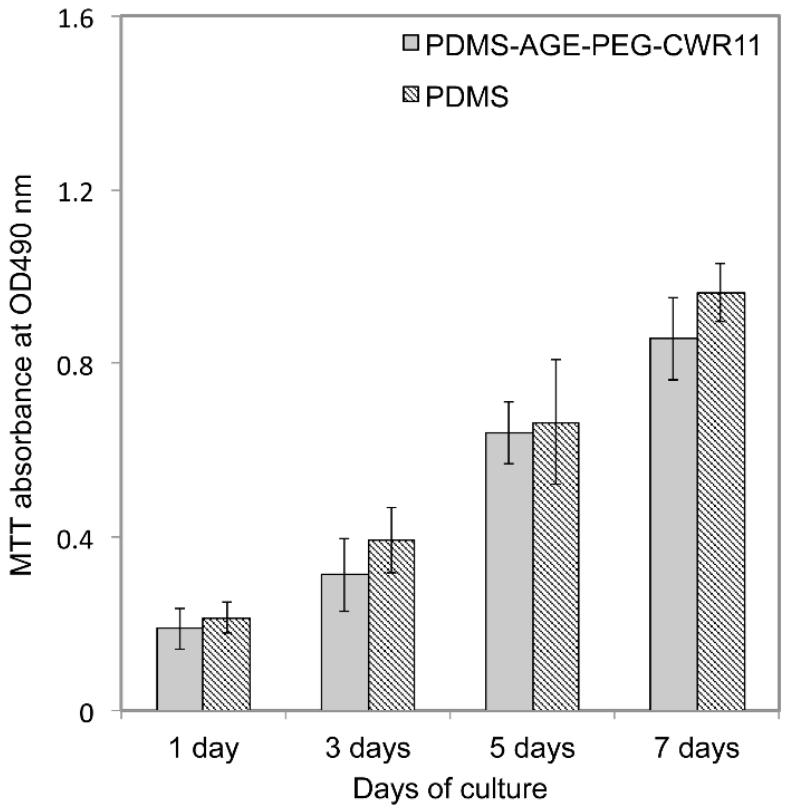

Figure 3.14. Cytotoxicity assay for CWR11-immobilized PDMS slides against mammalian smooth muscle cells.

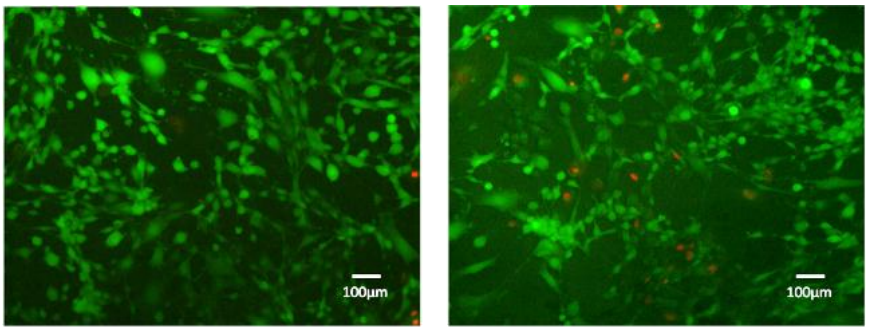

Figure 3.15. LIVE/DEAD staining of mammalian smooth muscle cells incubated with untreated PDMS (above) and peptide -immobilized PDMS samples (below).

The immobilized AMP displayed good selectivity towards prokaryotic cell membrane, with diminished ability to disrupt membranes composed of eukaryotic membrane components. This trend is commonly seen in many AMPs. A possible suggestion for this observation could be due to the difference in the membrane integrity and structure of these two membranes types. The bacterial outer cell membrane (made up of negatively charged phophatidylglycerol) possessed a much higher net negative charge, as compared to mammalian cells (made up of zwitterionic phosphatidylcholine and sphingomyelin), hence, improving electrostatic affinities of AMP towards the former [217]. Additionally, mammalian cell's phospholipid bilayer is well decorated with cholesterol, which acts to stabilize and maintain the membrane integrity. The presence of such membrane-stabilizing agents may interfere with the antimicrobial action of the AMPs, rendering short peptides ineffective in permeabilizing mammalian cell membrane [218].

The CWR11-immobilized slides showed good selectivity toward bacteria cells and not mammalian cells, opening the way for the use of this AMP immobilization platform on biomedical device relevant surface for antimicrobial functionalization.

3.3. Conclusion

In this study, a novel arginine and tryptophan-rich peptide, CWR11, with potent bactericidal properties and salt resistant traits, was successfully engineered. An immobilization platform was developed to tether the peptide onto a PDMS surface using a robust three-step covalent immobilization procedure. Surface characterization assays such as XPS and ATR-FTIR confirmed the viability of the chemical tethering protocol, with strong indications of successful peptide grafting onto the target surface. The peptide-impregnated surface showed potent, wide spectrum antimicrobial and anti-biofilm characteristics,

coupled with excellent biocompatibility properties. These results now open the way for use of engineered CWR11 peptide as a potential implant peptide candidate.

The involvement of plasma and UV treatment makes it difficult, however, to implement such strategy onto both the intraluminal and extraluminal surfaces of urinary catheters. Additionally, prolonged exposure to degradative UV radiation and subjection to multiple reaction steps involving harsh chemicals might have detrimental effect on catheter material, eventually leading to the device failure. Hence, further optimization to the immobilization platform is necessary to improve the efficacy and translatability of the AMP tethering platform, which forms the basis for the work reported in Chapter 4.

Chapter 4 Development of a catheter functionalized by a polydopamine-peptide coating with antimicrobial and anti-biofilm properties[2]

Chapter 3 reports the development of a synthetic AMP, CWR11, with potent broad spectrum antimicrobial activities and relatively high salt resistance, which showed huge potential as an antimicrobial coating candidate for urinary catheters. An immobilization platform was concurrently developed to covalently graft this arginine-, tryptophan-rich peptide onto a model PDMS surface. Although the peptide tethering platform showed good surface antimicrobial activities, there are several drawbacks associated with the AGE polymer brush immobilization strategy. For example, the requirement for surface plasma activation and subsequent UV radiation limits the applicability of the platform to only flat surfaces. Additionally, exposure to strong plasma treatment and prolonged chemical treatments can often compromise material integrity, leading to premature failure of biomedical devices.

This chapter aims to develop an AMP-based coating platform that eliminates the need for complex reaction steps and use of degradative radiation techniques that may lower peptide immobilization efficacy and compromise material integrity. Bioinspired

[2]A version of Chapter 4 has been published. This chapter is adapted and reprinted from "Lim K.Y., Chua RRY, Ho B, Tambyah PA, Hadinoto K, Leong SSJ., 2015, Development of a catheter functionalized by a polydopamine peptide coating with antimicrobial and antibiofilm properties, Acta Biomaterialia;15:127-38", with permission from Elsevier.

polydopamine (PD)-based surface functionalization is an attractive approach that can be easily adopted for AMP grafting. The development of a simple surface functionalization dip-coating technique using mussel-derived dopamine molecules was recently reported [159]. Upon prolonged immersion in nucleophillic buffer, dopamine molecules polymerize to form a thin PD film, decorated with active functional groups (amine and catechol), on substrate surfaces [159, 160]. The reactive catechol groups exposed on the PD coating can form strong chemical bonding with commonly found thiol or amine groups, through simple Michael's addition. These advantages merit the use of a PD coating for AMP immobilization on catheter surfaces, which is investigated in this chapter.

. AMP immobilization was conducted *via* a simple 2-step reaction scheme, (i) surface activation with PD polymerisation and (ii) attachment of CWR11 onto the PD-activated polymer surface. The resulting peptide-grafted PDMS surface demonstrated excellent antimicrobial and anti-biofilm properties. Upon translation onto urinary catheter surfaces, the AMP-coated catheter surface exhibited good bactericidal potency, comparable to commercial Dover silver coated catheters. The stability of the CWR11 coating was also verified under varying aqueous environments, over extended time periods. The findings of this chapter have been published in *Acta Biomaterialia* [8].

4.1. Materials and Methods

4.1.1. Materials

Synthetic peptides and chemicals were purchased from local and international vendors as per detailed in Chapter 3 (Section 3.1.1). *E. coli*, GFP-*P. aeruginosa* and *S. aureus* were used for surface antimicrobial and anti-biofilm assays. Additionally, Dover silver-

coated catheters were purchased from Covidien Private Limited (Singapore), and used as positive control for catheter antimicrobial assay.

4.1.2. Synthesis of CWR11-tethered PDMS slides

4.1.2.1. Synthesis of Polydimethylsiloxane (PDMS) slides

1.0 cm^2 square PDMS slides, for subsequent peptide immobilization, were synthesized using the same method as described in Section 3.1.6.1.

4.1.2.2. Coating of PDMS slides with polydopamine (PD)

A layer of PD was coated on a PDMS slide. Each PDMS slide was immersed in 1.0 mL of dopamine solution (5.0 mg/mL, in 50 mM Tris-HCl, pH 8.8), and the polymerization reaction allowed to occur for 72 h at 25^{o}C. The PD-coated slides were rinsed in copious amount of deionized water to remove any unattached dopamine molecules.

4.1.2.3. Immobilization of CWR11

CWR11 was attached onto the PD-coated PDMS slides (PDMS-PD). The PD-coated slides were immersed in CWR11 peptide solution (2.0 mg/mL in 50 mM Tris buffer, pH 8.8) for 72 h at 25^{o}C. The peptide-immobilized slides (PDMS-PD-CWR11) were washed with copious amount of water to remove any unbounded AMP.

CWR11 contains numerous tryptophan amino acid residues, which absorb strongly at 280 nm. Peptide concentration was quantified using the OD_{600} absorbance measurement, based on an empirical formula (Equation 3.1) developed by *Pace* et al. [181], as detailed in Section 3.1.2.

The absorbance of the CWR11 peptide solution before and after surface immobilization was measured at 280 nm using Nanodrop 2000c (Thermo Scientific, USA). The immobilized peptide concentration was estimated by subtracting the quantity of CWR11 in the AMP solution after immobilization from that before.

4.1.3. Surface characterization of PDMS-PD-CWR11

4.1.3.1. Contact angle measurement

Surface wettability property of PDMS-PD-CWR11 and control slides (PDMS and PDMS-PD) was determined using static contact angle measurement, as described in Section 3.1.7.1.

4.1.3.2. Atomic Force Microscopy (AFM)

Surface morphology and roughness of the PDMS samples (i.e. PDMS, PDMS-PD and PDMS-PD-CWR11) were analyzed using atomic force microscopy (AFM) (Asylum Research, Santa Barbara, CA). A monolithic silicon non-contact high resonance frequency cantilever (NCST type, Nanoworld, Switzerland) was employed to image surface morphology during non-contact tapping mode. Scan rates were set at 1 Hz with data resolution of 256 pixels x 256 pixels. Area of scanning per sample was fixed at 1.5 µm x 1.5 µm. Surface morphology imaging and roughness analysis were conducted using the Igor Pro MFP-3D software.

4.1.3.3. Attenuated total reflectance fourier transform infrared (ATR-FTIR) spectroscopy

The presence of amide bonds on PDMS-PD-CWR11 and control PDMS-PD surfaces was verified using ATR-FTIR spectroscopy as described in Section 3.1.7.4.

4.1.3.4. X-ray photoelectron spectroscopy (XPS)

Survey and high resolution surface elemental scanning and quantification was analyzed by XPS using a Thermo Scientific Theta Probe. Methodology of XPS scanning was similar to that described in Section 3.1.7.2.

4.1.4. Surface antimicrobial activity and bacterial attachment assays

4.1.4.1. Surface antimicrobial activity of PDMS-PD-CWR11 slides

The surface antimicrobial activity of the PDMS-PD-CWR11 slides against three target uropathogens were assayed using an established protocol [180], as described in Section 3.1.8.

4.1.4.2. Bacterial attachment assay on peptide-immobilized PDMS slides

Anti-biofilm property of the PDMS-PD-CWR11 surface was determined using a reported bacteria adherent protocol [219], identical to that detailed in Section 3.1.10.1. Confocal microscopy (FV1200, Olympus, Japan) and fluorescence spectroscopy (Infinite 200, Tecan, Switzerland) was conducted to qualitatively and quantitatively determine the degree of bacteria attachment on the respective surfaces.

Biofilm or bacterial growth of GFP-*P. aeruginosa* strain on PDMS slides was processed and viewed under a scanning electron microscope (JEOL, JSM 5600LV). Briefly, PDMS slides were incubated with GFP-*P. aeruginosa* (1×10^6 CFU/mL) in BPM for 24 h at 37°C. The slides were washed once with PBS to remove loosely adherent bacteria and fixed in 2 % glutaraldehyde overnight at 4°C. After fixation, the slides were treated with Osmium (OsO_4) for 30 min and washed 2 times (5 min each) with PBS. The slides were dehydrated through an ethanol series of 25 % - 50 % - 75 % - 95 % (each for 15 min) and 3 changes

of 100 % ethanol, each for 20 min, followed by critical point drying with CO_2 (Balzers critical point dryer, CPD 030). The slides were then coated with gold (BAL-TEC sputter coater) and kept in a 40°C oven before viewing.

4.1.5. CWR11 immobilization on silicone Foley catheter

Silicone Elastomer-coated Foley catheters (123616A, Bard, Covington, GA, USA) were cut into small segments of 1.0 cm in length (outer diameter = 0.6 cm; inner diameter = 0.2 cm) for peptide immobilization studies. CWR11 was immobilized onto the catheter surface using a similar protocol as described in Section 4.1.2, with minor adaptations. Briefly, the catheter samples were immersed in dopamine solution (5.0 mg/mL, in 50 mM Tris-HCl buffer, pH 8.8), for 72 h at 25^{o}C. The PD-coated catheters (Cat-PD) were rinsed thoroughly with deionized water and then immersed in a solution of CWR11 (2.0 mg/mL in 50 mM Tris-HCl buffer, pH 8.8) for 72 h at 25^{o}C. The peptide-immobilized catheters (Cat-PD-CWR11) were subsequently washed thoroughly with deionized water, dried in a nitrogen stream.

4.1.6. Surface antimicrobial and stability assays for CWR11-immobilized catheter samples

4.1.6.1. Catheter surface antimicrobial assay

CWR11-immobilized and respective control catheters were subjected to surface antimicrobial assay, as described in Section 3.1.8 and 4.1.4.1, with minor adaptation. Briefly, overnight *E. coli* culture was sub-cultured in fresh MH medium for 3 h to reach mid-log phase and appropriately diluted to a final concentration of 1 x 10^6 CFU/mL. 50.0 µL of bacteria suspension was injected into the intraluminal section of the catheter samples, and incubated at 25^{o}C for 3 h. After incubation, 10.0 µL of the inoculant was withdrawn for

colony forming unit (CFU) counting, while the remaining bacterial suspension, along with the catheter sample, was immersed in fresh medium and incubated overnight (37^{o}C, 16 – 20 h) for optical density measurement. The protocol was repeated in triplicate for *E. coli*, *S. aureus* and GFP-*P. aeruginosa*.

4.1.6.2. Catheter stability assay

To assess the long-term stability of the peptide-immobilized catheters, a leaching assay [180, 220], as described in Section 3.1.9, was conducted. Briefly, the Cat-PD-CWR11 samples were immersed in deionized water for 1, 3, 7, 14, 21 and 30 days and subjected to antimicrobial assay (Section 4.1.6.1). The effect of different aqueous environments on the antimicrobial performance of Cat-PD-CWR11 was also studied. The catheter samples were incubated in deionized water, PBS, air, synthetic urine (Surine) and urine for 3 days, and subjected to antimicrobial assay, as described in Section 4.1.6.1. Urine and Surine samples were analyzed and specifications are shown in Table 4.1.

Table 4.1. pH, albumin content and osmolarity of urine and synthetic urine samples.

	Urine	**Surine**
pH	6.2	8.2
Albumin content (mg/L)	<5.0	<5.0

4.1.7. Cytotoxicity assay

4.1.7.1. Cell viability assay using MTT

The PDMS-PD-CWR11 samples were also tested for their biocompatibility and toxicity to 3T3 fibroblast and SV-HUC-1 uroepithelial cells, as described in Section 3.1.11.2, with minor adjustments to the reported protocol. 3T3 cells were cultured in DMEM supplemented with 5% fetal bovine serum (Hyclone) while SV-HUC-1 cells were cultured in F-12K medium (Sigma) supplemented with 10% fetal bovine serum (Hyclone). Cells, at a concentration of ~5×10^4/well for 3T3 cells and 4×10^5/well for SV-HUC-1, were seeded in a 24-well plate and incubated at 37°C in a humidified atmosphere of 5% CO_2 overnight (~16 h) before PDMS samples (1 cm × 1 cm) were introduced. PDMS samples were added such that the PDMS-PD-CWR11 surfaces were at close proximity, but not pressed together, to the respective cells. The cultures were incubated for 24 h, after which the PDMS slides were removed and adhering cells were washed once with PBS, followed by addition of 1× MTT reagent (0.5 mg/mL, 500 µL) and incubated at 37 °C for 1 h. The MTT reagent was then removed, and the cells were washed once with PBS, followed by cell lysis with 100% DMSO (500 µL). Violet formazan crystals were allowed to dissolve in DMSO, with gentle agitation on a rocker for 30 min. Optical absorbance of the samples was measured at 570nm.

In addition, live/dead staining of SV-HUC-1 cells was carried out. Briefly, the cells were labeled with green fluorescent CFSE dye (Molecular Probes) before treatment with the respective PDMS samples. The cells were then washed with PBS and incubated with 1 µg/mL propidium iodide (PI) in F-12K medium, at 37 °C for 15 min. Subsequently, the cells were washed 5× with PBS, fixed at -20°C with methanol for 4 min and kept in PBS, 4°C, before viewing under confocal microscopy (Olympus FV1000).

4.1.7.2. Hemocompatibility assay

The hemolytic activities of the PDMS-PD-CWR11 and Cat-PD-CWR11 samples against erythrocyte cells were studied *via* a method established by *Shai* et al. [221], as described in Section 3.1.11.1.

4.1.8. Statistical analysis

All experiments were conducted in triplicate, with average and standard deviation calculated for all measurements. Statistical analysis was conducted using the SPSS software (Mac, version 21, IBM, Rochester NY, USA), as described in Section 3.1.12.

4.2. Results and discussion

4.2.1. Synthesis of CWR11-immobilized PDMS surface

Synthetic AMP, CWR11, which has potent and broad spectrum antimicrobial activity [180], was used as the model peptide in this study. CWR11 retained its bactericidal property upon attachment to the PDMS surface, thus fulfilling an important pre-requisite as a coating agent. This chapter reports the studies performed to develop a simple and readily scalable 2-step dip-coating method for CWR11 immobilization onto PDMS substrate surface, and subsequently Foley urinary catheter, with the overall aim to develop a CWR11-based antimicrobial coating for silicone catheters, which involves a simple and scalable synthesis platform.

Figure 4.1A shows the schematic of the peptide immobilization chemistry. The PDMS slide was coated with a thin layer of PD, achieved by dip coating in an alkaline dopamine solution. A thin film of CWR11 was then bound to the PD-coated surface upon incubation of the samples with the peptide solution. Representative slides of untreated PDMS, PDMS-PD and PDMS-PD-CWR11 samples are shown in Figure 4.1C. A characteristic brown coloration observed on the PDMS-PD sample suggested complete polymerization of dopamine molecules onto the polymer surface [222].

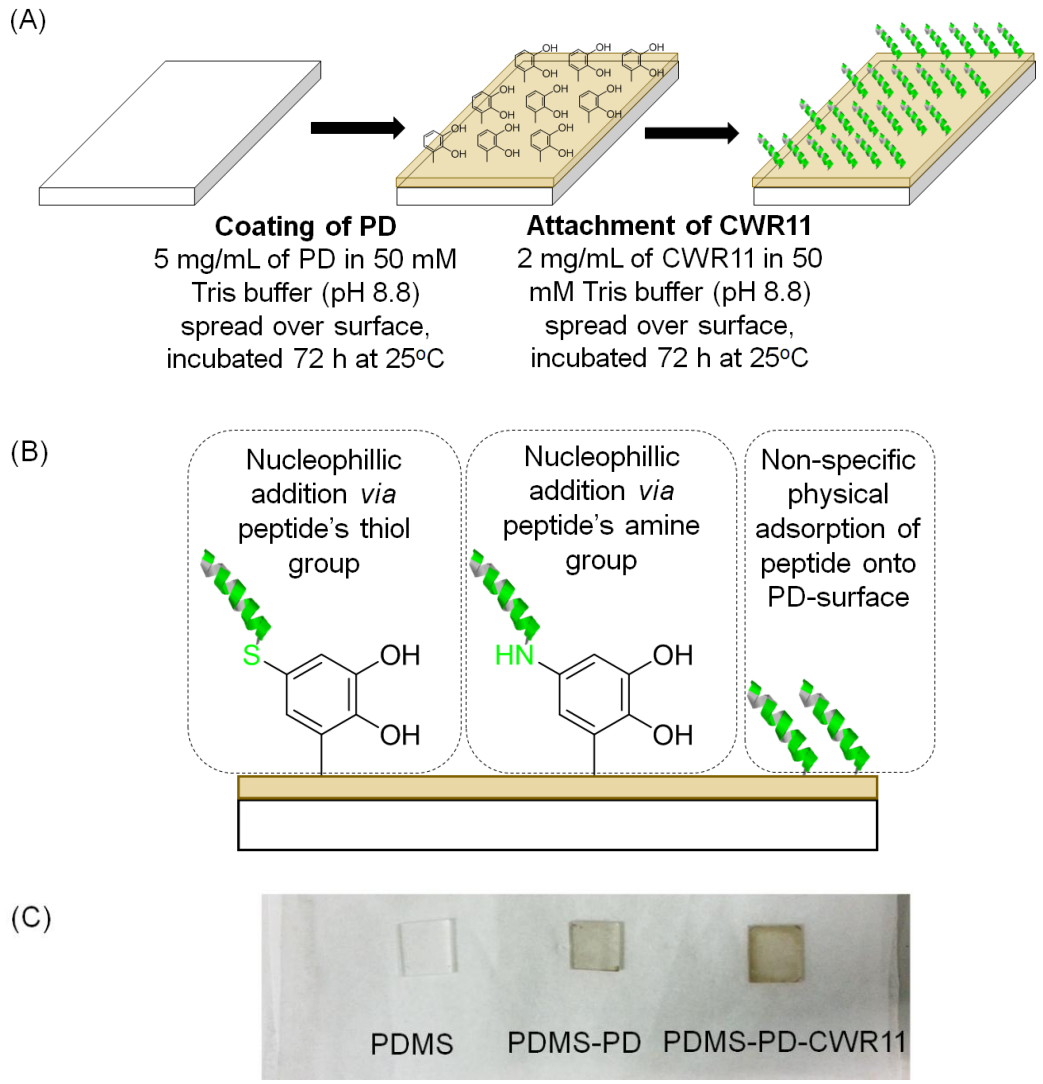

Figure 4.1. (A) Schematic of CWR11 tethering process on a PDMS surface. The PDMS substrate was first functionalized with a layer of polydopamine, followed by CWR11 attachment. (B) AMPs were attached to the surface *via* Michael addition / Schiff base reaction of the CWR11's inherent thiol (left) or/and amine group (middle) with exposed catechol functionalities and physical adsorption (right). (C) PDMS samples at different stages of the 2-step immobilization process.

Due to its robust chemistry, PD-mediated surface coating method has been widely utilized in a variety of applications such as stem cell engineering [160, 223], protein immobilization [224], DNA microarrays [225] and water membrane technologies [226].

Dopamine, a small molecule consisting of catechol and amine functionalities, polymerizes under mild alkaline condition to form a thin adherent film of PD on any type of organic or inorganic materials [159, 160, 227]. In an oxidising environment, the dopamine-hydrochloride molecules undergo covalent-oxidative polymerization and physical self-assembly of dopamine and its oxidative product, 5,6-dihydroxyindole (DHI), to form the PD layer. With increased exposure to alkaline conditions, the reaction equilibrium is shifted towards the covalent oxidative polymerization reaction, disrupting the self-assembled $(Dopamine)_2$/DHI physical trimer to form more Dopamine-DHI-DHI trimeric conjugate [227]. The co-existence of catechol and amine groups on the trimeric conjugate allows it to adhere to surfaces *via* multiple covalent bond formation [228, 229]. The brown precipitate observed on the PDMS-PD surface (Figure 4.1C) is attributed to the combined effect of covalent bond-forming oxidation reaction and oxidized product adherence to the PDMS surface. Moreover, due to the nature of dopamine molecule and manner of polymerization, catechol moieties are abundantly exposed on the PD coating. These catechol groups are oxidized to reactive o-quinone functional groups under alkaline condition, which offer convenient sites for covalent grafting of nucleophilic biomolecules *via* Michael addition and/or Schiff base reaction [159].

Despite the known capacity of PD coating to effectively immobilize bioactive molecules, the use of PD-functionalized polymer surfaces for AMP attachment remains relatively unexplored. In this study, we demonstrated a facile PD-based strategy for efficient immobilization of CWR11 onto inert silicon-based polymer, which imparts the target substrate surface with potent bactericidal properties.

The PDMS substrate surface was first functionalized with a thin layer of PD. Following PD coating, the samples were exposed to a concentrated CWR11 peptide solution, under oxidizing condition, for attachment of the AMP, *via* both covalent and physical adsorption

means [159] (Figure 4.1B). The abundance of reactive o-quinone groups and the hydrophilic nature of the PD film surface present an ideal platform for covalent and/or non-covalent CWR11 attachment [230-233].

4.2.2. PDMS-PD-CWR11 surface characterization

Changes in surface wettability of the PD-AMP-functionalized PDMS slides were assessed by water contact angle measurements [160]. PDMS is inherently hydrophobic, with a high contact angle of 104.0 ± 1.2^{o} (Figure 4.2A) [234]. Functionalization of PDMS with PD greatly enhanced the hydrophilicity of the polymer, decreasing the contact angle to 66.7 ± 2.5^{o}. Peptide immobilization did not significantly alter the contact angle of the PDMS-PD surface. A drastic enhancement in surface hydrophilicity was observed upon functionalizing the PDMS surface with PD, which is attributed to the presence of polar catechol and amine functional groups on the coating. The improvement in wettability of hydrophobic surfaces by PD coating is a well-established observation [160, 235]. Subsequent CWR11 immobilization did not significantly alter the contact angle. This behavior agrees with observations reported in previous studies that involved the grafting of growth factors and peptides onto PD-coated polystyrene (PS) and poly(lactic-co-glycolic acid) (PLGA) surfaces [160].

The surface morphology and roughness of PDMS, PDMS-PD and PDMS-PD-CWR11 samples were analyzed by AFM. The unmodified PDMS substrate possessed a smooth morphology (Figure 4.2B), with surface roughness of 521.7 ± 413.5 pm. PD polymerization on PDMS surface increased the surface roughness to 1.0 ± 0.8 nm. Attachment of CWR11 peptides onto the PD-coated surface further increased the surface roughness to 2.6 ± 2.0 nm. The sharp increment in surface roughness (by 2 nm) further verified peptide attachment.

To verify that the peptides were attached to the PD-functionalized polymer surface, ATR-FTIR analysis of the PDMS-PD-CWR11 samples was conducted to confirm the presence of amide bonds. Distinct peaks were observed at 1533 cm^{-1} and 1645 cm^{-1}, which are representative of amide I and II bands [210], respectively (Figure 4.2C). These characteristic peaks were absent in the PDMS-PD control samples.

(A)

	Contact angle (°)
PDMS	104.0 ± 1.2
PDMS-PD	66.7 ± 2.5
PDMS-PD-CWR11	62.3 ± 4.4

(B)

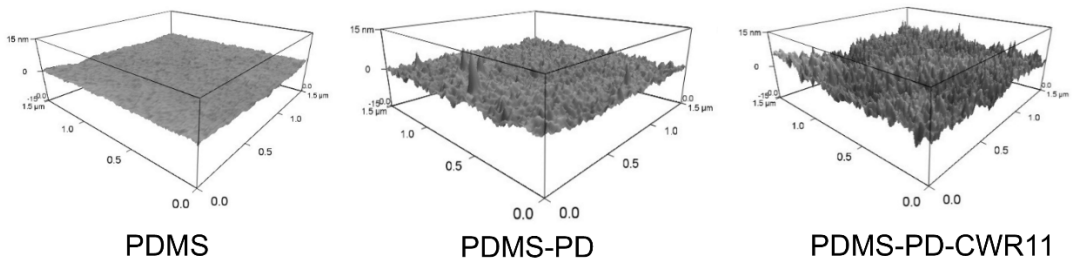

(C)

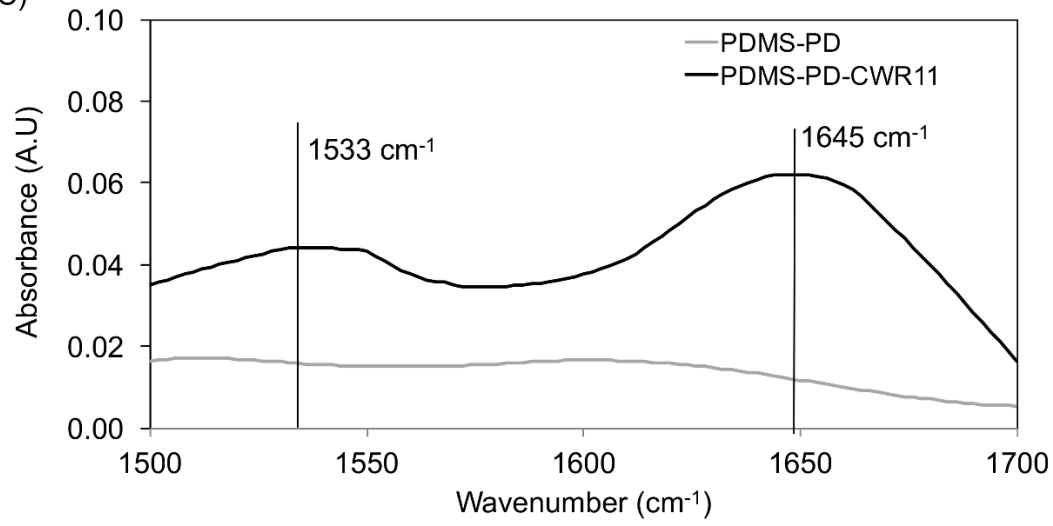

Figure 4.2. Surface characterization of PDMS-PD-CWR11 slides. (A) Contact angle measurements of deionized water on CWR11-immobilized and control PDMS surfaces. (B) AFM analysis of unmodified (left), PD-coated (middle) and CWR11-immobilized PDMS substrates. (C) ATR-FTIR spectrum for PDMS-PD-CWR11 (black) and PDMS-PD (grey) samples.

Surface elemental composition was investigated using XPS (Figure 4.3). The spectra revealed an increase in nitrogen/carbon (N/C) ratio for PDMS-PD sample (0.04 ± 0.00) compared to the unmodified PDMS (0.00 ± 0.00), which is attributed to the presence of amine group in the dopamine molecule [159]. A further increment in N/C ratio (0.13 ± 0.01) was observed with the immobilization of CWR11, which is due to the presence of multiple arginine amino acids in the peptide sequence. A high resolution XPS surface scan conducted for the samples showed that a small amount of sulfur was detected only on the PDMS-PD-CWR11 sample surface (Figure 4.3B). Analysis of the spectrum revealed a doublet at 163 eV, corresponding to carbon-linked sulfur group. The sulfur originated from the thiol group, derived from N-terminal cysteine residue of the peptide, which was attached to the PD-treated surface. This further confirmed the successful attachment of CWR11 onto the PD-modified PDMS surface. An additional doublet at binding energy of 168 eV, caused by oxidized sulfur species, was also present [236]. The alkaline Tris medium provides an oxidizing environment in which some of the thiol groups were oxidized, hence accounting for the peak at 168 eV.

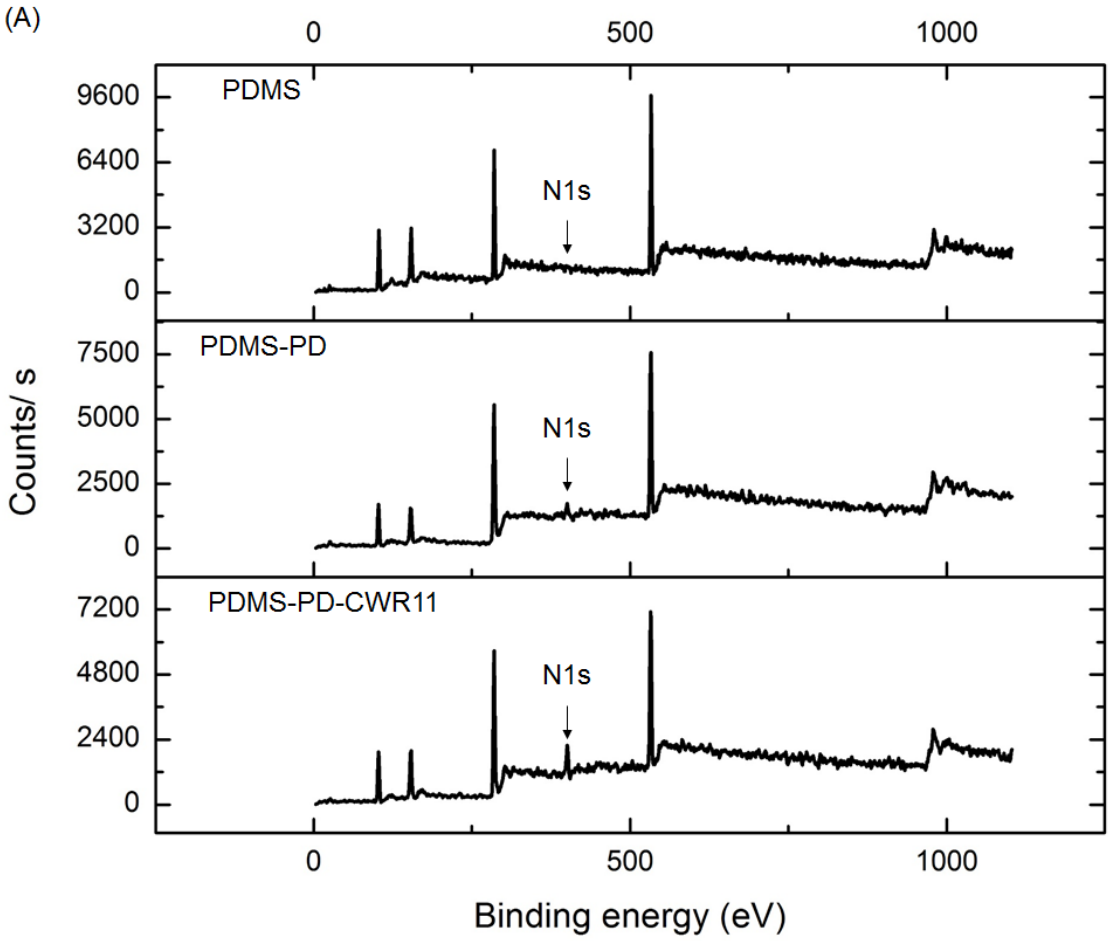
(A)
0
500
1000
PDMS
9600
6400
3200
0
N1s
PDMS-PD
7500
5000
2500
0
N1s
PDMS-PD-CWR11
7200
4800
2400
0
N1s
Counts/ s
0
500
1000
Binding energy (eV)

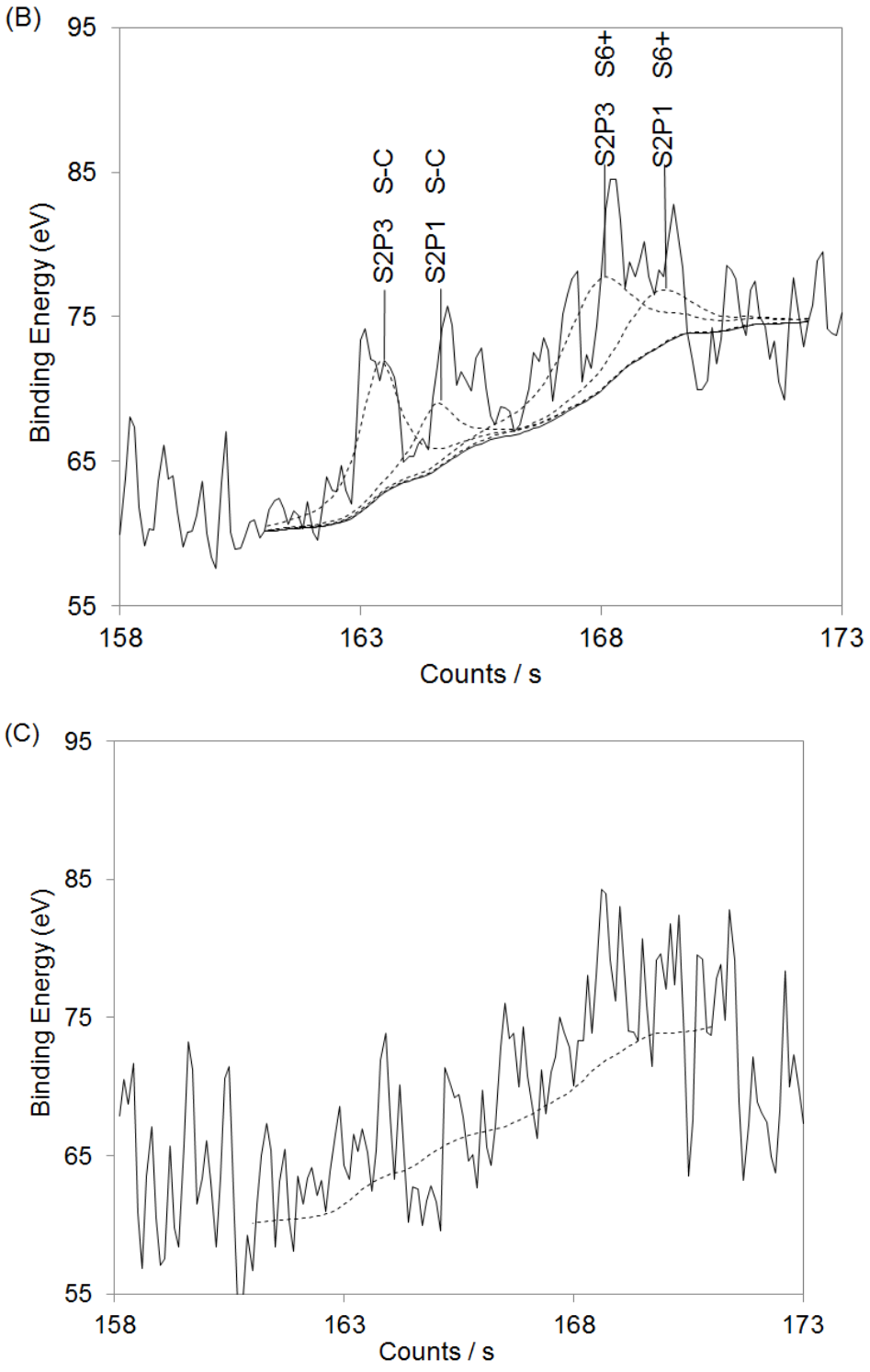

Figure 4.3. Surface characterization of PDMS-PD-CWR11 slides. (A) XPS survey spectra of PDMS, PDMS-PD and PDMS-PD-CWR11 samples for C, N, O and Si element. High resolution XP spectra of (B) PDMS-PD-CWR11 and (C) control (PDMS-PD) (C) slides for S2p detection. Dotted line represent fitted peaks, representing the charged conditions of the respective sulfur atoms, by deconvoluting the high resolution scanning spectrum.

Identification of characteristic amide bands in ATR-FTIR (Figure 4.2C), detection of higher surface nitrogen atomic percentage (Figure 4.3A) and the presence of sulfur atoms (Figure 4.3B) by XPS on peptide-immobilized surface also verified the successful grafting of CWR11 onto the PD-functionalized surface. These results agree with previously reported characterization of peptide attachment on PD-functionalized surfaces [237].

Compared to previously reported surface coupling methods, which require extensive surface modifications and complex reaction steps [153, 204, 238], this strategy offers a much simpler strategy for attaching peptides onto PDMS surfaces, where only two simple dip-coating steps are involved. Efficiency of peptide immobilization is comparable with similar studies that used multi-step immobilization platforms [153, 164, 239], with an estimated 3.41 ± 0.76 μg (1.78 ± 0.40 x 10^{-3} μmoles) of CWR11 tethered per cm^2 of PDMS surface, as estimated by absorbance measurement (data not shown).

4.2.3. Antimicrobial activity of CWR11-immobilized PDMS surface

To determine the antimicrobial performance of the PDMS samples, PDMS-PD-CWR11, PDMS-PD and unmodified PDMS surfaces were inoculated with 5.0 x 10^4 CFU of *E. coli* and incubated for 3 h. The inoculated bacteria suspensions were then subjected to bacteria CFU count. No visible colony was observed on the agar plate for culture from PDMS-PD-CWR11, while significant bacteria growth was observed for the unmodified and PD-coated controls (Figure 4.4A). This result indicates that attachment of CWR11 had conferred the PD-coated PDMS surface with potent bactericidal property. When the surface antimicrobial assays were repeated with *S. aureus* and GFP-*P. aeruginosa*, it was observed that PDMS-PD-CWR11 was effectively bactericidal against these UTI-relevant bacteria (Figure 4.4B). This result clearly shows that CWR11 retained its potent, broad-spectrum antimicrobial property upon attachment to the PD-functionalized surface.

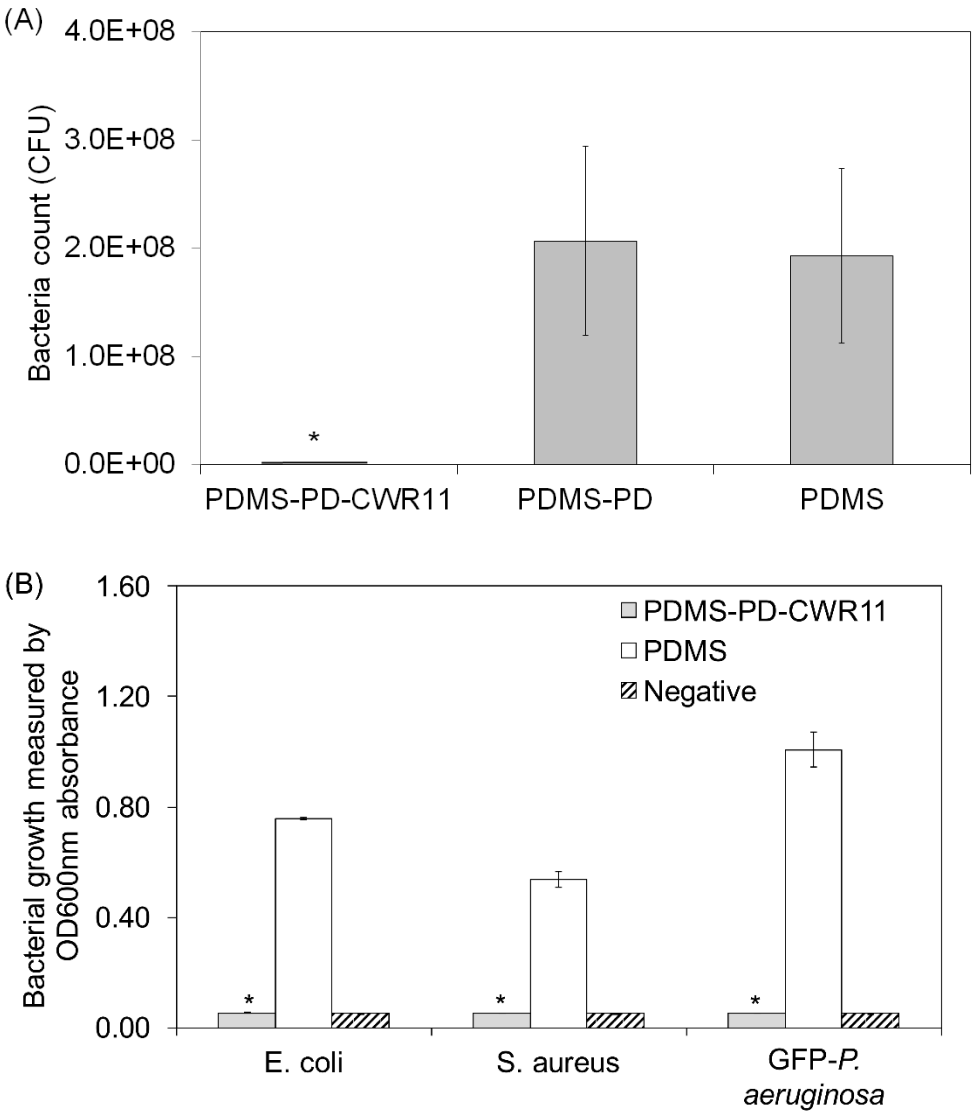

Figure 4.4. Surface antimicrobial activities of CWR11-immobilized PDMS slides. (A) Antibacterial activity of PDMS-PD-CWR11 and uncoated controls. (B) Antimicrobial activity of CWR11-immobilized PDMS slides against *E. coli*, *S. aureus* and *P. aeruginosa*. Optical density measurements (OD_{600}) of overnight MH medium were taken as an indication of bacterial growth. Negative control experiment was carried out using MH medium only. * indicates $p<0.05$ in comparison to untreated PDMS controls.

Many established immobilization strategies utilize long spacers such as polyethylene glycol (PEG) to covalently link the AMP to activated surface [145, 180, 238]. A study by *Bagheri* et al. suggested the importance of spacer in reducing steric hindrance imposed

upon the immobilized peptides [145]. However, in this immobilization study, CWR11 peptides were directly attached onto PD-activated surface. Surface antimicrobial assays demonstrated that the attached AMP retained its potent bactericidal properties, even in the absence of a long spacer. Similar observations were reported in earlier studies. *Kai Hilpert* et al. investigated the tethered bactericidal activities of some 9-, 12- and 13-mer peptides, using CAPE linker and streptavidin/biotin coupling chemistry [163]. The AMPs were directly attached onto the respective surfaces and demonstrated potent bactericidal properties against bacteria and fungi. In another recent study, covalent linkage of polybia-MPI to surface-functionalized polymer brushes without using long spacers did not compromise the antimicrobial property of the peptide [164]. The results from these studies suggest that the use of long spacers is not required to retain immobilized peptide activity, but the outcome may vary with peptide sequence, surface concentration, substrate surface, as well as the surface coupling chemistry [89, 150, 163, 240, 241]. By simplifying the peptide immobilization platform, the loss of peptides can be reduced and the PDMS surface-immobilized CWR11 concentration can be enhanced compared to multi-step immobilization platforms [180], which will increase the economic competitiveness of product development.

4.2.4. Anti-fouling property of CWR11-immobilized PDMS surface

Combating bacterial colonization and biofilm formation on biomedical devices has been a challenge for the medical community for several decades and it is essential that indwelling biomedical devices should possess certain degree of anti-biofilm property. Anti-fouling capacity was investigated by seeding GFP-*P. aeruginosa*, along with the CWR11-immobilized PDMS slides, in a biofilm-promoting medium, followed by 24 h incubation to allow cell attachment, before planktonic cells were eventually washed away. The

attachment of GFP-*P. aeruginosa* was determined by SEM and confocal microscopy imaging, and the amount of biofilm on the surface was quantitatively assayed using fluorescence spectroscopy. SEM images of the sample surfaces showed that the unmodified PDMS surface supported attachment of a large amounts of bacteria (Figure 4.5A). A slight decrease in cell attachment was observed for the PDMS-PD surface while bacteria attachment on the PDMS-PD-CWR11 surface was significantly reduced.

GFP expression facilitates the quantification of biofilm establishment on the surfaces using confocal microscopy. Confocal laser imaging of the sample surfaces demonstrated results that were consistent with those of SEM imaging (Figure 4.5B). Extensive biofilm formation was observed on the surface of the PDMS and PDMS-PD slides, while PDMS-PD-CWR11 slides showed a significantly reduced attachment on its surface significantly. Reduced biofilm formation on PDMS-PD-CWR11 compared to the control slides demonstrated the anti-biofilm potency of the peptide-immobilized surface.

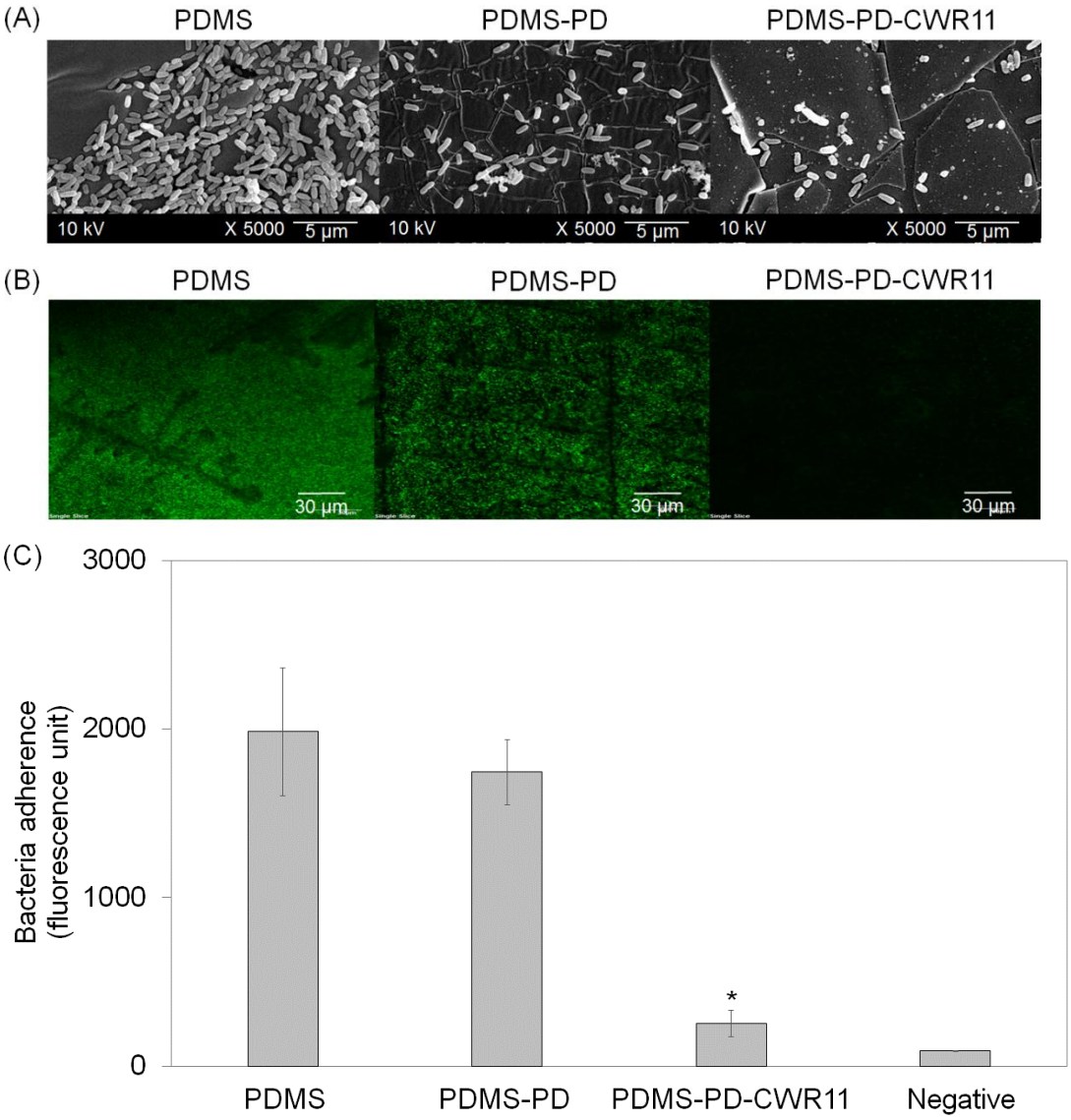

Figure 4.5. Anti-biofilm assessment of CWR11-immobilized slides. Treated and untreated PDMS samples were incubated with GFP-*P. aeruginosa* for 24 h, in biofilm-promoting environment. (A) SEM images and (B) confocal microscopy images of the PDMS-PD-CRW11 samples and the respective controls. (C) Fluorescence spectrometric measurements of PDMS-PD-CRW11 and control PDMS slides to quantitate biofilm formation on the respective surfaces. * indicates $p<0.05$ in comparison to untreated PDMS controls.

The PD coating alone was observed to have a minimal effect in preventing microbial adherence, which agrees with earlier reports that PD coating generally supports cell attachment [6, 159]. Conjugation of CWR11 on PD-functionalized PDMS prevented the

attachment of GFP-*P. aeruginosa* under biofilm-promoting environment, which indicates that the surface-immobilized CWR11 retained its membranolytic property. The highly bactericidal surface-immobilized CWR11 could have eliminated the bacteria before they could colonize the surface, thus preventing biofilm formation, and increases the 'antimicrobial life span' of the CWR11-immobilized surface.

4.2.5. Immobilization of CWR11 onto Foley catheter surfaces

The same peptide tethering platform was extended to immobilize CWR11 on commercially available Foley urinary catheters. The urinary catheter was first coated with a layer of PD (Cat-PD), followed by CWR11 attachment (Cat-PD-CWR11). The use of dip-coating in the immobilization process allowed both the intra- and extra-luminal surfaces of the catheter to be readily grafted with CWR11.

4.2.6. Antimicrobial performance and stability of CWR11-immobilized catheter

The antimicrobial performance of the CWR11-immobilized catheter was verified by introducing 5 x 10^4 CFU of bacteria, in a 50 µL suspension, to the intraluminal section of the sample. The catheter was incubated at room temperature (25^{o}C) for 3 h before being immersed in fresh medium for overnight culture. CFU count of the samples indicated that no bacterial growth was evident for the Cat-PD-CWR11 sample, whereas significant bacterial growth was observed in the control catheter (Figure 4.6A). The same results were obtained when the samples were subjected to OD_{600} measurement. Similar to the CWR11-immobilized PDMS samples, the peptide-immobilized catheter displayed potent bactericidal property against a broad spectrum of UTI-relevant bacteria, including gram-negative *E. coli* and GFP-*P. aeruginosa*, and gram-positive *S. aureus*.

The ability of the immobilized peptides to retain its activity in different environments was determined by exposing the Cat-PD-CWR11 samples to air, water, PBS, synthetic urine and urine for 3 days, followed by subjecting the samples to antimicrobial assays. The CFU determination result indicated that the CWR11-immobilized catheters retained its bactericidal property in all the environments tested (Figure 4.6B).

To investigate the long-term stability of the CWR11-immobilized catheters, Cat-PD-CWR11 were subjected to soft cleaning conditions for an extended period of time. OD_{600} measurements demonstrated that the samples retained excellent antimicrobial potency up to 21 days, completely inhibiting *E. coli* growth (Figure 4.6C). The prolonged stability of the AMP-coated surface suggests minimal peptide degradation [242].

The antimicrobial performance of Cat-PD-CWR11 was compared against commercially available Dover silver-coated catheters. Our results show that the Dover silver-coated catheter slightly outperformed Cat-PD-CWR11 in terms of inhibitory activity (Figure 4.6B and C). This could be due to the controlled release functionality of the Dover silver-coated catheters where the sustained, controlled release of silver ions effectively targets both planktonic and adherent bacteria [71]. In contrast, the tethered peptides on the Cat-PD-CWR11 surfaces may not be effective against planktonic bacteria that are not in proximity to the catheter surface, resulting in slightly higher bacteria growth upon overnight incubation. This will be addressed in the studies reported in the next chapter of this thesis.

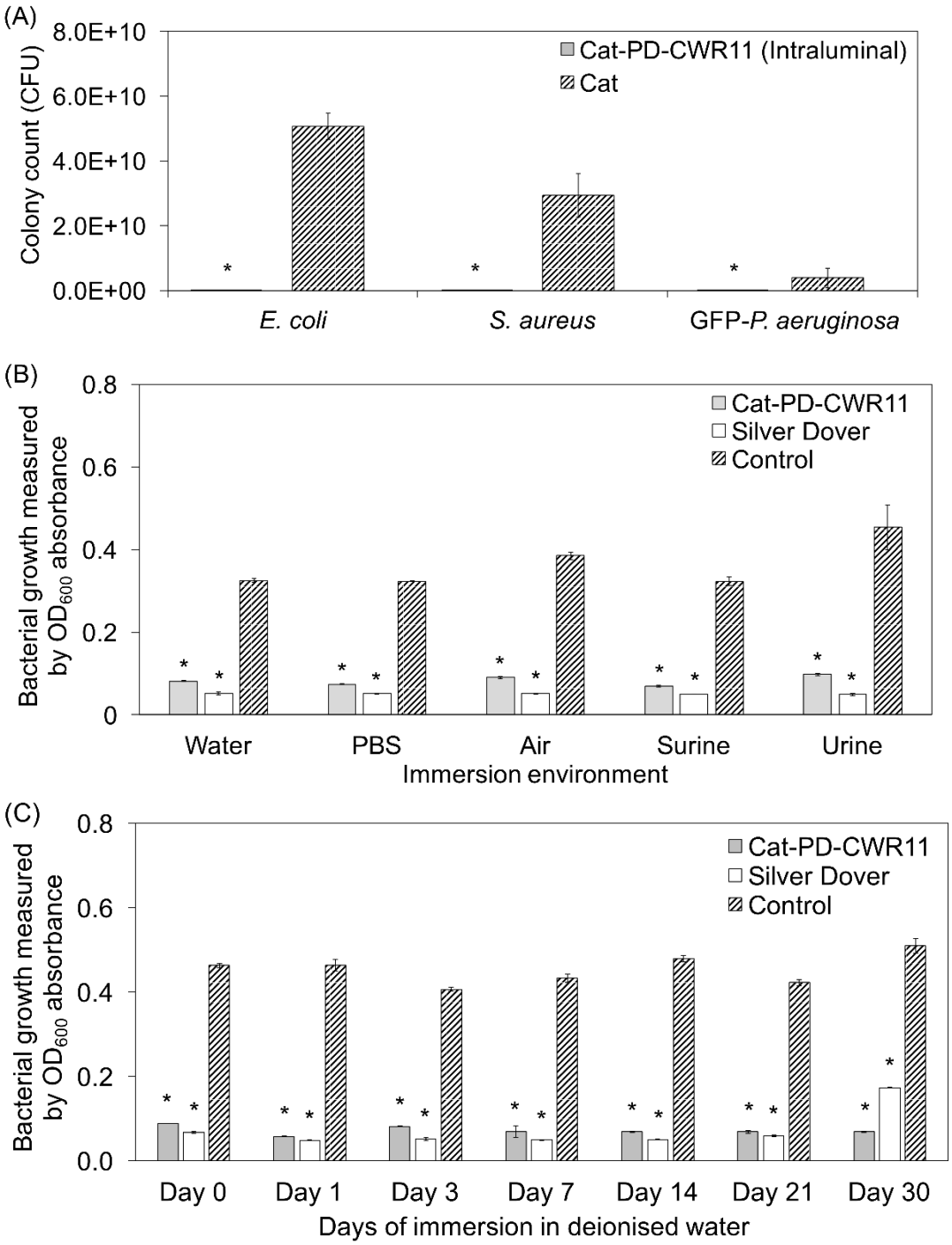

Figure 4.6. Antimicrobial behaviour of CWR11-immobilized catheter samples. (A) Antimicrobial activities of CWR11-immobilized catheter samples against *E. coli*, *S. aureus* and *P. aeruginosa*. (B) Antimicrobial activity of AMP-immobilized catheter after 3 days of incubation in various environments. (C) Stability of the CWR11-immobilized catheters compared to untreated and Silver Dover catheter over 30 days. * indicates $p<0.05$ in comparison to untreated catheter controls.

4.2.7. Cytotoxicity

Cytotoxicity of the peptide-immobilized samples needs to be evaluated since the PD and PD-CWR11 films are designed for indwelling urinary catheters. The effect of CWR11-immobilized slides on uroepithelial cell viability was tested using the MTT assay. The viability of cells in close proximity with CWR11-immobilized slides was higher than 95% and comparable with the control slides (i.e. PDMS and PDMS-PD) (Figure 4.7A). Live-dead staining of the cells were conducted and viewed under a confocal microscope. Viable cells were stained green while dead cells were identified by an additional red PI dye. PI is a high affinity DNA-binding dye that enters dead cells because of their compromised plasma membrane, giving a bright red nuclear staining, but is excluded from live cells with intact plasma membrane. Cells remained largely viable when placed in close proximity with PDMS-PD-CWR11 for 24 h, with negligible amount of PI staining detected (Figure 4.7B). Together, the MTT assays and live/dead staining showed that PD-CWR11 coating was not cytotoxic, but highly compatible with uroepithelial cells.

To evaluate the hemocompatibility of the PDMS-PD-CWR11 slide and Cat-PD-CWR11, the samples were tested for hemolytic tendency against hRBCs. Figure 4.7C shows the rate of hemolysis of the peptide-immobilized samples, compared to the controls. The unmodified and PD-coated controls showed negligible cytotoxicity while the hemolytic activities were slightly higher for the CWR11-immobilized samples (2.67 ± 0.28% for PDMS-PD-CWR11; 1.61 ± 0.35% for Cat-PD-CWR11). However, in accordance to clinical standards stipulated by ISO 10993 (Biological evaluation of medical devices), these values lie within the acceptable cytotoxicity levels determined for medical devices [243].

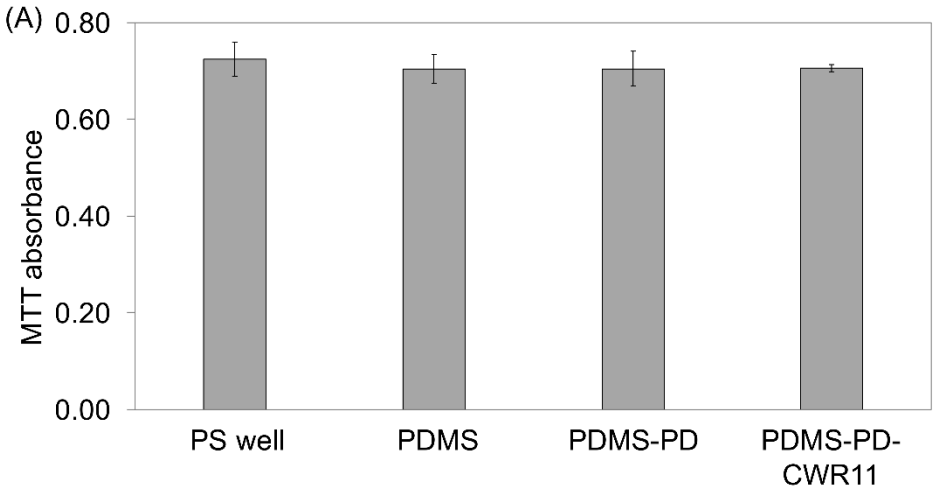
(A)
0.80
0.60
0.40
0.20
0.00
MTT absorbance
PS well
PDMS
PDMS-PD
PDMS-PD-CWR11

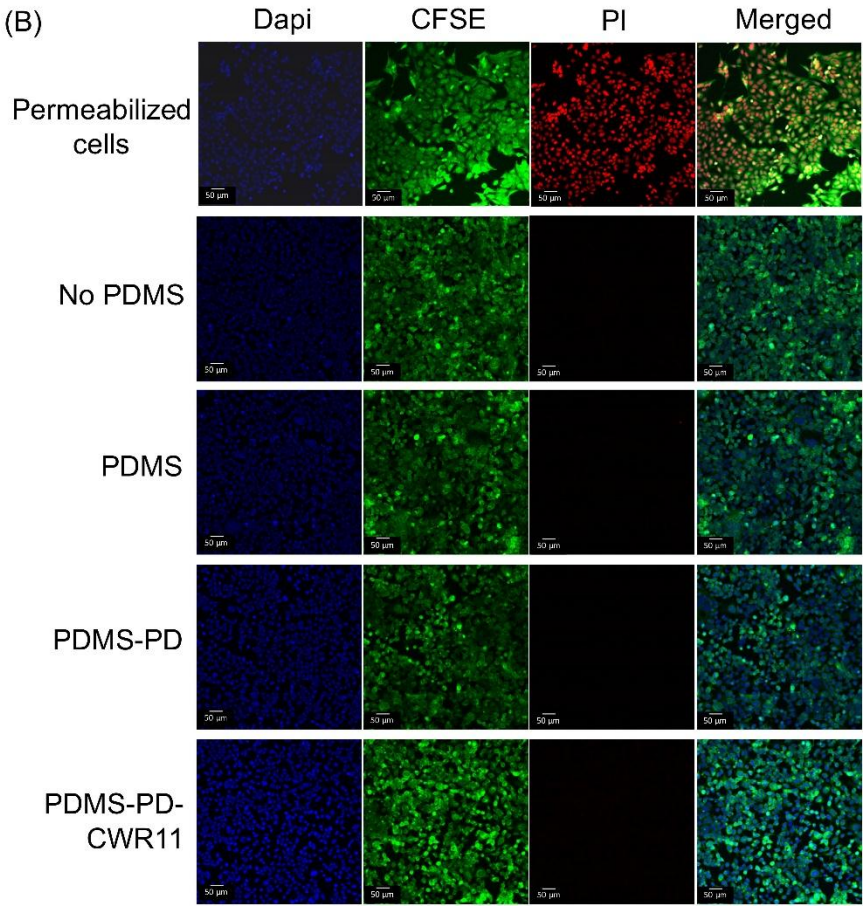
(B)
Dapi
CFSE
PI
Merged
Permeabilized cells
No PDMS
PDMS
PDMS-PD
PDMS-PD-CWR11

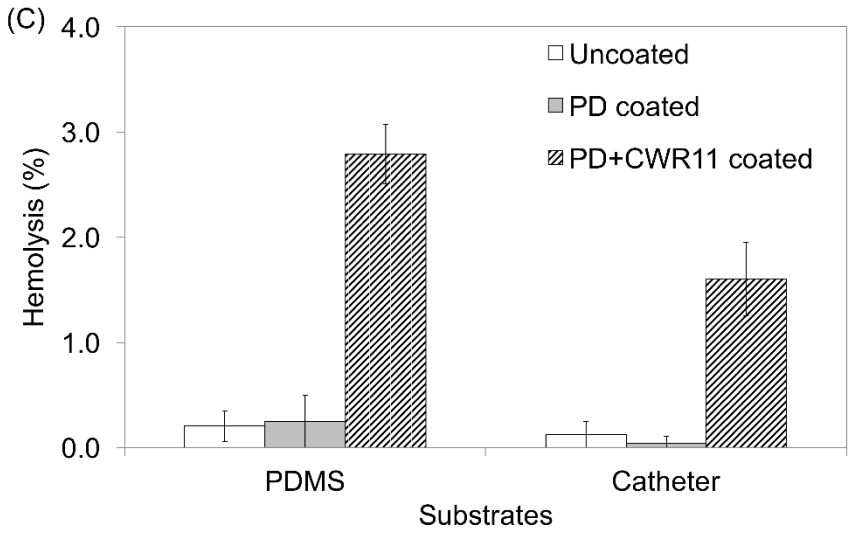

Figure 4.7. (A) Quantitative analysis of SV-HUC1 uroepithelial cells viability per cm^2 of peptide immobilized surface on PDMS-PD-CWR11 samples using MTT assay. (B) Live-dead fluorescence imaging of SV-HUC1 cells incubated with PDMS-PD-CWR11 slides, methanol-permeabilized cells and in the absence of PDMS slides (no PDMS). Shown are nuclei (blue); cytoplasm (green) and propidium iodide (PI)-stained dead cells (red). (C) Hemocompatibility assay of CWR11-immobilized PDMS slides and catheters against human erythrocyte cells.

4.3. Conclusion

In summary, a 2-step polydopamine-based surface immobilization strategy was developed for conjugation of a synthetic AMP, CWR11, onto model PDMS and commercially available Foley catheter. The facile immobilization platform provides a non-destructive and efficient avenue to attach CWR11 onto relevant biomedical devices. Compared to the AGE polymer brush-based platform developed in Chapter 3, this platform involves a much simpler immobilization process with improved AMP immobilization efficacy, which is readily scalable. The peptide-grafted polymer substrates demonstrated potent antimicrobial and anti-biofilm properties against relevant UTI causing bacteria, with excellent stability and biocompatibility. Overall, this CWR11 immobilization strategy

demonstrated excellent functionality and good potential for clinical application, which can be readily extended to other biomedical devices.

As expected of contact active antimicrobial coating, the two AMP immobilization platforms developed in Chapters 3 and 4 offer antimicrobial protection against bacteria that exist within close enough proximity to the surface. More often than not, however, planktonic bacteria that do not come into contact with the surface-tethered AMPs will continue to grow and multiply, leading to rapid bacteria proliferation that will eventually overwhelm the surface-immobilized AMP, resulting in the failure of the antimicrobial coating. To address this problem, a matrix-based coating with AMP controlled release functionality is hypothesized to be able to improve the long term efficacy of the AMP-based coating. An ideal release platform should exhibit high initial release for sterilization of the implant site, followed by sustained and prolonged release for prophylactic measure against possible bacterial infection. The need for an efficient, AMP controlled release coating motivates the initiation for development of a matrix-based platform for sustained peptide release, which forms the aim of the next chapter in this thesis.

Chapter 5 Dual layer coating for controlled release of antimicrobial peptides for prevention of CAUTI

By utilizing coupling strategies such as AGE polymer brush (Chapter 3) and PD-based (Chapter 4) grafting platforms, proof-of-concept demonstration that AMPs can be grafted onto model PDMS and commercial urinary catheter surfaces to render these surfaces contact active was achieved. The AMP-immobilized surfaces exhibited potent, broad-spectrum antimicrobial action against uropathogens such as *E. coli*, *P. aeruginosa* and *S. aureus*. These surfaces also demonstrated excellent anti-biofilm properties and good biocompatibility with hRBCs and uroepithelial cells. However, despite the effective bactericidal functionalities, these contact active surfaces are only effective against microbes that lie within close proximity to the PDMS or catheter surfaces. Planktonic bacteria colonies that are reasonably distant from the surfaces cannot be efficiently targeted and hence can continue to proliferate. Upon prolonged catheter indwelling, the rapidly proliferating planktonic bacteria will eventually dominate and gradually reduce the efficacy of the contact active AMP-immobilized surface, eventually rendering it impotent.

To address this problem, this chapter aims to develop an AMP-based controlled release coating that can target both bacteria near the catheter surface as well as planktonic bacteria to curb their growth at the initial stage. To achieve this, the coating should possess a site sterilization function, inhibiting and/or killing any planktonic bacteria immediately upon implantation to prevent subsequent exponential growth. Systemic administration of antibiotics is often utilized to target such planktonic bacteria growth. However, this method

is impeded by the inefficiency of drug delivery to the target site as well as potential systemic toxicity [8], especially in the case of CAUTI. The use of antibiotics which can induce antibiotic resistant pathogen development is also undesirable. A targeted antibacterial agent delivery system, that ensures sustained, localized and specific drug release is touted as the preferred treatment method [24]. An optimal depot formulation should exhibit high initial release of antimicrobial compound during the early post-implantation period while the immune system is weakened or compromised. A slow and sustained release profile should follow for prophylactic treatment [170, 244].

Biodegradable, matrix-based polymers have facilitated controlled release of antibacterial drugs in microparticle- and implant-based depot formulations [245-247]. These polymers degrade and metabolize naturally *in vivo* to non-toxic by-products [248]. Poly-ε-caprolactone (PCL), in particular, has been frequently featured for drug delivery [247], tissue engineering [223] and medical device coating applications [249]. The excellent biocompatibility and gradual biodegradability of PCL renders it one of the most suitable biomaterials for controlled drug release application. *Chang* et al. showed that by encapsulating antibiotic (gentamycin) in PCL, it is possible to retain sustained drug release for up to 14 days [250]. In contrast to other polymers such as polylactic acid, polyglycolic acid and poly(lactic-co-glycolic acid), PCL possesses superior rheological properties and solid morphology due to increased crystallinity and hydrophobicity [251], thus allowing easier handling of the polymer. Additionally, PCL degradation is more gradual and produces non-toxic carbon dioxide and water as by-products. These properties merit the use of PCL as an AMP-encapsulating layer for this study.

In 2008, *Artem* et al., through the use of peptide array technology and Artificial Neural Networks, a powerful machine learning technique to create quantitative *in-silico* models of antibiotic activities, developed an arginine-, tryptophan-rich 9-mer synthetic peptide,

HHC36 [252]. The synthetic AMP possessed potent, broad spectrum antimicrobial activity with excellent biocompatibility against mammalian cells. A further conformational study on HHC36 reveals that the arginine-, tryptophan-rich peptide adopted a turn conformation in aqueous buffer and folds instinctively in the presence of bacterial membrane mimicry to adopt an enhanced turned configuration. Further examination with isothermal titration calorimetry and acrylamide fluorescence quenching demonstrated preferential attachment of HHC36 towards negatively charge membrane surface, accounting for the excellent selectivity of the synthetic peptide [253]. The short amino acid sequence (9 amino acids), abundance of tryptophans (four tryptophan residues) and lack of cysteine also aids to ensure ease of identification as well as reduce synthesis process complexity. These properties make HHC36 an ideal candidate agent for controlled release antimicrobial coating. In fact, since being reported in 2009, HHC36 has been selected as the choice agent for delivery in a variety of controlled release studies [170, 254, 255]. For these similar reasons, HHC36 was chosen as the candidate AMP for the current controlled release study.

Specifically, this chapter reports the development of a platform comprising a layer-by-layer assembly of thin films to facilitate the sustained release of arginine-, tryptophan-rich HHC36. To achieve a coating that can facilitate sustained AMP release, PCL films, impregnated with HHC36, were surface-coated with a thin 1-palmitoyl-2-oleoyl-sn-glycero-3-phosphocholine (POPC) film to modulate the release of HHC36. POPC is a major component of the eukaryotic cell membrane and offers significant resistance against bacteria growth [170], while showing excellent biocompatibility. Synthesis of the coating, efficacy of the AMP release profile and antimicrobial functionality of the PCL-POPC coating were studied. The coating was subsequently applied on commercial silicone catheters to examine its short and long term antimicrobial and anti-biofilm against UTI-relevant bacterial strains.

5.1. Materials and methods

5.1.1. Materials

Synthetic peptides HHC36 (KRWWKWWRR) and CHHC36 (CKRWWKWWRR), chemicals and silver Dover control catheters were purchased from local and international vendors as detailed in Section 3.1.1. *E. coli*, GFP-*P. aeruginosa* and *S. aureus* (as described in Section 3.1.1) were used for subsequent antimicrobial and anti-biofilm assays.

5.1.2. Processing of HHC36-impregnated PCL-POPC film (PCL(P)-POPC(P)) in 96-well plate

PCL coating in 96-well plate was prepared using a drop-and-dry technique. 10% (w/v) PCL solution was prepared by dissolving 0.5 g PCL pellet in 5.0 mL 2,2,2-trifluoroethanol (TFE). 5.0 mg AMP were subsequently loaded into 500 µL 10% (w/V) PCL solution and mixed thoroughly by vortexing. 100 µL of the HHC36-rich PCL solution was pipetted into each well and dried at 25^{o}C for 24 h to form a single layer HHC36-impregnated PCL film (PCL(P)).

POPC (Avanti Polar Lipids Inc., USA) was dissolved in ethanol (500 µL) to obtain a final concentration of 26 mM POPC. 100 µL of the POPC solution was pipetted onto the PCL(P) surface, and dried under atmospheric condition at room temperature (25^{o}C, 24 h). During the drying process, a portion of the total loaded AMPs from the basal PCL layer diffuses out and gets trapped within the newly formed POPC superficial layer forming the dual layer AMP-rich PCL-POPC coating (PCL(P)-POPC(P)).

5.1.3. Coating surface characterization

5.1.3.1. Scanning electron microscope (SEM)

Surface morphologies of PCL(P) and PCL(P)-POPC(P) coating were processed and viewed under a SEM (JSM6390LA, JEOL, Japan). Briefly, sample coatings were sputter-coated with a thin layer of platinum (JFC-1600, JEOL, Japan) and kept in a 40^{o}C oven before viewing.

5.1.3.2. Energy dispersive X-ray spectroscopy (EDS)

Coating morphology and surface elemental distribution were studied using EDS as described in Section 3.1.7.3.

5.1.3.3. Attenuated total reflectance fourier transform infrared (ATR-FTIR) spectroscopy

Coating of POPC film and impregnation of AMP into the PCL(P)-POPC(P) coating were verified using ATR-FTIR spectroscopy. Methodology for ATR-FTIR analysis was elaborated in Section 3.1.7.4.

5.1.4. AMP release profile

In vitro AMP release kinetics of the PCL(P)-POPC(P) coating were measured by absorbance measurement at 280 nm using Nanodrop 1000c (Thermo Scientific, USA). PCL(P)-POPC(P) coating in each well was immersed with 200 µL of PBS solution and incubated at 25^{o}C. After 24 h incubation, the PBS solution was withdrawn and sampled for peptide release, and the well was replenished with fresh PBS. The PBS withdrawal and refreshing process was conducted at regular time points (i.e. day 1, 3, 5, 8, 11, 14, 21 and

30). The AMP content was analyzed by absorbance measurement to assess the peptide cumulative release rate over 30 days at regular time intervals. A series of HHC36 standards from 4 µg/mL to 1000 µg/mL were used for calibration purpose.

5.1.5. Released peptide conformation and functionality

5.1.5.1. CD spectroscopy

Far UV spectroscopy analysis of the released and native HHC36 in (i) PBS (pH 7.4) and (ii) 10 mM SDS was performed using CD analysis, as detailed in Section 3.1.4.

5.1.5.2. Fluorescence emission spectroscopy

Fluorescence emissions of released and native HHC36 were measured with a fluorescence spectrometer (LS5, Perkin Elmer, USA) at 25^{o}C using a quartz cuvette of 0.5 cm pathlength. Emission spectra were recorded between 300 nm and 500 nm, with excitation at 280 nm. Excitation and emission slit widths were set to 5.0 nm. Sample conditions were similar to those described for CD analysis (Section 5.1.5.1).

5.1.5.3. PCL(P)-POPC(P) coating antimicrobial assays

PCL(P)-POPC(P) coated wells were subjected to antimicrobial assay as described in Section 3.1.8, with minor adaptations. Briefly, *E. coli* culture was sub-cultured in *Luria* broth (LB) medium to mid-log phase and further diluted to provide a final bacterium density of ~1 x 10^6 CFU/mL. 50 µL of the bacterial suspension, along with 150 µL of fresh LB medium, was added to PCL(P)-POPC(P) coated wells and incubated at 25^{o}C for 24 h. Bacterial growth in the resulting suspension was assayed through CFU enumeration, as described in Section 3.1.8. Long term antimicrobial activity of the coating was investigated. Briefly, PCL(P)-POPC(P) coated wells were subjected to 10 consecutive cycles of antimicrobial

assay as described above. CFU of overnight bacteria suspensions were enumerated, after every cycle of antimicrobial assay, as an indication of bacterial growth.

5.1.6. PCL(P)-POPC(P) coating on silicone Foley catheter

Silicone Foley catheter (16 Fr, Multigate, Australia) were cut into 1.0 cm segments for PCL(P)-POPC(P) coating. The coating process was conducted *via* a simple dip-and-dry method, similar to that as described in Section 5.1.2. Briefly, the catheter samples were immersed in 10% (w/v) PCL solution containing 10.0 mg/mL HHC36, in TFE solvent for 10 s. Catheter segments were withdrawn and left to dry under room temperature (25^{o}C) for 24 h. The single layer AMP-laden PCL-coated catheter (Cat-PCL(P)) was then dipped into a POPC solution (26 µM POPC in ethanol) for 10 s. Coated catheter samples were withdrawn and dried overnight at 25^{o}C for 24 h. The dual layer coated catheters (Cat-PCL(P)-POPC(P)) were kept at 4^{o}C for future experiments.

5.1.7. Antimicrobial and anti-biofilm assay for Cat-PCL(P)-POPC(P)

5.1.7.1. Antimicrobial assay against planktonic bacteria

Cat-PCL(P)-POPC(P) and uncoated control catheters were subjected to antimicrobial assay against planktonic *E. coli*, *S. aureus* and GFP-*P. aeruginosa*. Overnight bacterial suspension was sub-cultured in LB medium to mid-log phase and further diluted to provide a final bacterium density of ~1 x 10^6 CFU/mL. 50 µL of the bacterial suspension, along with 450 µL of fresh LB medium, was added to 2.0 mL microtubes containing the catheter samples and incubated at 25^{o}C for 24 h. OD_{600} of the resulting bacterial suspension was measured subsequently as an indication of bacteria growth. The assay was repeated in triplicate for *E. coli*, *S. aureus* and GFP-*P. aeruginosa*. Long term antimicrobial performance of the coated catheters was evaluated in a similar fashion. Briefly, catheter

samples were subjected to 5 consecutive cycles of antimicrobial assays as described above. OD_{600} measurements of overnight bacteria suspensions were recorded, after every cycle of antimicrobial assay, as an indication of bacterial growth. Bacteria adherence on the respective catheter surfaces, when subjected to prolonged and repeated bacteria exposure, was examined using an anti-biofilm assay described in Section 5.1.7.2.

5.1.7.2. Anti-biofilm assay against planktonic bacteria

The anti-biofilm property of the Cat-PCL(P)-POPC(P) and control catheters was evaluated by a bacterial adherence assay [256]. The catheter samples were immersed into microtubes, containing ~2.0 x 10^7 CFU *E. coli* in nutrient rich LB medium. The samples were incubated at 37^{o}C overnight (24 h) to promote biofilm development. After incubation, catheter samples were removed, rinsed thrice and re-immersed into 1 mL of fresh PBS solution. Adherent bacteria cells were then removed from the catheter surface by sonication (10 min) followed by vortexing (5 min). Viable bacterial counts were assessed by serial dilution on MH plates.

5.1.7.3. Determination of biofilm and bacteria growth using SEM

Biofilm or bacterial growth of GFP-*P. aeruginosa* on 1 cm catheter segments was viewed under a scanning electron microscope (JSM 5600LV, JEOL, Japan) using a similar methodology as detailed in Section 4.1.4.2. Briefly, catheters were incubated with GFP-*P. aeruginosa* (5 × 10^7 CFU/ml) in biofilm promoting medium (BPM) for 48 h at 37°C. The catheters were washed three times with PBS to remove loosely adherent bacteria and divided longitudinally into halves. Samples were fixed in 2% glutaraldehyde for 24 h at 4°C. After fixation, the catheters were treated with osmium (OsO_4) for 30 min and washed twice (5 min each) with PBS. The catheters were dehydrated through an ethanol series of 25–

50–75–95% (each for 15 min) and three changes of 100% ethanol (each for 20 min), followed by critical point drying with CO_2 (CPD 030, Balzers critical point dryer, Liechtenstein). The catheters were then coated with gold (BAL-TEC sputter coater, USA) and incubated in an oven at 40 °C before viewing.

5.1.8. Biocompatibility assays

5.1.8.1. Hemocompatibility assay

Cytotoxicity of Cat-PCL(P)-POPC(P) samples against hRBC was investigated using a hemolytic assay established by *Shai* et al. [257]. Detailed methodology was described in Section 4.1.7.2.

5.1.8.2. Uroepithelial cell viability assay

Cat-PCL(P)-POPC(P) and untreated control catheter samples were tested for cytotoxicity against a SV-HUC-1 uroepithelial cells by MTT assay as described in Section 4.1.7.1.

5.2 Results and discussion

In view of the need to develop an alternative CAUTI therapy that is independent of antibiotics while having improved efficacy and economics feasibility for longer term catheterization, this chapter reports the development of a catheter coating platform for sustained release of AMPs. An ideal controlled release platform for CAUTI treatment should (1) not promote the development of multiple antibiotic resistance, (2) possess controlled and sustained release kinetics, and (3) display good biocompatibility with surrounding uroepithelial cells [170]. With these pre-requisites in mind, a layer-by-layer coating composed of PCL and POPC, for the delivery of a model AMP, HHC36 was developed. HHC36 is also an arginine-, tryptophan-rich synthetic AMP with proven antimicrobial action against both gram-negative and gram-positive bacterial strains [252], which merits its use in this study. Compared to CWR11, HHC36 showed favorable antimicrobial capability against the uropathogens of our interest (Table 5.1). The potent bactericidal property is crucial to sustain the antimicrobial action of the controlled release coating for an extended period of time, especially during the later phase where AMP release becomes thin.

Table 5.1. Reported MIC of HHC36 [252] and CWR11 against tested uropathogens.

	Minimum Inhibitory Concentration (μM)	
	CWR11	**HHC36**
E. coli	5.2 ± 0.5	4.05 ± 1.91
S. aureus	5.5 ± 0.0	3.74 ± 3.92
GFP-*P. aeruginosa*	2.5 ± 0.0	2.15 ± 1.06

Figure 5.1A shows the schematic of the proposed dual layer PCL(P)-POPC(P) controlled release coating; a layer of biodegradable PCL, impregnated with high concentration of HHC36, was layered with a thin film of POPC, which acts as a diffusion boundary layer to modulate HHC36 release. The synthesis process which involved two simple drip-and-dry processes is shown in Figure 5.1B.

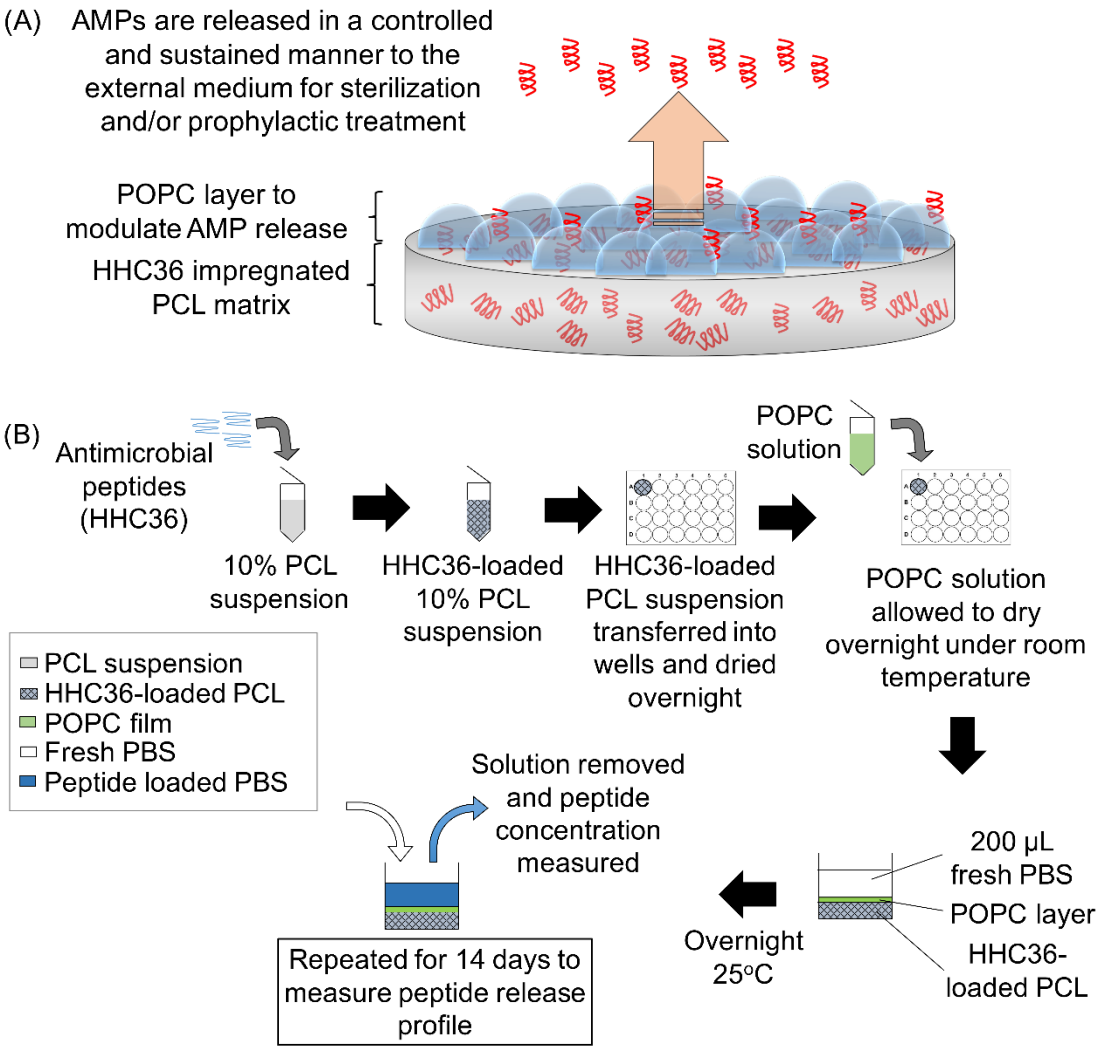

Figure 5.1. (A) Schematic of HHC36-impregnated PCL-POPC coating process. PCL formed the basal layer while a thin film of POPC was coated on top as a boundary for peptide diffusion. AMPs were loaded into both layers. AMP release was recorded daily for an extended period of 14 days. (B) Schematic of dual layer PCL(P)-POPC(P) controlled release coating. HHC36 was abundantly impregnated in both layers. Upon exposure to aqueous medium, HHC36 is released in a controlled and sustained manner.

PCL is a biodegradable polymer with excellent physical properties. Due to its slow degradation rate and excellent permeability, PCL makes an apt candidate material for sustained delivery of therapeutic agent over prolonged period [258, 259]. It is a semi-crystalline polymer with regular structure, accounting for its superior mechanical toughness

[260], which enables easy handling. Unlike commonly used polymers, such as poly(D,L-lactic-co-glycolic acid), PCL does not produce acidic by-products upon degradation. This, along with its excellent mechanical properties and good permeability, renders PCL an attractive controlled release polymer for biomedical application. A layer of POPC was coated onto the surface of PCL. POPC, a close mimic of eukaryotic membrane phospholipid, acts as a diffusion barrier to enhance sustainability of peptide release. The use of POPC as an efficient boundary to enhance release kinetics has been demonstrated in a recent study by *Kazemzadeh-Narbat* et al. [170].

Specifically, PCL matrix encapsulated with HHC36 was prepared by dissolving PCL and AMP in 2,2,2-trifluoroethanol (TFE), and subsequently dried overnight under atmospheric condition (Figure 5.1B). The TFE solvent, a helix-inducing chemical, is hypothesized to aid in stabilizing peptide helices during the casting process, conserving AMP structural robustness for subsequent antimicrobial activity, upon release [261].

5.2.1. Characterization of PCL-POPC AMP controlled release coating

5.2.1.1. SEM analysis

The surface morphologies of AMP-loaded PCL and PCL-POPC coatings were characterized by SEM. The PCL(P) coating has an uneven and porous surface morphology (Figure 5.2A, top), containing relatively large pores, measuring 143.63 ± 24.15 μm^2 in area. The addition of a POPC layer improved the smoothness of the surface morphology (Figure 5.2A, bottom).

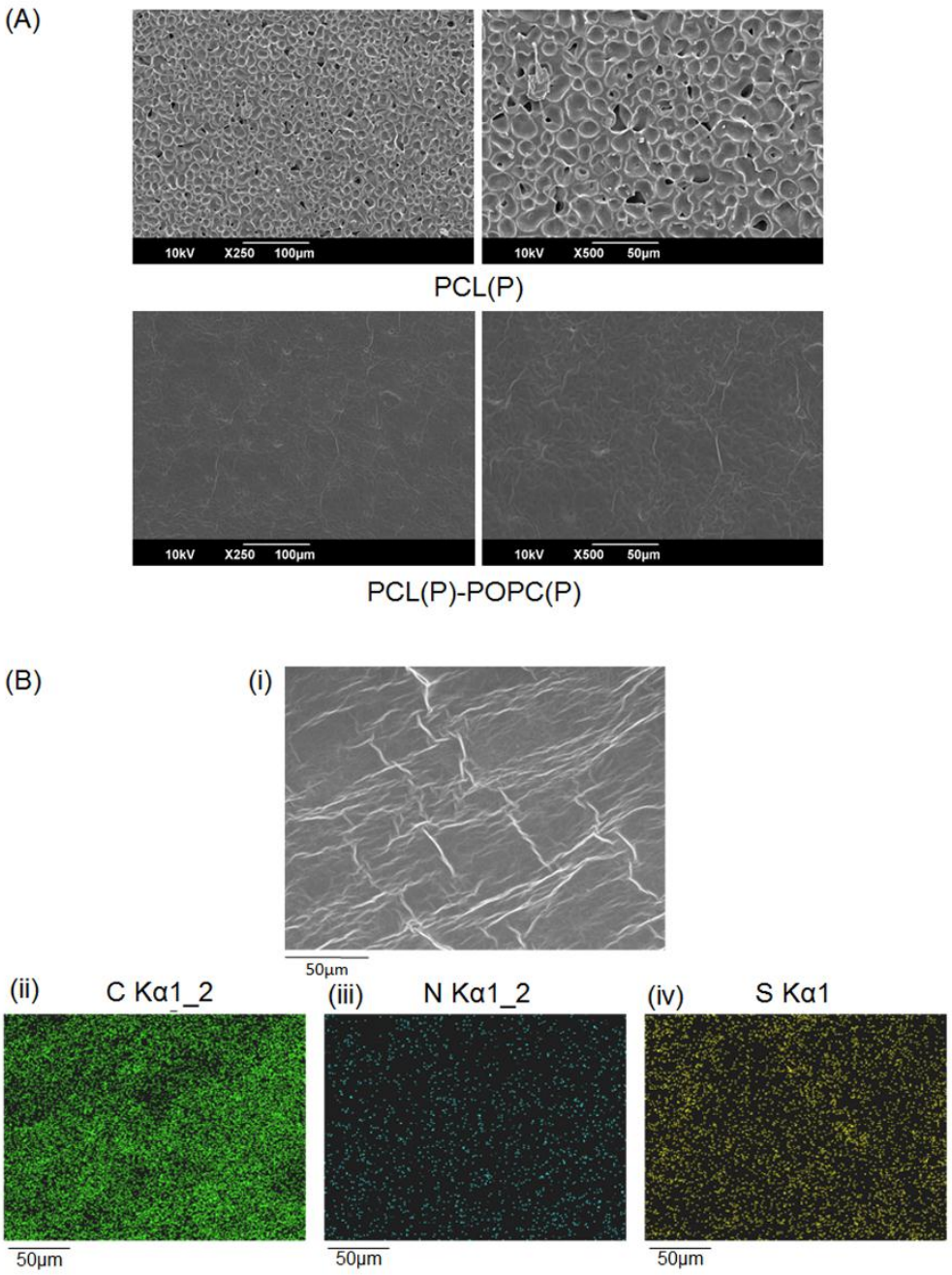

Figure 5.2. (A) SEM micrographs of PCL(P) layer (top) and PCL(P)-POPC(P) layer (bottom). (B) A FESEM and EDS elemental mapping of PCL(P)-POPC(P) surface showed a smooth morphology and homogeneous distribution of AMPs on the surface. (B)(i) High magnification FESEM images of PCL(P)-POPC(P) surface morphology. High concentration of HHC36 is embedded within the dual layer assembly. PCL(P)-POPC(P) coating surface elemental mapping of atomic carbon (B)(ii), nitrogen (B)(iii) and sulphur (B)(iv).

5.2.1.2. EDS analysis

Higher resolution surface analysis of PCL(P)-POPC(P) was carried out by FESEM imaging coupled with an EDS elemental mapping. Figure 5.2B shows the FESEM image (Figure 5.2Bi) and elemental mapping of carbon (C) (Figure 5.2Bii), nitrogen (N) (Figure 5.2Biii) and sulphur (S) (Figure 5.2Biv) elements for the AMP-embedded PCL-POPC surface. High magnification FESEM imaging of PCL(P)-POPC(P) coating surface morphology agrees well with the SEM result. The porous PCL layer is covered by a uniform layer of physically attached POPC, presenting a smooth morphology. Carbon is abundantly present on the PCL-treated surface (77.3 %), followed by oxygen (17.2 %) and nitrogen (3.4 %). Sulphur is present in very small quantities, i.e., at an atomic percentage of 2.1 %. HHC36 was engineered to carry an additional cysteine amino acid at its N-terminal in this study, for easy peptide detection by sulphur elemental mapping. The detection of small amount of sulphur element on the coating verified the successful impregnation of AMP into the dual layer coating. The results obtained from the sulphur elemental mapping (Figure 5.2Biv) illustrates that the cysteine-tagged HHC36 was uniformly distributed across the surface coating.

5.2.1.3. ATR-FTIR analysis

Figure 5.3 shows the ATR-FTIR spectra of the PCL and PCL(P)-POPC(P) coatings. Distinctive peaks corresponding to POPC were observed on the PCL(P)-POPC(P) spectrum. Characteristic vibration bands at 2923 cm^{-1} and 2853 cm^{-1} corresponds to CH_2 anti-symmetric stretch and CH_2 symmetric stretch of POPC, respectively. The POPC's C=O stretching band is observed at 1746 cm^{-1}. The wave numbers 1464 cm^{-1} and 1203 cm^{-1} are attributed to CH2 scissoring and PO_2^- anti-symmetric stretching. Strong absorbance at 1086 cm^{-1} is likely due to both PO_2^- and CO-O-CH_2 symmetric stretching

[170]. Additional transmittance peaks are observed at 1536 cm^{-1} and 1675 cm^{-1} wavenumber. The doublet, representative of amide I and II bands [262], originates from the AMPs that were embedded within the POPC and PCL coating.

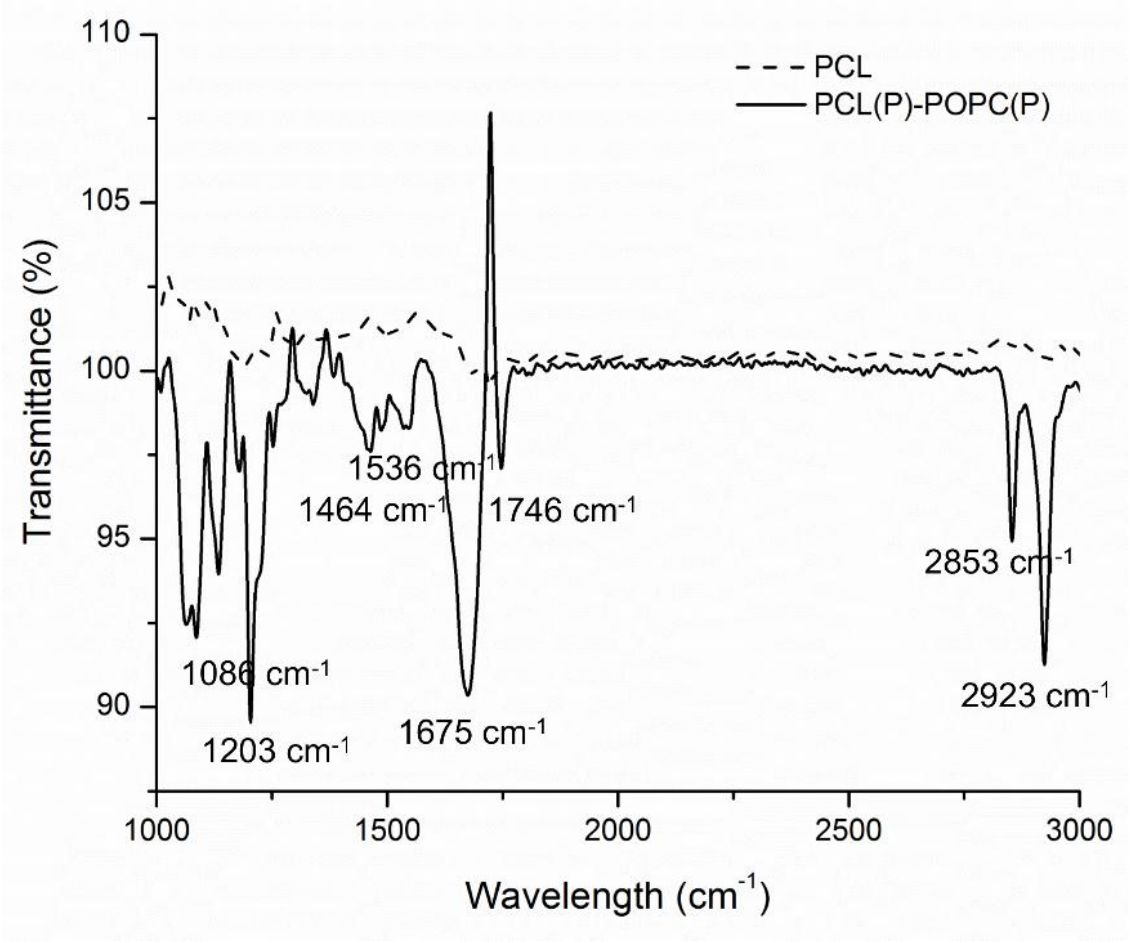

Figure 5.3. ATR-FTIR spectra of PCL (dash line) compared to PCL(P)-POPC(P) (solid line) layer. Impregnation of AMP and coating with additional POPC film gives rise to additional corresponding transmittance peaks.

The highly porous nature of the HHC36-loaded PCL film, as observed in SEM imaging (Figure 5.2A), provides a high surface area for AMP release. To control the burst release profile of the peptides, a thin film of POPC was applied as a diffusion barrier to regulate the release kinetics. During the solvent drying process, some AMPs from the basal PCL

matrix are expected to diffuse out and remain trapped within the top POPC layer, embedding the superficial layer with a significant amount of peptides. These superficial peptides is the first to be released, accounting for the burst release section of the release profile. After which, HHC36 embedded deeper within the basal PCL layer is gradually released over the course of the immersion period. An AMP-rich dual layer PCL-POPC coating was thus developed. The efficacy of POPC as a diffusion boundary has been widely studied and well verified [170]. SEM imaging of a smooth superficial layer (Figure 5.2A) and observation of distinctive peaks in ATR-FTIR spectroscopy (Figure 5.3) confirmed the embedding of a HHC36-rich POPC film above the porous PCL layer. Surface EDS elemental mapping showed uniform distribution of AMPs on the coating (Figure 5.2B), further verifying homogeneous impregnation of peptides throughout both the PCL and POPC films.

5.2.2. *In vitro* HHC36 release profile from PCL(P)-POPC(P) coating

Figure 5.4 shows the release profile of the HHC36-impregnated PCL-POPC coating over 30 days (solid line). This time span corresponds to the span of long term catheterization performed in hospitals, which typically lies between 2 weeks to a month. The PCL(P)-POPC(P) coating released 18 % of AMPs in the first 24 h, after which a slower release of peptides which accumulated to 43 % of the loaded peptides was observed by day 14. Peptide release from PCL(P)-POPC(P) coating, from day 7 to 14 remained significantly high, i.e., at 20 µg/day, where the released peptide concentration remained higher than the HHC36 minimum inhibitory concentration (MIC). In contrast to PCL(P), in which significant AMP release was observed only until day 3 (dashed line), PCL(P)-POPC(P) exhibited a more sustained control release profile.

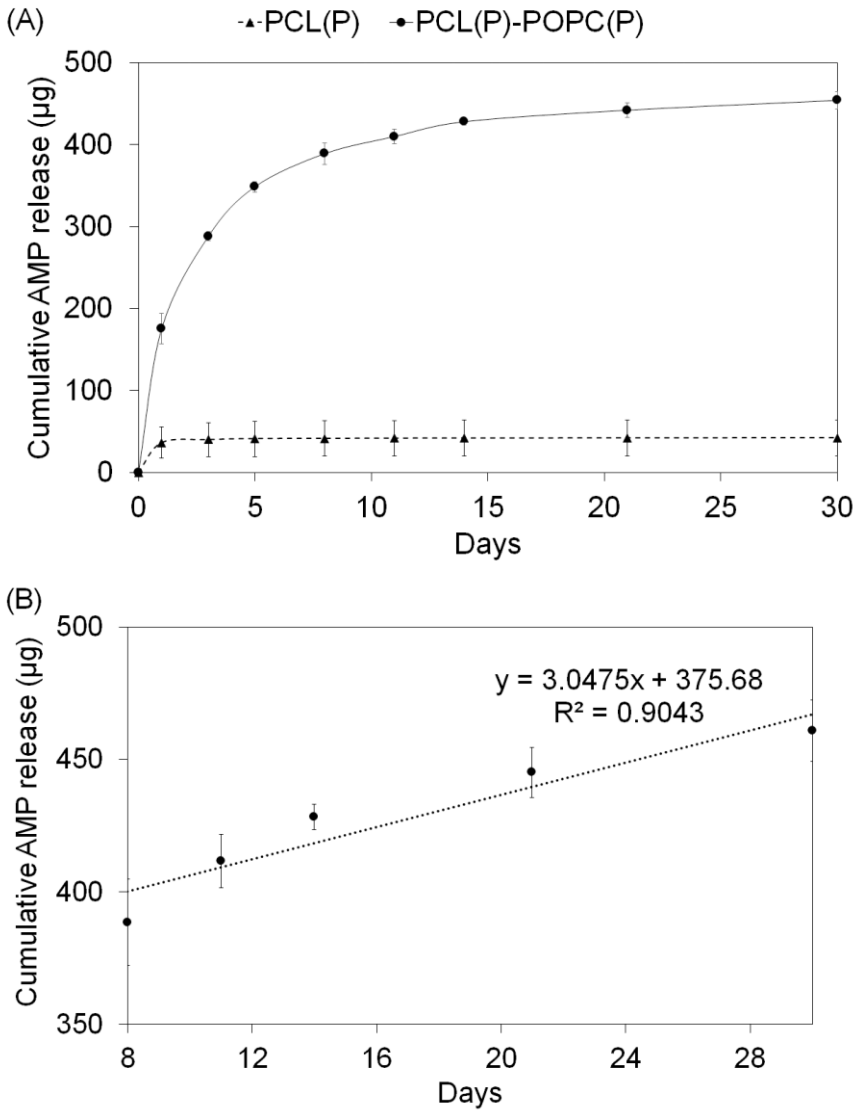

Figure 5.4. (A) Kinetics of HHC36 release from PCL(P)-POPC(P) (solid line) and PCL(P) (dashed line) coating over 30 days. (B) AMP release profile from PCL(P)-POPC(P) from day 8 to 30 follow closely a first order release kinetics.

The *in vitro* peptide release profile obtained from the PCL(P)-POPC(P) coating exhibited a two-phase release kinetics (Figure 5.4). First, an initial burst release of peptide within the first 24 hours that accounted for the release of 18% of the peptide was observed, which is hypothesized to be driven by concentration-induced diffusion. This burst release is likely due to the combinatorial effects of AMP molecules that were at or near the solvent-coating

interface, which diffused readily into the supernatant solution and the release of POPC-encapsulated peptides due to the swelling of the superficial POPC layer upon contact with PBS [170]. Such burst release profile is commonly observed in various diffusion-governed controlled release setup [170, 247, 263]. In the second release phase, HHC36 was progressively released from the dense PCL layer, closely following a first order kinetic release for day 8 to 30. The PBS solution penetrated into the PCL polymer matrix, hydrolysed the polymer, thus releasing the entrapped the AMPs. At the end of 14 days, ~43% of the total encapsulated AMPs were released. Although not included in the scope of the study, it is hypothesized that the remaining entrapped HHC36 will be gradually released over time, with progressive degradation of the PCL polymer [247, 264]. Further optimization to the controlled release platform for enhanced and more sustained release kinetics are currently underway and described in Section 6.2.3.

5.2.3. Released HHC36 peptide stability

5.2.3.1. CD studies of AMP secondary structure after release from the PCL(P)-POPC(P) layer

The integrity and antimicrobial potency of the released AMPs were studied by CD spectroscopy. Various structure-activity studies proposed that an AMP's ability to fold into amphipathic or amphiphilic conformation plays a crucial role in determining its bactericidal action [265]. The structural integrity of the released peptides were analysed by CD. Figure 5.5 compares the molar ellipticity of HHC36 released from the PCL(P)-POPC(P) layer and native HHC36 in PBS (A) and membrane mimicking 10 mM SDS environments (B). The PCL(P)-POPC(P) released and native HHC36 showed identical turned structures in water, with 2 distinct negative troughs at 225 nm and 198 nm. In the presence of 10 mM SDS,

both peptides adopted discrete alpha helical configurations. This result confirms that the released HHC36 possessed comparable conformation to the native peptides.

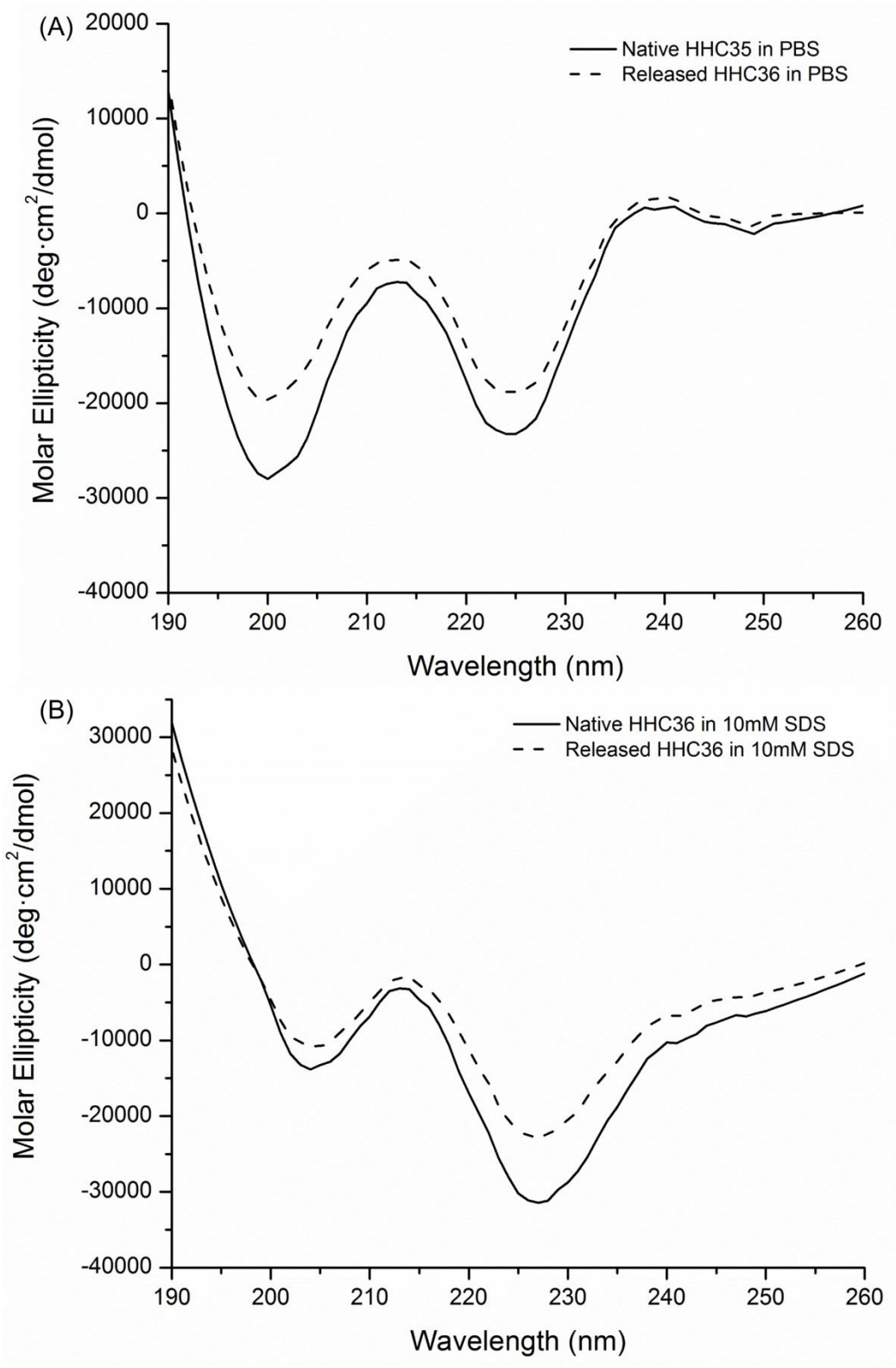

Figure 5.5. Far-UV CD spectra of native (black line) and released (dash line) peptides from the PCL(P)-POPC(P) coating in PBS (A) and 10 mM SDS (B).

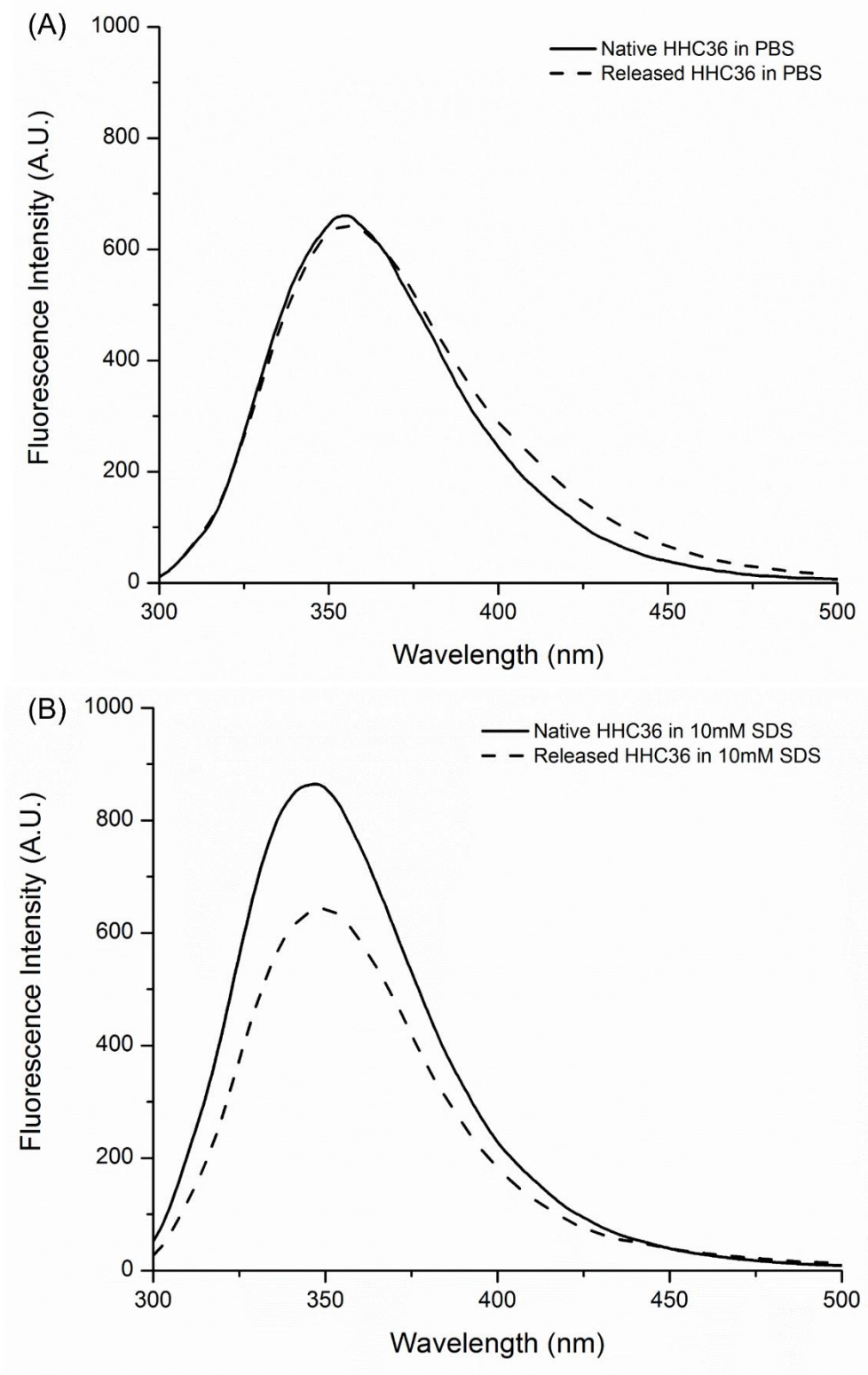

Figure 5.6. Fluorescence emission spectra of native (black line) and released (dash line) peptides from the PCL(P)-POPC(P) coating in PBS (A) and 10 mM SDS (B). Excitation was fixed at 280 nm.

5.2.3.2. Fluorescence spectroscopy to characterize peptide-membrane interaction

Fluorescence emission spectra were recorded to determine peptides' association with bacteria membrane. The emission spectra, under both PBS and 10 mM SDS environments, were comparable to those of the native peptide at the same concentration (Figure 5.6). Both released and native AMPs registered a fluorescence maxima at 354 nm and 346 nm in PBS and 10 mM SDS, respectively. A blue shift of the same magnitude, i.e., 8 nm, was observed for both AMPs. The similarities in emission spectra illustrated matching membrane interaction and insertion for the released and native HHC36.

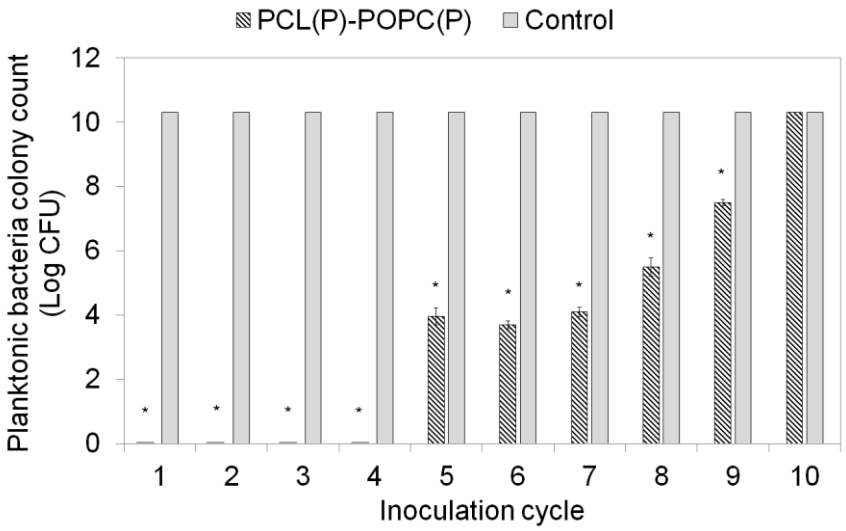

Figure 5.7. Antimicrobial property of the PCL(P)-POPC(P) coated and untreated wells with repeated bacterial inoculation, up to 10 cycles. AMP release coating illustrated potent antimicrobial activity, significantly inhibiting bacterial growth up to 9 cycles of inoculation. * indicates $p<0.05$ in comparison to negative controls.

5.2.3.3. Antimicrobial assay of released HHC36

Antimicrobial potency of the released HHC36 was evaluated by a simple antimicrobial assay. The lack of visible bacteria colony, upon overnight incubation of the PCL(P)-

POPC(P) coating with 5 x 10^4 CFU *E. coli*, illustrated that the released AMPs retained their antimicrobial potency, killing all planktonic microbes upon their release. Coating was subjected to further cycles of repeated bacterial inoculations. Bacterial growth was significantly inhibited up to the ninth cycle of inoculation (Figure 5.7). Bacterial growth was completely inhibited on the first four rounds of bacterial inoculation. On the fifth round of inoculation, an increase in bacteria count is observed. This could be due to the drop in amount of AMP released from the PCL(P)-POPC(P) coating below its MIC, hence unable to completely inhibit the growth of the inoculated bacteria. Bacteria growth rate was inhibited to similar extent from the 5^{th} to 7^{th} cycle of bacterial inoculation. The result seemed to suggest that the amount of AMP released from the PCL(P)-POPC(P) coating on the 5^{th}, 6^{th} and 7^{th} round of bacteria inoculation stays relatively constant, accounting for the similarity in CFU for the respective cycles. Antimicrobial properties of the PCL(P)-POPC(P) coating continue to drop subsequently, eventually completely losing its bactericidal functionality on the 9^{th} inoculation cycle. The result demonstrates that bactericidal property of HHC36 was preserved upon prolonged encapsulation within PCL-POPC matrix and subsequent release.

The use of strong organic solvent, extended periods of drying under humid atmospheric environment and prolonged residence within the highly hydrophobic PCL polymer could often compromise peptide integrity, resulting in peptide inactivation and denaturation. To investigate the integrity of the encapsulated, and subsequently, released peptides, secondary structure of released HHC36 was studied using CD spectroscopy, and compared with native peptides (Figure 5.5). The CD fingerprint of native HHC36 is comparable to that reported in the literature for HHC36 [253]. Figure 5.5 shows that the CD spectra of the released HHC36 closely resemble those of the native peptide. The AMP's inherent mixed turn conformation in PBS, and alpha helical conformational

adaptation in the presence of membrane-mimicking SDS, were retained in the peptide encapsulation and subsequent release process. The fluorescence emission spectrum of tryptophan-rich AMPs is often used as a criterion to determine the extent of AMP penetration into bacteria membrane [266, 267]. A blue shift, decrease in the wavelength at which emission peak occurs, is representative of the peptide's insertion into the hydrophobic acyl chain region of the bacterial phospholipid membrane [268]. Similarities in the emission maxima and fluorescence intensity confirm the conservation of the peptide's structure and membrane permeabilizing functionality. The membrane permeabilizing potency of the released HHC36 remained unaffected by the encapsulation process, as illustrated by identical magnitude of blue shifts (8 nm) for the released and native HHC36 peptides. Antimicrobial activity of the released AMP was verified using an antimicrobial assay. The released HHC36 retained its bactericidal properties, completely killing the inoculated 5 x 10^4 CFU *E. coli*. Antimicrobial action of the encapsulated AMPs was also shown to be retained with prolonged encapsulation (Figure 5.7). The use of TFE, a common helix stabilizing agent [261] as solvent is hypothesized to play a crucial role in preserving the structural integrity of the peptide during the encapsulation process. The pivotal role of TFE in protecting peptide integrity and antimicrobial functionality against harsh environmental conditions, such as pH, temperature and denaturing reagent, is highlighted in a recent study [269]. The use of TFE as a solvent in this study resulted in the HHC36 peptides adopting a highly stable alpha helical secondary conformation, which opens the way for subsequent encapsulation and release steps.

5.2.4. Coating PCL(P)-POPC(P) onto silicone Foley catheters

The same PCL(P)-POPC(P) coating platform was extended onto commercially available silicone Foley catheters. Figure 5.8A shows the schematic for the coating

procedure. The catheter was coated with layers of HHC36-rich PCL polymer and POPC. Figure 5.8B compares the untreated and coated silicone catheter in terms of physical appearance. The coating process renders the catheter with a continuous, translucent polymer coating on the catheter surface. FESEM imaging of the coated catheter's cross section showed that the PCL(P)-POPC(P) layer was approximately 10 μm thick (Figure 5.8C). The coating was applied to both the intraluminal and extraluminal catheter surfaces, to render antimicrobial protection for both surfaces of the catheter for superior protection against bacteria.

(A)

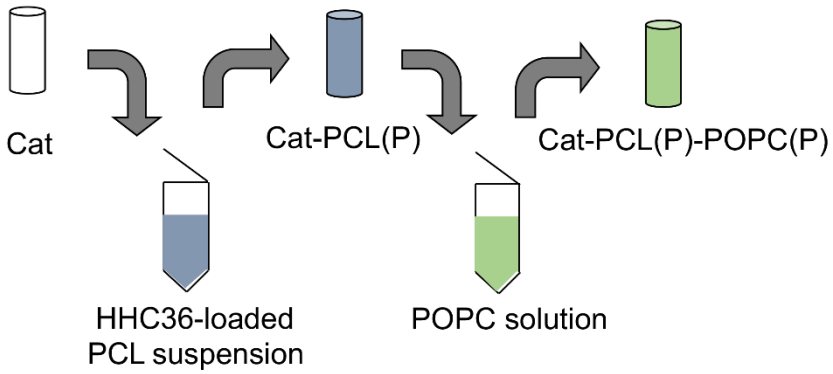

(B)

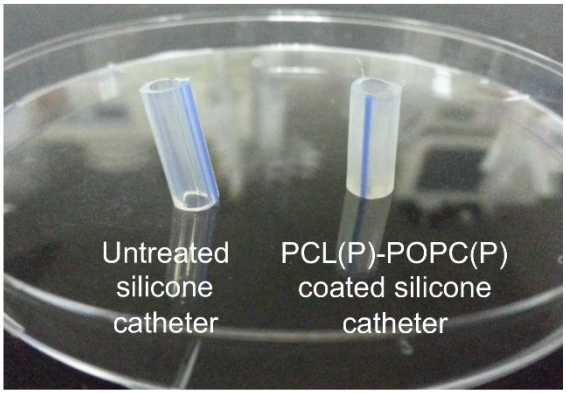

(C)

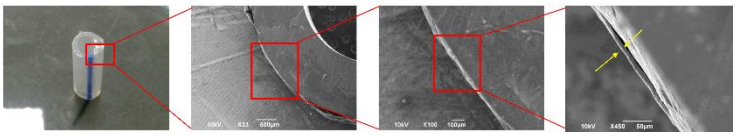

Figure 5.8. Coating of AMP-impregnated PCL-POPC onto silicone Foley catheters. (A) Schematic of AMP-impregnated dual layer coating process onto silicone catheter surface. (B) Cat-PCL(P)-POPC(P) showed a transparent and translucent surface. (C) Cross-sectional SEM micrographs of Cat-PCL(P)-POPC(P) at various magnifications (0x, 33 x, 100 x and 450 x). The coating thickness (indicated by yellow arrows) was ascertained to be approximately 10 µm.

5.2.5. Antimicrobial and anti-biofilm activity of Cat-PCL(P)-POPC(P)

The presence of PCL(P)-POPC(P) coating on the silicone catheter resulted in excellent antimicrobial activity against *E. coli* (Figure 5.10A), which is comparable to that of the

commercial silver Dover catheter. Similar antimicrobial results were observed against *S. aureus* and GFP-*P. aeruginosa*, demonstrating the efficacy of HHC36-loaded catheters against UTI-related pathogen strains.

To examine if Cat-PCL(P)-POPC(P) possessed an antifouling property, biofilm assays were performed, where the catheter was incubated with 1 x 10^8 CFU *E. coli* for 18-24 h. Negligible amount of bacteria was found adhering onto the treated catheter surface (Figure 5.10B). Cat-PCL(P)-POPC(P) slightly outperformed the silver Dover catheter in preventing bacteria adherence, where the former achieved almost 100.0 ± 0.0 % reduction in bacteria adhesion versus 95.9 ± 1.5 % reduction for the latter relative to untreated controls.

After 24 hours of incubation with 1 x 10^7 CFU GFP-*P. aeruginosa*, Cat-PCL(P)-POPC(P) and untreated catheter surfaces were examined by SEM. Figure 5.10 (bottom) shows a dense network of cellular multilayers on the untreated silicone catheter, which is surrounded and enveloped by a protective matrix. In contrast to the untreated catheter surface, no viable bacteria can be observed on the Cat-PCL(P)-POPC(P) surface, even upon prolonged incubation with GFP-*P. aeruginosa*. Small cell debris can occasionally be seen attached to the coating surface (as indicated by the yellow arrows in Figure 5.10), indicating that planktonic microbes were lysed prior to surface attachment. It is suggested that planktonic bacteria were targeted and killed by the released AMPs before they can execute any sort of interaction and attachment onto the coating surface. Such trait is commonly observed in antimicrobial compound releasing coating [270, 271].

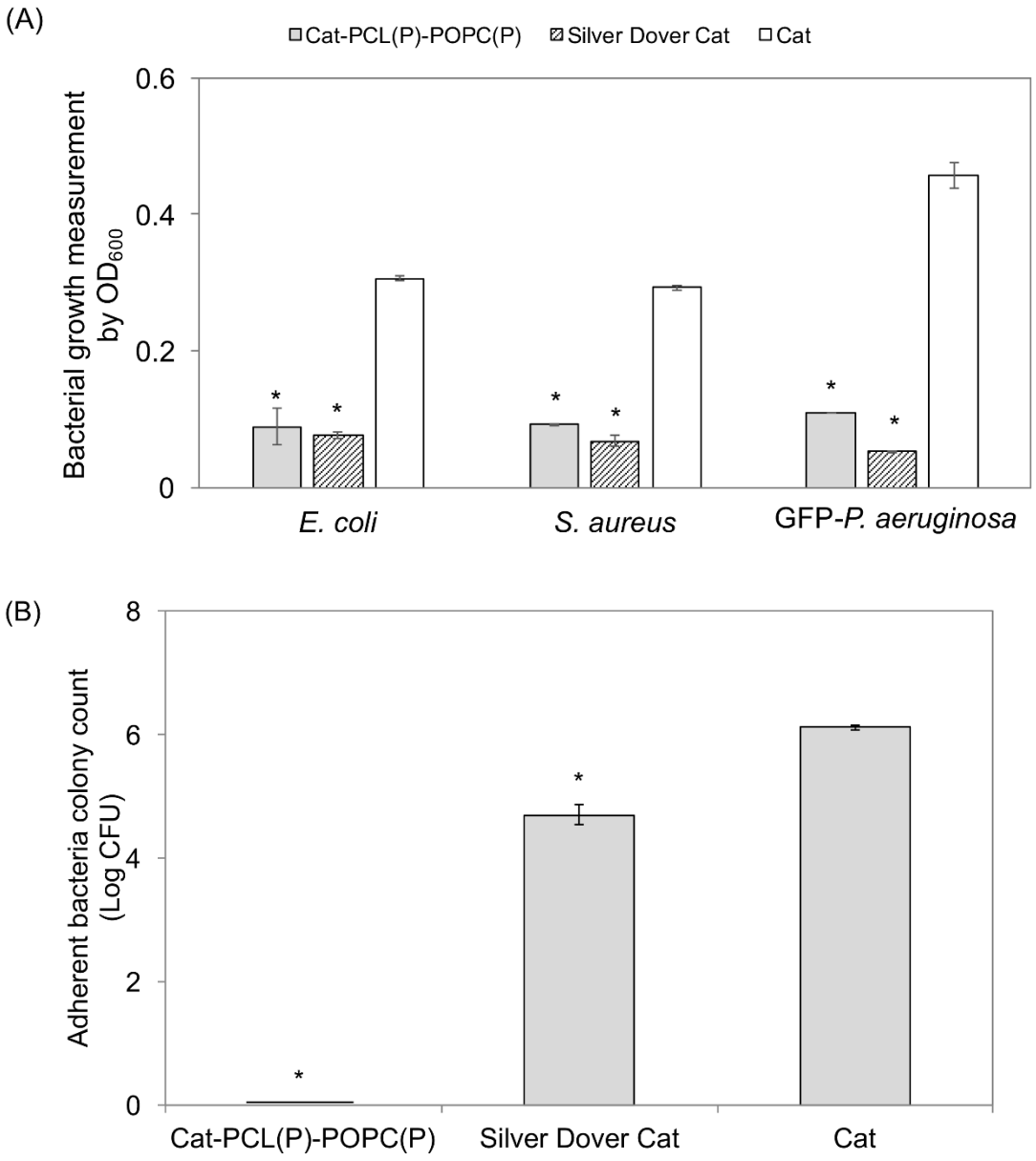

Figure 5.9. Antimicrobial and anti-biofilm property of Cat-PCL(P)-POPC(P). (A) Antimicrobial activities of Cat-PCL(P)-POPC(P) against *E. coli*, *S. aureus* and GFP-*P. aeruginosa*. Optical density (OD600) of overnight bacterial cultures were recorded as an indication of bacteria growth. Untreated and silver Dover catheters were used as negative and positive controls, respectively. (B) Anti-biofilm assessment of Cat-PCL(P)-POPC(P). Coated and untreated catheters were exposed to a high concentration of *E. coli* (~1 x 10^7 CFU) and incubated at 37 ^{o}C for 24 h. The extent of biofilm development was quantitated by adherent bacteria counts. * indicates $p<0.05$ in comparison to untreated control catheters.

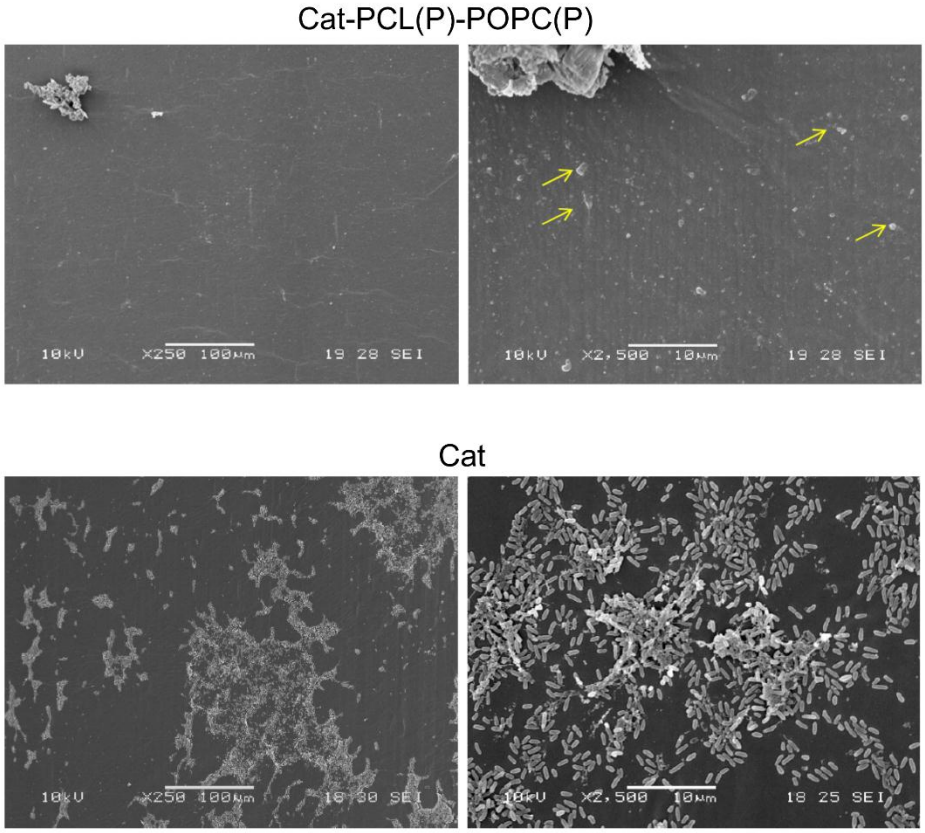

Figure 5.10. SEM imaging of coated and untreated catheters upon overnight exposure to high bacteria exposure after 24 h incubation. Yellow arrow indicating lysed cell debris due to antimicrobial action of released HHC36.

To investigate if the PCL(P)-POPC(P) coating was effective when challenged repetitively with bacteria, the coated catheter was subjected to 5 successive rounds of bacteria incubation followed by antimicrobial assays (Figure 5.11). Bacteria growth was significantly inhibited relative to the uncoated surfaces in the first four cycles of assay, but eventually succumbed to bacteria colonization in the fifth round of incubation with fresh bacteria (Figure 5.12A). Compared to Cat-PCL(P)-POPC(P), the bactericidal efficacy of the commercial silver Dover catheter was lost upon the second round of bacteria incubation. Bacterial growth rate of the sample incubated with silver Dover catheter was similar to that

of the untreated control for the third, fourth and fifth inoculation cycles. Plugging of hydrogel pores by bacterial binding could result in lesser silver ions released for significant antimicrobial action from the third inoculation cycle onwards for the silver Dover catheter. Figure 5.12B shows a 3 log reduction in *E. coli* attachment to the Cat-PCL(P)-POPC(P) and silver Dover catheter surfaces, in contrast to the untreated silicone catheter. The released antimicrobial agents from Cat-PCL(P)-POPC(P) and silver Dover catheter is hypothesized to significantly resist bacteria adherence and delay onset of biofilm development.

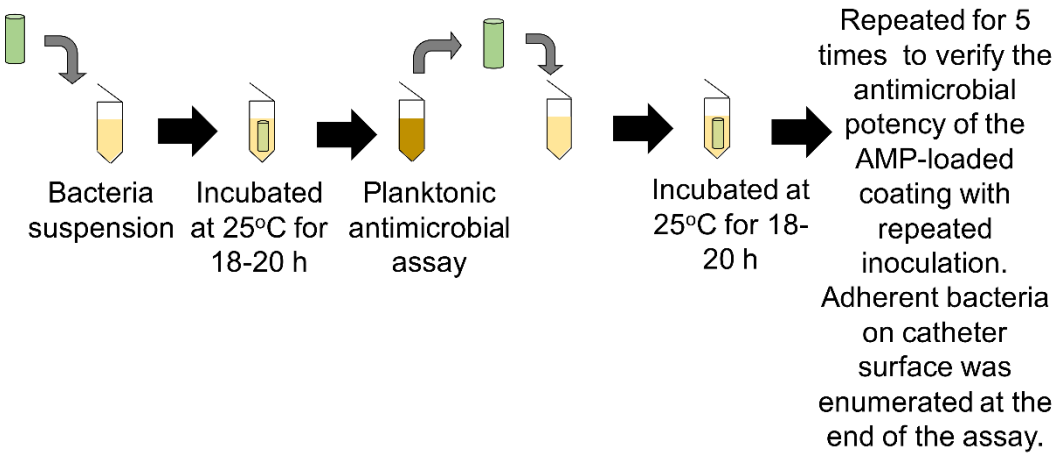

Figure 5.11. Antimicrobial activities of Cat-PCL(P)-POPC(P) against *E. coli* after 5 cycles of bacteria inoculation at every 24 h interval. At every 24 h interval, the samples were incubated with a fresh suspension of bacteria culture at equal volume for another 24 h, and the OD_{600} of the overnight culture was recorded as an indication of *E. coli* growth.

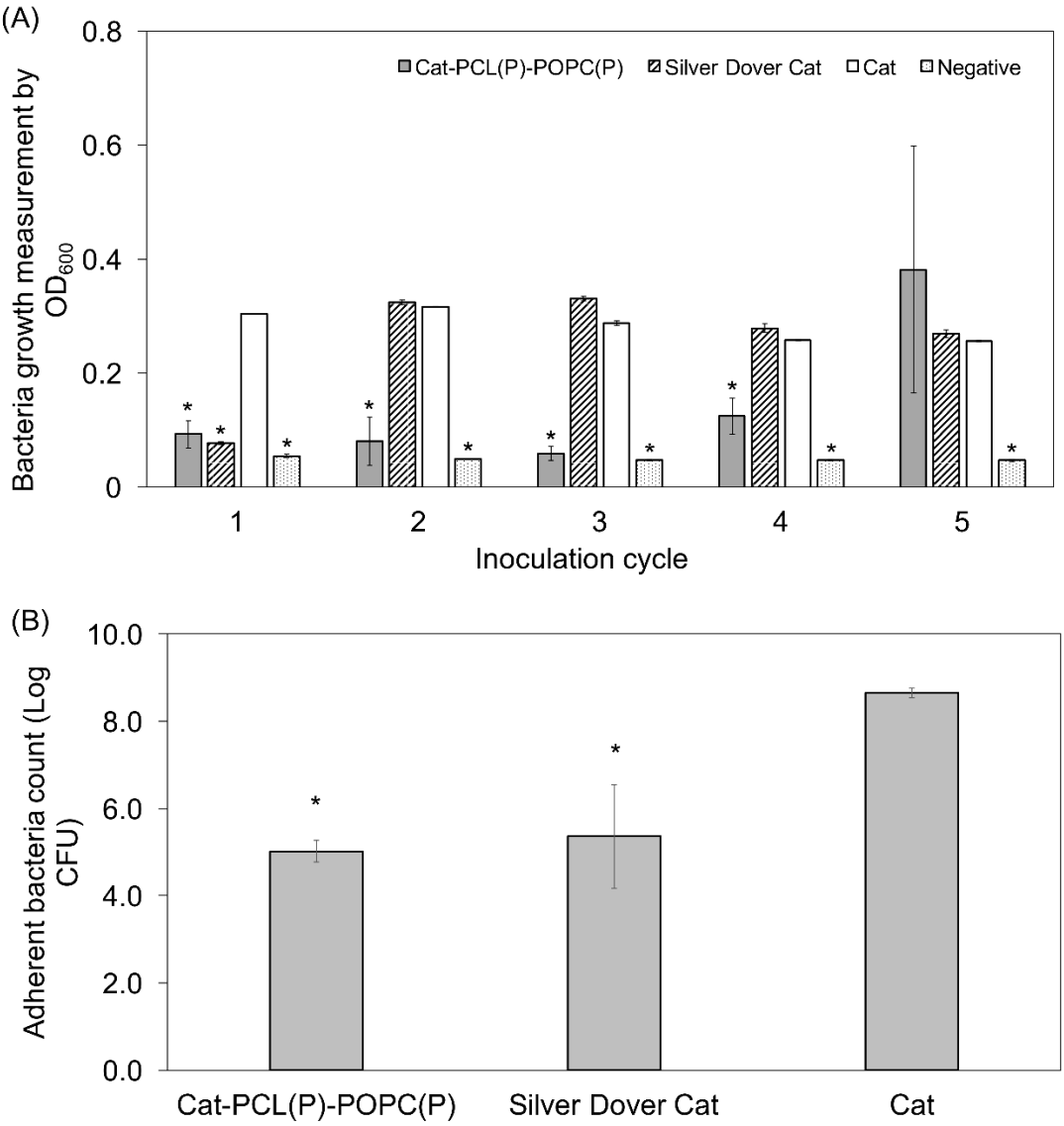

Figure 5.12. Antimicrobial activity of Cat-PCL(P)-POPC(P) when challenged with repeated bacteria incubation. (A) In the first four cycles, Cat-PCL(P)-POPC(P) significantly inhibited bacterial growth but lost its bactericidal action during the fifth inoculation cycle. (B) Adherent bacteria count on Cat-PCL(P)-POPC(P) and control catheters after five cycles of bacteria inoculation. * indicates $p<0.05$ in comparison to untreated control catheters.

5.2.6. Biocompatibility of Cat-PCL(P)-POPC(P)

5.2.6.1. hRBC hemolysis

The hemocompatibility of Cat-PCL(P)-POPC(P) was examined by comparingthe hRBC hemolytic rate of Cat-PCL(P)-POPC(P) with the untreated silicone catheters (Figure 5.13A). Although the coated catheter demonstrated a slightly higher hemolytic rate (2.14 ± 0.08 %) in contrast to the untreated control (0.34 ± 0.08 %), the hemolytic value of the former still falls within the acceptable clinical cytotoxicity level (10%) [145, 163].

5.2.6.2. Uroepithelial cell viability assay

The cytotoxic effect of Cat-PCL(P)-POPC(P) on uroepithelial cell viability was evaluated through a simple MTT assay. The released HHC36 was non-cytotoxic towards human SV-HUC-1 uroepithelial cells, with a near 100% cell viability achieved upon overnight incubation with Cat-PCL(P)-POPC(P) (Figure 5.13B).

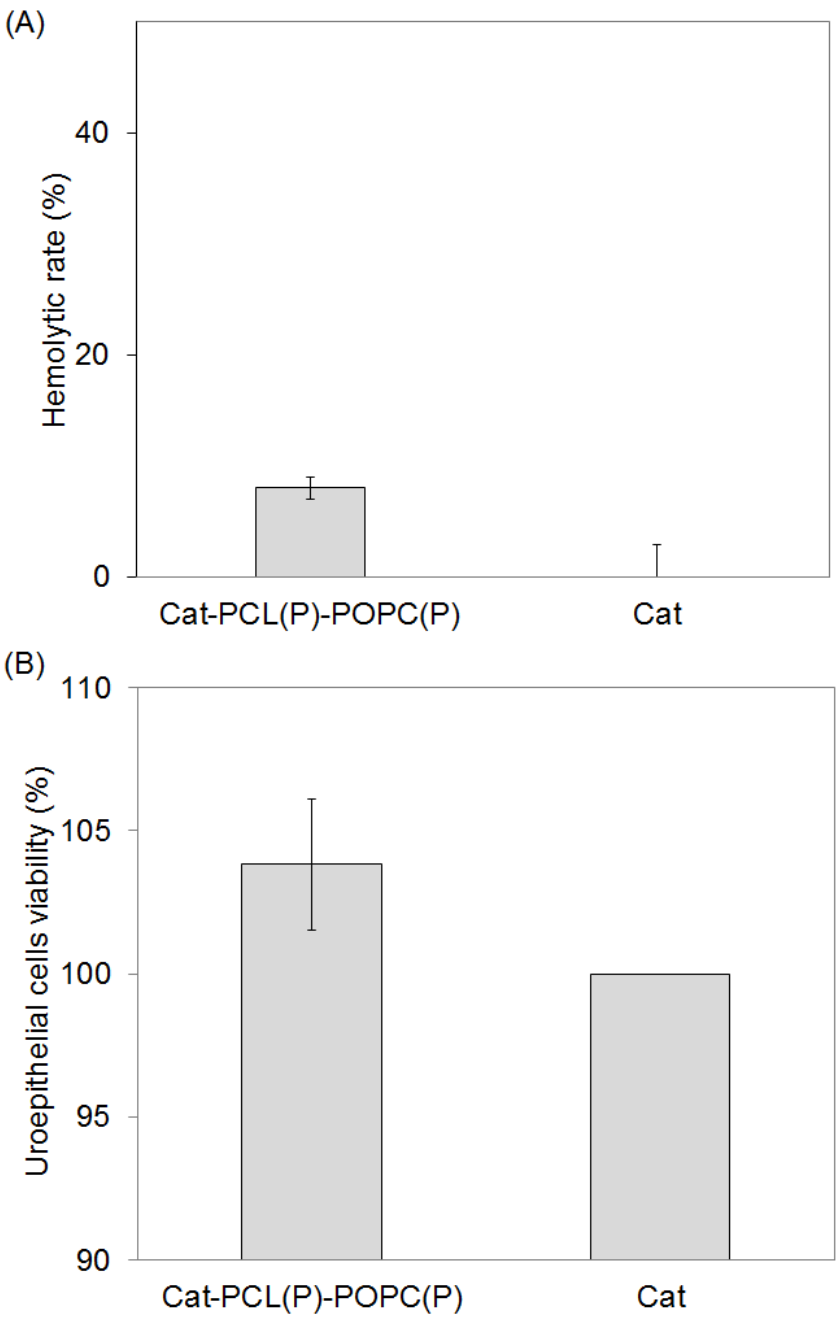

Figure 5.13. Biocompatibillity assay of Cat-PCL(P)-POPC(P). (A) The hemolytic activity of coated and control catheters after incubation with 5% hRBCs for 1 h at 37°C. A low extent of hemolysis was observed for the AMP-coated catheter. (B) Uroepithelial cell viability assay upon overnight incubation with Cat-PCL(P)-POCP(P). Released HHC36 showed excellent biocompatibility with uroepithelial cell, achieving ~100% cell viability.

HHC36 has been demonstrated to be highly hemocompatible, with minimal RBC lysis even at a high concentration of 251 μM [272]. Biocompatibility assay with uroepithelial cells and hRBCs confirmed that released HHC36 from the PCL(P)-POPC(P) coating retained its excellent selectivity, where a low hemolysis rate (~2%) and high cell viability (~100%) was attained.

5.3. Conclusion

This chapter reports the development and proof-of-concept demonstration of the feasibility of a thin adherent multilayer coating, based on PCL and POPC, impregnated with AMP for sustained antimicrobial protection. The coating layer was created using a simple “drip and dry” method, which is expected to be readily scalable. Encapsulation of HHC36 into the polymer layers did not compromise the peptide’s integrity and functionality. The deployment of a POPC layer as a diffusing barrier enabled more controlled and sustained peptide release, with a moderate burst release, followed by an optimal first order release kinetics. Transfer of the PCL-POPC coating to the silicone catheter showed good efficacy, where the coated catheters exhibited potent antimicrobial and anti-biofilm action against multiple UTI-relevant bacterial strains, inhibiting bacterial growth up to 4 days of bacteria exposure. The coated implant also demonstrated good biocompatibility against both hRBC and uroepithelial cells. Overall, this dual layer coating demonstrated excellent functionality, highlighting its potential as a therapy or prophylactic measure for curbing CAUTI in both short and long term catheterization.

Chapter 6 Overall conclusion and future directions

6.1. Overall conclusion

The drastic increase in nosocomial infection frequency and rise of antibiotic resistant bacteria have prompted the research community to search for an antimicrobial alternative. The potent, broad spectrum antimicrobial property coupled with low resistance development tendencies of AMPs have rendered these short peptides one of the most viable candidates to replace antibiotics in treating bacterial infection. The aim of this research project was to develop an effective AMP-based antimicrobial coating for silicon surfaces that can be readily translated to urinary catheters. Two types of AMP coating platforms were successfully developed; i.e., (i) contact active and (ii) controlled release platforms.

Chapter 3 presents the development of an in-house synthetic AMP (CWR11) which was rationally engineered to possess effective, salt-resistant antimicrobial action against both gram-positive and gram-negative uropathogens. CWR11 exhibited membrane lytic action of mechanism which was confirmed qualitatively using FESEM analysis, and quantitatively *via* NPN uptake and PI fluorescence assays. The synthetic peptide was subsequently immobilized onto model PDMS surfaces *via* an 'AGE-polymer brush' based chemical coupling strategy. Inert silicone surfaces were first activated with plasma radiation before being functionalized with AGE polymer brushes. Heterobifunctional PEG linkers and subsequently CWR11, were grafted onto reactive epoxide terminal groups of these AGE polymer brushes. The successful surface immobilization of CWR11 was verified by surface

characterization assays such as water contact angle measurements, surface atomic XPS spectroscopy and ATR-FTIR spectroscopy. The CWR11-immobilized PDMS surface exhibited broad spectrum microbial killing and anti-biofilm properties against prevalent uropathogens such as *E. coli*, GFP-*P. aeruginosa* and *S. aureus*. Superb biocompatibility with hRBCs and SMCs illustrated the non-cytotoxic nature of the AMP-immobilized surface. However, the requirement for plasma surface activation limits the applicability of this immobilization platform to only flat surfaces. Moreover, prolonged exposure to strong plasma radiation and intense UV can also potentially compromise material integrity, leading to premature failure of the material. For these reasons, another AMP immobilization platform was next developed to overcome these challenges.

In Chapter 4, an alternative PD-based immobilization platform was developed for CWR11 grafting. Unlike the previous chemical coupling strategy, where plasma surface activation was required, the PD-based platform involves a simple surface activation process that can be easily achieved by dip-coating. Briefly, the inert PDMS surface was functionalized with a thin PD layer by extended immersion in alkaline PD solution. Reactive catechol groups exposed on the PDMS-PD surface present viable sites for subsequent CWR11 grafting. The candidate peptide can be grafted onto the PD functionalized surface *via* (1) sulfhydryl chemistry between the peptide's thiol and PD's catechol groups, (2) Michael's addition between peptide's amine and PD's catechol groups, and/or (3) non-specific physical adsorption. The 'dip-coating'-based platform meant ease of application to substrates of any shape and size. Moreover, the whole immobilization process involves the use of mild reagents (50 mM Tris buffer), which minimized the possibility of material degradation due to damaging radiation or strong corrosive chemicals. The short dual-step immobilization process yielded a four-fold higher peptide grafting efficacy, as compared to the previous three-step process, i.e. to achieve an immobilized peptide surface

concentration of 3.41 ± 0.76 μg/cm^2 compared to 0.8 ± 0.2 μg/cm^2, respectively. The immobilization of peptides was also subsequently confirmed by increased surface roughness (as determined by AFM analysis) and nitrogen atomic percentage (as measured by XPS spectroscopy). The CWR11-impregnated PDMS exhibited good antimicrobial activity, completely inhibiting 5 x 10^4 CFU of selected uropathogen growth, within 3 hours of bacteria incubation. The PDMS-PD-CWR11 samples showed superior anti-biofilm properties which significantly resisted bacteria adherence even under biofilm promoting environment. The same immobilization strategy was applied to graft CWR11 on silicone urinary catheter surfaces. CWR11-immobilized silicone Foley catheters demonstrated similar antimicrobial and anti-biofilm properties as the peptide-treated PDMS surfaces, as well as excellent stability, thus opening the way for the development of an AMP-based contact active antimicrobial urinary catheter for CAUTI prevention.

In Chapters 3 and 4, CWR11 was successfully immobilized onto model PDMS and silicone catheter surfaces. Despite the potent surface bactericidal action, these CWR11-immobilized surfaces are only contact active which implies that they are only efficient against bacteria which are in close proximity to the surface. Planktonic bacteria are not effectively targeted and can proliferate extensively, eventually overcoming the surface-immobilized AMP, rendering the contact active surface useless. To address this limitation, an AMP coating with controlled release functionality is needed to further improve antimicrobial efficacy. In Chapter 5, an AMP-impregnated layer-by-layer coating was developed, which composed of basal PCL polymer matrix layered with a thin POPC film. The assembly illustrated an ideal peptide release kinetics, with a moderate burst release in the first 24 h for thorough site sterilization, killing any planktonic bacteria present in the environment. Sustained, significant AMP released was observed for the subsequent 30 days as prophylactic measure against possible subsequent bacterial infection. To the best

of our knowledge, this is the first polymer-based AMP release platform developed to curb bacteria colonization. Characterization assays with CD and fluorescence spectroscopy demonstrated conservation of AMP's conformational integrity and bactericidal mechanism upon encapsulation and subsequent release from dual layer assembly. In the second part of the study, the PCL-POPC coating platform was applied to silicone Foley urinary catheters. The coated catheters (Cat-PCL(P)-POPC(P)) exhibited superior antimicrobial and anti-biofilm properties against prevalent uropathogens. When challenged with multiple bacterial inoculation cycles, Cat-PCL(P)-POPC(P) retained good antibacterial functionality and significantly inhibited bacterial growth (5×10^4 CFU *E. coli*) up to 4 cycles of repeated inoculation. The excellent AMP release profile, coupled with the stability of the released peptides, indicate great potential for development of the PCL-POPC coating platform for AMP controlled release functionality on urinary catheters for treatment and/or prevention of CAUTI in both short and long term-catheterized patients.

The results from this thesis provides proof-of-concept demonstration for the deployment of AMPs and their immobilization on biomedically-relevant surfaces to eradicate bacteria colonization and biofilm formation. These scalable AMP-based antimicrobial coating platforms are also expected to be readily translated to other biomedical devices and implants (e.g. intravascular stents, artificial heart valves, and contact lenses), as well as food and pharmaceutical packaging where bacterial contamination is a common problem. Overall, the outcomes of these studies have contributed to new knowledge in strategies for rational engineering of peptides for enhanced peptide functionality and improved knowledge in structural-activity relationship of AMPs. This new knowledge will advance research in the design and synthesis of novel and potent antimicrobial products with desired properties. The proof-of-concept demonstration that AMPs can retain their antimicrobial potency in the tethered form opens the possibility for AMPs to be utilized as

antimicrobial coating agents. *In vivo* studies to determine the safety and efficacy of AMP-immobilized catheters in animal models are currently underway. The overall outcome of this research project provides strong evidence that AMP-based coating shows great potential as an effective therapy to address CAUTI for short and term long catheterization.

6.2. Future directions

With the engineering of synthetic peptide CWR11, development of PD-based immobilization platform and formulation of dual layer PCL-POPC coating, we had successfully come up with AMP-based coating that can be applied onto urinary catheter surfaces to impart antimicrobial contact active or controlled release functionalities. However, this is not the final product, and is still far from clinical applicability. There are still several areas that need to be further optimized, including enhancement of AMP grafting efficacy and optimization of immobilization factors for PD-based immobilization platform to increase contact active antimicrobial potency, augmentation of PCL-based controlled release platform to improve AMP release profile for a better and more sustained antimicrobial performance. With the optimization studies done, it is critical that these coatings be tested in mice models to investigate their antimicrobial efficacy and biocompatibility under *in vivo* condition.

6.2.1. Optimization of PD-based AMP immobilization strategy

Enhancement and optimization of the PD-based AMP immobilization strategy, reported in Chapter 4, will be performed to further improve the AMP grafting efficiency and specificity to optimize the development of an efficient contact active antimicrobial surface. The platform developed so far allows peptides to be attached to the PD-coated surface *via* three different coupling methods, i.e., sulfhydryl linkages, Michael's addition and/or

physical adsorption. Having such diverse and random peptide immobilization chemistries may pose challenges for future product development and scale up manufacture as it can potentially lead to undesirable batch-to-batch inconsistencies. The use of controlled covalent immobilization strategy which employs the thiol group on CWR11 is proposed. These thiol groups will specifically react with thiol or maleimide groups that can be functionalized onto PD-coated surfaces using specific moieties such as heterobifunction PEG moieties utilized in the immobilization platform reported in Chapter 3. The surface peptide concentration and antimicrobial performances achieved using this platform will be compared with those achieved *via* random immobilization (as reported in Chapter 4) to assess the effect of thiol coupling on peptide immobilization and bactericidal efficacy.

Various studies have highlighted the correlation between immobilized peptide concentration on subsequent surface bactericidal action. It is generally proposed that there is a positive correlation between AMP concentration and antimicrobial efficacy. Based on the immobilization platform reported in Chapter 4, as each surface catechol group is assumed to be coupled to one peptide molecule, the concentration of immobilized peptides is thus limited by the number of reactive catechol group on the PD-coated surface. The problem of limited surface active groups can be circumvented by utilizing multi-branch linkers to allow more AMPs to be attached to a single reaction site on the surface. The use of this platform can then facilitate further studies to investigate the significance of immobilized peptide concentration on surface bactericidal activity. A potential difficulty for this would be to find a compatible multi-branch linker. Current conventional way involves building polymer brushed onto the surface often involving harsh treatment conditions and complicated process, defeating the purpose of developing the PD-based immobilization platform.

6.2.2. Study of the effect of immobilization factors on the antimicrobial activity of tethered peptides

Numerous factors such as the role of spacers, linker chain length, surface peptide concentration and immobilized peptide orientation have been highlighted by separate studies as crucial elements determining the efficacy of immobilized peptides' activity. Admittedly, the real influence of these factors in affecting surface antimicrobial activity is very often found to be platform- and peptide-specific. To further optimize the antimicrobial performance of tethered AMPs in PD-based platform, it is considered important to better understand the effect of the above-mentioned factors on the immobilized AMP activity.

The effect of linker chain length on immobilized AMPs' bactericidal action has been widely debated. While some studies emphasized the importance of long spacers for peptide structural flexibility and antimicrobial potency [145], others debunked the need for an additional linker as the additional step might compromise AMP tethering efficiency [148]. Systematic studies to evaluate the role of spacers and the subsequent effect of varying the spacer length on immobilized peptide antimicrobial activity using the current PD-based immobilization platform are planned. Briefly, PEG linker with varying length (e.g. 200 Da, 500 Da, 5000 Da) will be used for specific AMP attachment to reactive PD surfaces. Comparison of the antimicrobial potency of the respective AMP-immobilized platforms will shed light on the role of linker length on grafted peptides' bactericidal action.

Peptide conformation is also extremely crucial in driving bacterial membrane permeabilization and hence bactericidal action. However, few studies have been conducted to investigate the effect of orientation and conformation of tethered AMPs on their corresponding membrane permeation mechanism. The complex immobilization process of previously reported coupling strategies place constraints on the feasibility of

such studies, as the use of multifarious surface functionalization chemistry and multiple linkers and/or spacers tend to lower signal to noise ratio, and hence resolution of the analysis result. The simpler PD-based coupling strategy presented in Chapter 4 makes the surface peptide structural-activity relationship study more viable. The use of biophysical analytical tools, such as elipsometry, Quartz Crystal Microbalance with dissipation (QCM-D) and surface CD, to non-destructively monitor peptide immobilization and tethered peptide conformation at real time will be performed. Correlation between peptide orientation, surface density and conformational flexibility can thus be evaluated and will be crucial to further improve PD-based AMP immobilization platform for maximum antimicrobial potency. However, the aforementioned analytical tools only provide indirect or low resolution imaging of the surface immobilized peptides. Higher resolution equipment, such as solid state NMR, is needed.

6.2.3. Optimization of PCL-based controlled release platform

In Chapter 5, a PCL-POPC dual layer assembly was introduced as an AMP-based controlled release platform. Despite the superb release kinetics and sustained antimicrobial action against planktonic bacteria, further optimization can be conducted to enhance the coating performance. For example, the current PCL-POPC platform reports a relatively slow peptide release rate, releasing ~48% of the total loaded AMP after 30 days. Modifications to the basal PCL matrix and physically adsorbed POPC layer can therefore be made to enhance the release rate. PEG can be incorporated within the dense hydrophobic PCL network to enable faster and more efficient escape of peptides that are trapped deep within the matrix. *Chen* et al. demonstrated in an earlier study that more than 90% of the total incorporated drug was released in PLLA-PEG-PLLA microparticles, as compared to the 45% observed in pure PLLA setup [273]. The authors suggested that the

introduced PEG fragments act as ‘water pumps’, facilitating drug escape. In a similar way, it is hypothesized that by introducing PEG hydrophilic channels/pockets into the PCL matrix, more AMPs can be released within the 30 days treatment period. A systematic study will be conducted to determine the ideal PEG content in order to achieve ideal AMP release profile.

In the platform reported in Chapter 5, POPC, which serves as barrier to modulate peptide release, was physically adsorbed onto the PCL matrix surface. Such physical adsorption may pose downstream problems for product design and development, as it could potentially lead to batch-to-batch variability. The search for an alternative AMP-compatible diffusion barrier is ongoing, where poly(SBMA-co-AAM) is considered an interesting potential candidate. In a recent study, Wang *et al*. developed a multilayer silver release platform grafted with a superficial poly(SBMA-co-AAM) layer as diffusion boundary [274]. Sustained silver release was observed for 50 days. The zwitterionic poly(SBMA-co-AAM) coating has also been demonstrated to effectively reduce bacterial adherence and biofilm formation. The excellent release modulating property, coupled with good anti-biofilm functionality, makes poly(SBMA-co-AAM) an excellent potential alternative to POPC. However, further studies are needed to investigate the compatibility of the polymer layer with peptides. On top of that, although poly(SBMA-co-AAM) has been shown to demonstrate excellent physical properties as well as release modulating functionality, attachment of it is still dependent on physical attachment, which is still non-ideal as a long term solution. A boundary layer that can be covalently attached to the basal AMP-impregnated PCL layer is still much needed.

6.2.4. *In vivo* safety and efficacy studies in animal models

Upon completion of the platform optimization studies and in view of the ultimate aim to use these AMP-based coatings for clinical applications, it is critical that the safety and efficacy of these AMP-impregnated platforms are investigated in mice models. Established experimental protocols reported in earlier studies [256] will be adapted to assess the antimicrobial capability of the optimised AMP-coated catheters. Briefly, 7 to 8 weeks old mice will be anesthetized and transurethrally implanted with AMP-coated and control catheters. 1 x 10^7 CFU of bacteria suspension is then immediately introduced into the bladder lumen. The animals will be sacrificed at appropriate time points (i.e., 6 h or 24 h). Catheters will then be retrieved from the bladder, immersed in PBS, and sonicated for 10 min followed by vortexing vigorously for 5 mins to detach any adherent bacterial on catheter surface, to demonstrate anti-biofilm property of these antimicrobial catheters under *in vivo* situation. Bladders and kidneys from mice will also be homogenized in PBS and serially diluted for CFU enumeration to test for antimicrobial efficacy of coating against planktonic bacteria. *In vivo* biocompatibility of antimicrobial catheters can be verified by investigating the viability of the surrounding murine uroepithelial cells, through extensive cell sectioning and live/dead staining. The downsizing of the respective platforms onto a mouse catheter might adversely affect their antimicrobial potency, hence unable to exert similar extent of bactericidal action as seen when applied on the PDMS and catheter. Based on preliminary results, further optimizations, such as increased peptide loading, might be required to ensure good *in vivo* antimicrobial potency in mouse models.

References

[1] McFee RB. Nosocomial or Hospital-acquired Infections: An Overview. Disease-a-Month. 2009;55:422-38.

[2] Klevens RM, Edwards JR, Richards CL, Horan TC, Gaynes RP, Pollock DA, et al. Estimating health care-associated infections and deaths in US hospitals, 2002. Public health reports. 2007;122:160.

[3] Tambyah PA, Oon J. Catheter-associated urinary tract infection. Current Opinion in Infectious Diseases. 2012;25.

[4] Regev-Shoshani G, Ko M, Miller C, Av-Gay Y. Slow Release of Nitric Oxide from Charged Catheters and Its Effect on Biofilm Formation by Escherichia coli. Antimicrob Agents Chemother. 2010;54:273-9.

[5] Donlan RM, Costerton JW. Biofilms: Survival Mechanisms of Clinically Relevant Microorganisms. Clinical Microbiology Reviews. 2002;15:167-93.

[6] Sileika TS, Kim H-D, Maniak P, Messersmith PB. Antibacterial Performance of Polydopamine-Modified Polymer Surfaces Containing Passive and Active Components. ACS Appl Mater Interfaces. 2011;3:4602-10.

[7] Warren JW. Catheter-associated urinary tract infections. Int J Antimicrob Agents. 2001;17:299-303.

[8] Lim K, Chua RRY, Ho B, Tambyah PA, Hadinoto K, Leong SSJ. Development of a catheter functionalized by a polydopamine peptide coating with antimicrobial and antibiofilm properties. Acta Biomaterialia. 2015;15:127-38.

[9] Gosbell I. Methicillin-Resistant Staphylococcus Aureus. Am J Clin Dermatol. 2004;5:239-59.

[10] Kim JS, Kuk E, Yu KN, Kim J-H, Park SJ, Lee HJ, et al. Antimicrobial effects of silver nanoparticles. Nanomedicine: Nanotechnology, Biology and Medicine. 2007;3:95-101.

[11] Lok C-N, Ho C-M, Chen R, He Q-Y, Yu W-Y, Sun H, et al. Silver nanoparticles: partial oxidation and antibacterial activities. JBIC Journal of Biological Inorganic Chemistry. 2007;12:527-34.

[12] Cook GS, Costerton J. Foley Catheter Biofilm Formation Comparison Study in an In-Vitro Assay. unknown publication date, http://www bacterin com/pdf/whitepaper pdf. 1991.

[13] Hola V, Peroutkova T, Ruzicka F. Virulence factors in Proteus bacteria from biofilm communities of catheter-associated urinary tract infections. FEMS Immunol Med Microbiol. 2012;65:343-9.

[14] Rauschmann MA, Wichelhaus TA, Stirnal V, Dingeldein E, Zichner L, Schnettler R, et al. Nanocrystalline hydroxyapatite and calcium sulphate as biodegradable composite carrier material for local delivery of antibiotics in bone infections. Biomaterials. 2005;26:2677-84.

[15] Dave RN, Joshi HM, Venugopalan VP. Novel Biocatalytic Polymer-Based Antimicrobial Coatings as Potential Ureteral Biomaterial: Preparation and In Vitro Performance Evaluation. Antimicrob Agents Chemother. 2011;55:845-53.

[16] Liedberg H, Lundeberg T. Assessment of silver-coated urinary catheter toxicity by cell culture. Urological Research. 1989;17:359-60.

[17] Ha US, Cho Y-H. Catheter-associated urinary tract infections: new aspects of novel urinary catheters. Int J Antimicrob Agents. 2006;28:485-90.

[18] Hancock REW, Lehrer R. Cationic peptides: A new source of antibiotics. Trends Biotechnol. 1998;16:82-8.

[19] De Lucca AJ, Walsh TJ. Antifungal Peptides: Novel Therapeutic Compounds against Emerging Pathogens. Antimicrobial Agents and Chemotherapy. 1999;43:1-11.

[20] Theis T, Stahl U. Antifungal proteins: targets, mechanisms and prospective applications. Cellular and Molecular Life Sciences CMLS. 2004;61:437-55.

[21] Andersen JH, Jenssen H, Sandvik K, Gutteberg TJ. Anti-HSV activity of lactoferrin and lactoferricin is dependent on the presence of heparan sulphate at the cell surface. Journal of Medical Virology. 2004;74:262-71.

[22] McPhee JB, Scott MG, Hancock REW. Design of host defence peptides for antimicrobial and immunity enhancing activities. Combinatorial Chemistry and High Throughput Screening. 2005;8:257-72.

[23] Yeaman MR, Yount NY. Mechanisms of Antimicrobial Peptide Action and Resistance. Pharmacological Reviews. 2003;55:27-55.

[24] Zilberman M, Elsner JJ. Antibiotic-eluting medical devices for various applications. Journal of Controlled Release. 2008;130:202-15.

[25] Jacobsen SM, Stickler DJ, Mobley HLT, Shirtliff ME. Complicated Catheter-Associated Urinary Tract Infections Due to Escherichia coli and Proteus mirabilis. Clinical Microbiology Reviews. 2008;21:26-59.

[26] Nicolle L. Catheter associated urinary tract infections. Antimicrobial Resistance and Infection Control. 2014;3:23.

[27] Lawrence EL, Turner IG. Materials for urinary catheters: a review of their history and development in the UK. Medical Engineering & Physics. 2005;27:443-53.

[28] Healthwise. Indwelling Foley Catheter for Women. 2012.

[29] Barford JMT, Coates ARM. The pathogenesis of catheter-associated urinary tract infection. Journal of Infection Prevention. 2009;10:50-6.

[30] Foxman B. Epidemiology of urinary tract infections: incidence, morbidity, and economic costs. The American Journal of Medicine. 2002;113:5-13.

[31] Johnson JR. Virulence factors in Escherichia coli urinary tract infection. Clinical Microbiology Reviews. 1991;4:80-128.

[32] Schwan WR. Survival of uropathogenic Escherichia coli in the murine urinary tract is dependent on OmpR. Microbiology. 2009;155:1832-9.

[33] Tambyah PA, Halvorson KT, Maki DG. A Prospective Study of Pathogenesis of Catheter-Associated Urinary Tract Infections. Mayo Clinic Proceedings.74:131-6.

[34] Curtis Nickel J, Downey J, Costerton JW. Movement of pseudomonas aeruginosa along catheter surfaces A mechanism in pathogenesis of catheter-associated infection. Urology.39:93-8.

[35] Katsikogianni M, Missirlis Y. Concise review of mechanisms of bacterial adhesion to biomaterials and of techniques used in estimating bacteria-material interactions. Eur Cell Mater. 2004;8.

[36] Withman B, Gunasekera TS, Beesetty P, Agans R, Paliy O. Transcriptional Responses of Uropathogenic Escherichia coli to Increased Environmental Osmolality Caused by Salt or Urea. Infect Immun. 2013;81:80-9.

[37] Elvy J, Colville A. Catheter associated urinary tract infection: what is it, what causes it and how can we prevent it? Journal of Infection Prevention. 2009;10:36-41.

[38] Agha Moghaddam N, Hosseini-Moghaddam SMM, Talebi M, Pourshafie MR. Diversity of Bacteria Isolated From Long- and Short-term Catheterized Patients. Journal of Medical Bacteriology. 2014;3:28-35.

[39] Reed D, Kemmerly SA. Infection Control and Prevention: A Review of Hospital-Acquired Infections and the Economic Implications. The Ochsner Journal. 2009;9:27-31.

[40] Apisarnthanarak A, Thongphubeth K, Sirinvaravong S, Kitkangvan D, Yuekyen C, Warachan B, et al. Effectiveness of multifaceted hospitalwide quality improvement programs featuring an intervention to remove unnecessary urinary catheters at a tertiary care center in Thailand. Infection Control. 2007;28:791-8.

[41] Bruminhent J, Keegan M, Lakhani A, Roberts IM, Passalacqua J. Effectiveness of a simple intervention for prevention of catheter-associated urinary tract infections in a community teaching hospital. American Journal of Infection Control.38:689-93.

[42] Loeb M, Hunt D, O'Halloran K, Carusone SC, Dafoe N, Walter SD. Stop Orders to Reduce Inappropriate Urinary Catheterization in Hospitalized Patients: A Randomized Controlled Trial. Journal of General Internal Medicine. 2008;23:816-20.

[43] Blodgett TJ. Reminder Systems To Reduce the Duration of Indwelling Urinary Catheters: A Narrative Review. Urologic nursing. 2009;29:369-79.

[44] Stekkinger E, van der Linden PJQ. A Comparison of Suprapubic and Transurethral Catheterization on Postoperative Urinary Retention after Vaginal Prolapse Repair: A Randomized Controlled Trial. Gynecologic and Obstetric Investigation. 2011;72:109-16.

[45] Dixon L, Dolan LM, Brown K, Hilton P. RCT of urethral versus suprapubic catheterization. British Journal of Nursing. 2010;19:S7-S13.

[46] Hakvoort RA, Thijs SD, Bouwmeester FW, Broekman AM, Ruhe IM, Vernooij MM, et al. Comparing clean intermittent catheterisation and transurethral indwelling catheterisation for incomplete voiding after vaginal prolapse surgery: a multicentre randomised trial. BJOG: An International Journal of Obstetrics & Gynaecology. 2011;118:1055-60.

[47] Maki DG, Tambyah PA. Engineering out the risk for infection with urinary catheters. Emerging Infectious Diseases. 2001;7:342-7.

[48] Meddings J, Rogers MAM, Krein SL, Fakih MG, Olmsted RN, Saint S. Reducing unnecessary urinary catheter use and other strategies to prevent catheter-associated urinary tract infection: an integrative review. BMJ Quality & Safety. 2013.

[49] Clarke K. Diagnosis, Treatment and Prevention of Catheter-Associated Urinary Tract Infections. J Womens Health, Issues Care 3. 2014;3:2.

[50] Hooton TM, Bradley SF, Cardenas DD, Colgan R, Geerlings SE, Rice JC, et al. Diagnosis, Prevention, and Treatment of Catheter-Associated Urinary Tract

Infection in Adults: 2009 International Clinical Practice Guidelines from the Infectious Diseases Society of America. Clinical Infectious Diseases. 2010;50:625-63.

[51] Wagenlehner FME, Cek M, Naber K, Kiyota H, Bjerklund-Johansen T. Epidemiology, treatment and prevention of healthcare-associated urinary tract infections. World Journal of Urology. 2012;30:59-67.

[52] Pestova E, Millichap JJ, Noskin GA, Peterson LR. Intracellular targets of moxifloxacin: a comparison with other fluoroquinolones. J Antimicrob Chemother. 2000;45:583-90.

[53] Richmond MH, Sykes RB. The β-Lactamases of Gram-Negative Bacteria and their Possible Physiological Role. In: Rose AH, Tempest DW, editors. Adv Microb Physiol: Academic Press; 1973. p. 31-88.

[54] Rahal JJ, Simberkoff MS. Bactericidal and Bacteriostatic Action of Chloramphenicol Against Meningeal Pathogens. Antimicrob Agents Chemother. 1979;16:13-8.

[55] Sato K, Matsuura Y, Inoue M, Une T, Osada Y, Ogawa H, et al. In vitro and in vivo activity of DL-8280, a new oxazine derivative. Antimicrob Agents Chemother. 1982;22:548-53.

[56] Nailor MD, Sobel JD. Antibiotics for Gram-Positive Bacterial Infection: Vancomycin, Teicoplanin, Quinupristin/Dalfopristin, Oxazolidinones, Daptomycin, Telavancin, and Ceftaroline. Medical Clinics.95:723-42.

[57] Snydman DR, Jacobus NV, McDermott LA, Lonks JR, Boyce JM. Comparative In Vitro Activities of Daptomycin and Vancomycin against Resistant Gram-Positive Pathogens. Antimicrob Agents Chemother. 2000;44:3447-50.

[58] King A, Phillips I, Kaniga K. Comparative in vitro activity of telavancin (TD-6424), a rapidly bactericidal, concentration-dependent anti-infective with multiple mechanisms of action against Gram-positive bacteria. J Antimicrob Chemother. 2004;53:797-803.

[59] Kolář M, Urbánek K, Látal T. Antibiotic selective pressure and development of bacterial resistance. Int J Antimicrob Agents.17:357-63.

[60] Neu HC. The Crisis in Antibiotic Resistance. Science. 1992;257:1064-73.

[61] Rai M, Kon K, Ingle A, Duran N, Galdiero S, Galdiero M. Broad-spectrum bioactivities of silver nanoparticles: the emerging trends and future prospects. Appl Microbiol Biotechnol. 2014;98:1951-61.

[62] Dizaj SM, Lotfipour F, Barzegar-Jalali M, Zarrintan MH, Adibkia K. Antimicrobial activity of the metals and metal oxide nanoparticles. Materials Science and Engineering: C. 2014;44:278-84.

[63] Prabhu S, Poulose E. Silver nanoparticles: mechanism of antimicrobial action, synthesis, medical applications, and toxicity effects. International Nano Letters. 2012;2:1-10.

[64] Wang R, Neoh KG, Kang E-T, Tambyah PA, Chiong E. Antifouling coating with controllable and sustained silver release for long-term inhibition of infection and encrustation in urinary catheters. Journal of Biomedical Materials Research Part B: Applied Biomaterials. 2014:n/a-n/a.

[65] Ansari M. Evaluation of antibacterial activity of silver nanoparticles against MSSA and MRSA on isolates from skin infections. Biology and Medicine. 2011.

[66] Sondi I, Salopek-Sondi B. Silver nanoparticles as antimicrobial agent: a case study on E. coli as a model for Gram-negative bacteria. J Colloid Interface Sci. 2004;275:177-82.

[67] Monteiro DR, Gorup LF, Silva S, Negri M, de Camargo ER, Oliveira R, et al. Silver colloidal nanoparticles: antifungal effect against adhered cells and biofilms of Candida albicans and Candida glabrata. Biofouling. 2011;27:711-9.

[68] Percival SL, Woods E, Nutekpor M, Bowler P, Radford A, Cochrane C. Prevalence of silver resistance in bacteria isolated from diabetic foot ulcers and efficacy of silver-containing wound dressings. Ostomy/wound management. 2008;54:30-40.

[69] Saint S, Veenstra DL, Sullivan SD, Chenoweth C, Fendrick A. THe potential clinical and economic benefits of silver alloy urinary catheters in preventing urinary tract infection. Archives of Internal Medicine. 2000;160:2670-5.

[70] Saint S, Elmore JG, Sullivan SD, Emerson SS, Koepsell TD. The efficacy of silver alloy-coated urinary catheters in preventing urinary tract infection: a meta-analysis. The American Journal of Medicine.105:236-41.

[71] Beattie M, Taylor J. Silver alloy vs. uncoated urinary catheters: a systematic review of the literature. Journal of Clinical Nursing. 2011;20:2098-108.

[72] Desai DG, Liao KS, Cevallos ME, Trautner BW. Silver or Nitrofurazone Impregnation of Urinary Catheters Has a Minimal Effect on Uropathogen Adherence. The Journal of Urology.184:2565-71.

[73] Johnson JR, Roberts PL, Olsen RJ, Moyer KA, Stamm WE. Prevention of Catheter-Associated Urinary Tract Infection with a Silver Oxide-Coated Urinary Catheter: Clinical and Microbiologic Correlates. J Infect Dis. 1990;162:1145-50.

[74] Schumm K, Lam TB. Types of urethral catheters for management of short‐term voiding problems in hospitalised adults. The Cochrane Library. 2008.

[75] Riley DK, Classen DC, Stevens LE, Burke JP. A large randomized clinical trial of a silver-impregnated urinary catheter: Lack of efficacy and staphylococcal superinfection. The American Journal of Medicine.98:349-56.

[76] Davenport K, Keeley FX. Evidence for the use of silver-alloy-coated urethral catheters. Journal of Hospital Infection.60:298-303.

[77] Brosnahan J, Jull A, Tracy C. Types of urethral catheters for management of short‐term voiding problems in hospitalised adults. The Cochrane Library. 2004.

[78] Srinivasan A, Karchmer T, Richards A, Song X, Perl TM. A prospective trial of a novel, silicone-based, silver-coated foley catheter for the prevention of nosocomial urinary tract infections. Infection Control. 2006;27:38-43.

[79] Guggenbichler JP, Böswald M, Lugauer S, Krall T. A new technology of microdispersed silver in polyurethane induces antimicrobial activity in central venous catheters. Infection. 1999;27:S16-S23.

[80] Kumon H, Hashimoto H, Nishimura M, Monden K, Ono N. Catheter-associated urinary tract infections: impact of catheter materials on their management. Int J Antimicrob Agents.17:311-6.

[81] Darouiche RO, Smith JA, Jr., Hanna H, Dhabuwala CB, Steiner MS, Babaian RJ, et al. Efficacy of antimicrobial-impregnated bladder catheters in reducing

catheter-associated bacteriuria: a prospective, randomized, multicenter clinical trial. Urology.54:976-81.

[82] Darouiche RO, Safar H, Raad II. In Vitro Efficacy of Antimicrobial-Coated Bladder Catheters in Inhibiting Bacterial Migration along Catheter Surface. J Infect Dis. 1997;176:1109-12.

[83] Stensballe J, Tvede M, Looms D, Lippert FK, Dahl B, Tønnesen E, et al. Infection Risk with Nitrofurazone-Impregnated Urinary Catheters in Trauma PatientsA Randomized Trial. Ann Intern Med. 2007;147:285-93.

[84] Johnson JR, Berggren T, Conway AJ. Activity of a nitrofurazone matrix urinary catheter against catheter-associated uropathogens. Antimicrob Agents Chemother. 1993;37:2033-6.

[85] Driver M. Coatings for biomedical applications. 2012 ed. Cambridge, UK: Woodhead Publishing Limited; 2012.

[86] Johnson JR, Delavari P, Azar M. Activities of a Nitrofurazone-Containing Urinary Catheter and a Silver Hydrogel Catheter against Multidrug-Resistant Bacteria Characteristic of Catheter-Associated Urinary Tract Infection. Antimicrob Agents Chemother. 1999;43:2990-5.

[87] Lee S-J, Kim SW, Cho Y-H, Shin W-S, Lee SE, Kim C-S, et al. A comparative multicentre study on the incidence of catheter-associated urinary tract infection between nitrofurazone-coated and silicone catheters. Int J Antimicrob Agents.24:65-9.

[88] Fisher LE, Hook AL, Ashraf W, Yousef A, Barrett DA, Scurr DJ, et al. Biomaterial modification of urinary catheters with antimicrobials to give long-term broadspectrum antibiofilm activity. J Controlled Release. 2015;202:57-64.

[89] Onaizi SA, Leong SSJ. Tethering antimicrobial peptides: Current status and potential challenges. Biotechnology Advances. 2011;29:67-74.

[90] Skarnes RC, Watson DW. Antimicrobial factors of normal tissues and fluids. Bacteriological reviews. 1957;21:273.

[91] Brogden KA. Antimicrobial peptides: pore formers or metabolic inhibitors in bacteria? Nat Rev Micro. 2005;3:238-50.

[92] Steiner H, Hultmark D, Engstr √∂m Ö, Bennich H, Boman H. Sequence and specificity of two antibacterial proteins involved in insect immunity. 1981.

[93] Ganz T, Selsted ME, Lehrer RI. Defensins. European journal of haematology. 1990;44:1-8.

[94] Zasloff M. Magainins, a class of antimicrobial peptides from Xenopus skin: isolation, characterization of two active forms, and partial cDNA sequence of a precursor. Proceedings of the National Academy of Sciences. 1987;84:5449-53.

[95] Wang G, Li X, Wang Z. APD2: the updated antimicrobial peptide database and its application in peptide design. Nucleic Acids Research. 2009;37:D933-D7.

[96] Boman HG. Peptide antibiotics and their role in innate immunity. Annual review of immunology. 1995;13:61-92.

[97] Brogden KA, Ackermann M, Huttner KM. Detection of anionic antimicrobial peptides in ovine bronchoalveolar lavage fluid and respiratory epithelium. Infection and immunity. 1998;66:5948-54.

[98] Harris F, Dennison SR, Phoenix DA. Anionic antimicrobial peptides from eukaryotic organisms. Curr Protein Pept Sci. 2009;10:585-606.

[99] Harris F, R Dennison S, A Phoenix D. Anionic antimicrobial peptides from eukaryotic organisms and their mechanisms of action. Curr Chem Biol. 2011;5:142-53.

[100] Gennaro R, Zanetti M. Structural features and biological activities of the cathelicidin,Äêderived antimicrobial peptides. Peptide Science. 2000;55:31-49.

[101] Bechinger B, Zasloff M, Opella SJ. Structure and orientation of the antibiotic peptide magainin in membranes by solid,Äêstate nuclear magnetic resonance spectroscopy. Protein Science. 1993;2:2077-84.

[102] Turner J, Cho Y, Dinh N-N, Waring AJ, Lehrer RI. Activities of LL-37, a Cathelin-Associated Antimicrobial Peptide of Human Neutrophils. Antimicrobial Agents and Chemotherapy. 1998;42:2206-14.

[103] Falla TJ, Karunaratne DN, Hancock REW. Mode of Action of the Antimicrobial Peptide Indolicidin. Journal of Biological Chemistry. 1996;271:19298-303.

[104] Harwig SSL, Kokryakov VN, Swiderek KM, Aleshina GM, Zhao C, Lehrer RI. Prophenin-1, an exceptionally proline-rich antimicrobial peptide from porcine leukocytes. FEBS Letters. 1995;362:65-9.

[105] Ganz T. Versatile Defensins. Science. 2002;298:977-9.

[106] Lai R, Liu H, Hui Lee W, Zhang Y. An anionic antimicrobial peptide from toad Bombina maxima. Biochemical and Biophysical Research Communications. 2002;295:796-9.

[107] Andersson M, Boman A, Boman HG. Ascaris nematodes from pig and human make three antibacterial peptides: isolation of cecropin P1 and two ASABF peptides. Cell Mol Life Sci. 2003;60:599-606.

[108] Samakovlis C, Kylsten P, Kimbrell D, Engstr √∂m AÆ, Hultmark D. The andropin gene and its product, a male-specific antibacterial peptide in Drosophila melanogaster. The EMBO journal. 1991;10:163.

[109] Hara S, Yamakawa M. Moricin, a Novel Type of Antibacterial Peptide Isolated from the Silkworm, Bombyx mori. Journal of Biological Chemistry. 1995;270:29923-7.

[110] Zhao C, Ganz T, Lehrer RI. Structures of genes for two cathelin-associated antimicrobial peptides: prophenin-2 and PR-39. FEBS Letters. 1995;376:130-4.

[111] Lehrer RI. Primate defensins. Nature Reviews Microbiology. 2004;2:727-38.

[112] Fehlbaum P, Bulet P, Michaut L, Lagueux M, Broekaert WF, Hetru C, et al. Insect immunity. Septic injury of Drosophila induces the synthesis of a potent antifungal peptide with sequence homology to plant antifungal peptides. Journal of Biological Chemistry. 1994;269:33159-63.

[113] Eckert R, Qi F, Yarbrough DK, He J, Anderson MH, Shi W. Adding Selectivity to Antimicrobial Peptides: Rational Design of a Multidomain Peptide against Pseudomonas spp. Antimicrobial Agents and Chemotherapy. 2006;50:1480-8.

[114] Boman HG, Agerberth B, Boman A. Mechanisms of action on Escherichia coli of cecropin P1 and PR-39, two antibacterial peptides from pig intestine. Infection and Immunity. 1993;61:2978-84.

[115] Ouhara K, Komatsuzawa H, Yamada S, Shiba H, Fujiwara T, Ohara M, et al. Susceptibilities of periodontopathogenic and cariogenic bacteria to antibacterial peptides, ℂ≤-defensins and LL37, produced by human epithelial cells. Journal of Antimicrobial Chemotherapy. 2005;55:888-96.

[116] Wieprecht T, Dathe M, Beyermann M, Krause E, Maloy WL, MacDonald DL, et al. Peptide Hydrophobicity Controls the Activity and Selectivity of Magainin 2 Amide in Interaction with Membranes. Biochemistry. 1997;36:6124-32.

[117] Huang HW. Action of Antimicrobial Peptides:‚Äâ Two-State Model‚Äâ. Biochemistry. 2000;39:8347-52.

[118] Chen F-Y, Lee M-T, Huang HW. Evidence for membrane thinning effect as the mechanism for peptide-induced pore formation. Biophysical journal. 2003;84:3751-8.

[119] Laver D. The barrel-stave model as applied to alamethicin and its analogs reevaluated. Biophysical journal. 1994;66:355-9.

[120] He K, Ludtke SJ, Worcester DL, Huang HW. Neutron scattering in the plane of membranes: structure of alamethicin pores. Biophysical journal. 1996;70:2659-66.

[121] Yang L, Harroun TA, Weiss TM, Ding L, Huang HW. Barrel-stave model or toroidal model? A case study on melittin pores. Biophysical journal. 2001;81:1475-85.

[122] Shai Y. Mechanism of the binding, insertion and destabilization of phospholipid bilayer membranes by Œ±-helical antimicrobial and cell non-selective

membrane-lytic peptides. Biochimica et Biophysica Acta (BBA) - Biomembranes. 1999;1462:55-70.

[123] Yamaguchi S, Huster D, Waring A, Lehrer RI, Kearney W, Tack BF, et al. Orientation and dynamics of an antimicrobial peptide in the lipid bilayer by solid-state NMR spectroscopy. Biophysical journal. 2001;81:2203-14.

[124] Ghosh JK, Shaool D, Guillaud P, Cicéron L, Mazier D, Kustanovich I, et al. Selective Cytotoxicity of Dermaseptin S3 toward IntraerythrocyticPlasmodium falciparum and the Underlying Molecular Basis. Journal of Biological Chemistry. 1997;272:31609-16.

[125] Gazit E, Boman A, Boman HG, Shai Y. Interaction of the Mammalian Antibacterial Peptide Cecropin P1 with Phospholipid Vesicles. Biochemistry. 1995;34:11479-88.

[126] Oren Z, Lerman JC, Gudmundsson GH, Agerberth B, Shai Y. Structure and organization of the human antimicrobial peptide LL-37 in phospholipid membranes: relevance to the molecular basis for its non-cell-selective activity. Biochemical Journal. 1999;341:501-13.

[127] Matsuzaki K, Murase O, Fujii N, Miyajima K. An Antimicrobial Peptide, Magainin 2, Induced Rapid Flip-Flop of Phospholipids Coupled with Pore Formation and Peptide Translocation†. Biochemistry. 1996;35:11361-8.

[128] Wang G. Post-translational Modifications of Natural Antimicrobial Peptides and Strategies for Peptide Engineering. Current biotechnology. 2012;1:72-9.

[129] Strandberg E, Tiltak D, Ieronimo M, Kanithasen N, Wadhwani P, Ulrich AS. Influence of C-terminal amidation on the antimicrobial and hemolytic activities of cationic α-helical peptides. Pure Appl Chem. 2007;79:717-28.

[130] R Dennison S, HG Morton L, A Phoenix D. Effect of amidation on the antimicrobial peptide aurein 2.5 from Australian southern bell frogs. Protein Pept Lett. 2012;19:586-91.

[131] Sato AK, Viswanathan M, Kent RB, Wood CR. Therapeutic peptides: technological advances driving peptides into development. Curr Opin Biotechnol. 2006;17:638-42.

[132] Brinckerhoff LH, Kalashnikov VV, Thompson LW, Yamshchikov GV, Pierce RA, Galavotti HS, et al. Terminal modifications inhibit proteolytic degradation of an immunogenic mart-127–35 peptide: Implications for peptide vaccines. Int J Cancer. 1999;83:326-34.

[133] Dennison SR, Phoenix DA. Influence of C-Terminal Amidation on the Efficacy of Modelin-5. Biochemistry. 2011;50:1514-23.

[134] Andreu D, Ubach J, Boman A, Wåhlin B, Wade D, Merrifield RB, et al. Shortened cecropin A-melittin hybrids Significant size reduction retains potent antibiotic activity. FEBS Letters. 1992;296:190-4.

[135] Xu W, Zhu X, Tan T, Li W, Shan A. Design of Embedded-Hybrid Antimicrobial Peptides with Enhanced Cell Selectivity and Anti-Biofilm Activity. PLoS One. 2014;9:e98935.

[136] Zhu WL, Nan YH, Hahm K, Shin SY. Cell selectivity of an antimicrobial peptide melittin diastereomer with D-amino acid in the leucine zipper sequence. Journal of biochemistry and molecular biology. 2007;40:1090.

[137] Giuliani A, Pirri G, Bozzi A, Giulio A, Aschi M, Rinaldi AC. Antimicrobial peptides: natural templates for synthetic membrane-active compounds. Cell Mol Life Sci. 2008;65:2450-60.

[138] Lee DL, Powers JP, Pflegerl K, Vasil ML, Hancock REW, Hodges RS. Effects of single d-amino acid substitutions on disruption of β-sheet structure and hydrophobicity in cyclic 14-residue antimicrobial peptide analogs related to gramicidin S. The journal of peptide research : official journal of the American Peptide Society. 2004;63:69-84.

[139] Matsuzaki K. Control of cell selectivity of antimicrobial peptides. Biochimica et Biophysica Acta (BBA) - Biomembranes. 2009;1788:1687-92.

[140] Hong SY, Oh JE, Lee K-H. Effect of d-amino acid substitution on the stability, the secondary structure, and the activity of membrane-active peptide. Biochem Pharmacol. 1999;58:1775-80.

[141] Tsai C-W, Hsu N-Y, Wang C-H, Lu C-Y, Chang Y, Tsai H-HG, et al. Coupling Molecular Dynamics Simulations with Experiments for the Rational Design of Indolicidin-Analogous Antimicrobial Peptides. J Mol Biol. 2009;392:837-54.

[142] Christensen DJ, Gottlin EB, Benson RE, Hamilton PT. Phage display for target-based antibacterial drug discovery. Drug Discovery Today. 2001;6:721-7.

[143] Kay BK, Kasanov J, Yamabhai M. Screening Phage-Displayed Combinatorial Peptide Libraries. Methods. 2001;24:240-6.

[144] Sainath Rao S, Mohan KVK, Atreya CD. A Peptide Derived from Phage Display Library Exhibits Antibacterial Activity against <italic>E. coli</italic> and <italic>Pseudomonas aeruginosa</italic>. PLoS One. 2013;8:e56081.

[145] Bagheri M, Beyermann M, Dathe M. Immobilization Reduces the Activity of Surface-Bound Cationic Antimicrobial Peptides with No Influence upon the Activity Spectrum. Antimicrob Agents Chemother. 2009;53:1132-41.

[146] Ferreira L, Zumbuehl A. Non-leaching surfaces capable of killing microorganisms on contact. J Mater Chem. 2009;19:7796-806.

[147] Costa F, Carvalho IF, Montelaro RC, Gomes P, Martins MCL. Covalent immobilization of antimicrobial peptides (AMPs) onto biomaterial surfaces. Acta Biomaterialia. 2011;7:1431-40.

[148] Haynie SL, Crum GA, Doele BA. Antimicrobial activities of amphiphilic peptides covalently bonded to a water-insoluble resin. Antimicrob Agents Chemother. 1995;39:301-7.

[149] Glinel K, Jonas AM, Jouenne T, Leprince J, Galas L, Huck WTS. Antibacterial and Antifouling Polymer Brushes Incorporating Antimicrobial Peptide. Bioconjugate Chem. 2009;20:71-7.

[150] Humblot V, Yala J-F, Thebault P, Boukerma K, Héquet A, Berjeaud J-M, et al. The antibacterial activity of Magainin I immobilized onto mixed thiols Self-Assembled Monolayers. Biomaterials. 2009;30:3503-12.

[151] Willcox MDP, Hume EBH, Aliwarga Y, Kumar N, Cole N. A novel cationic-peptide coating for the prevention of microbial colonization on contact lenses. Journal of Applied Microbiology. 2008;105:1817-25.

[152] Chen R, Cole N, Willcox MDP, Park J, Rasul R, Carter E, et al. Synthesis, characterization and in vitro activity of a surface-attached antimicrobial cationic peptide. Biofouling. 2009;25:517-24.

[153] Gabriel M, Nazmi K, Veerman EC, Nieuw Amerongen AV, Zentner A. Preparation of LL-37-Grafted Titanium Surfaces with Bactericidal Activity. Bioconjugate Chem. 2006;17:548-50.

[154] Tan XW, Goh TW, Saraswathi P, Nyein CL, Setiawan M, Riau A, et al. Effectiveness of Antimicrobial Peptide Immobilization for Preventing Perioperative Cornea Implant-Associated Bacterial Infection. Antimicrob Agents Chemother. 2014;58:5229-38.

[155] Cho W-M, Joshi BP, Cho H, Lee K-H. Design and synthesis of novel antibacterial peptide-resin conjugates. Bioorg Med Chem Lett. 2007;17:5772-6.

[156] Wang Z, Han X, He N, Chen Z, Brooks CL. Molecular Structures of C- and N-Terminus Cysteine Modified Cecropin P1 Chemically Immobilized onto Maleimide-Terminated Self-Assembled Monolayers Investigated by Molecular Dynamics Simulation. The Journal of Physical Chemistry B. 2014;118:5670-80.

[157] Yameen B, Farrukh A. Polymer Brushes: Promises and Challenges. Chemistry – An Asian Journal. 2013;8:1736-53.

[158] Li X, Li P, Saravanan R, Basu A, Mishra B, Lim SH, et al. Antimicrobial functionalization of silicone surfaces with engineered short peptides having broad spectrum antimicrobial and salt-resistant properties. Acta Biomaterialia. 2014;10:258-66.

[159] Lee H, Dellatore SM, Miller WM, Messersmith PB. Mussel-Inspired Surface Chemistry for Multifunctional Coatings. Science. 2007;318:426-30.

[160] Yang K, Lee JS, Kim J, Lee YB, Shin H, Um SH, et al. Polydopamine-mediated surface modification of scaffold materials for human neural stem cell engineering. Biomaterials. 2012;33:6952-64.

[161] Lee YB, Shin YM, Lee J-h, Jun I, Kang JK, Park J-C, et al. Polydopamine-mediated immobilization of multiple bioactive molecules for the development of functional vascular graft materials. Biomaterials. 2012;33:8343-52.

[162] Steven MD, Hotchkiss JH. Covalent immobilization of an antimicrobial peptide on poly(ethylene) film. J Appl Polym Sci. 2008;110:2665-70.

[163] Hilpert K, Elliott M, Jenssen H, Kindrachuk J, Fjell CD, Körner J, et al. Screening and Characterization of Surface-Tethered Cationic Peptides for Antimicrobial Activity. Chem Biol. 2009;16:58-69.

[164] Basu A, Mishra B, Jan Leong SS. Immobilization of polybia-MPI by allyl glycidyl ether based brush chemistry to generate a novel antimicrobial surface. Journal of Materials Chemistry B. 2013;1:4746-55.

[165] Epand RM, Vogel HJ. Diversity of antimicrobial peptides and their mechanisms of action. Biochimica et Biophysica Acta (BBA) - Biomembranes. 1999;1462:11-28.

[166] Oren Z, Lerman JC, Gudmundsson GH, Agerberth B, Shai Y. Structure and organization of the human antimicrobial peptide LL-37 in phospholipid membranes: relevance to the molecular basis for its non-cell-selective activity. Biochem J. 1999;341:501-13.

[167] Dathe M, Wieprecht T. Structural features of helical antimicrobial peptides: their potential to modulate activity on model membranes and biological cells. Biochimica et Biophysica Acta (BBA) - Biomembranes. 1999;1462:71-87.

[168] Li Y, Wei S, Wu J, Jasensky J, Xi C, Li H, et al. Effects of Peptide Immobilization Sites on the Structure and Activity of Surface-Tethered Antimicrobial Peptides. The Journal of Physical Chemistry C. 2015;119:7146-55.

[169] Sobczak M, Dębek C, Olędzka E, Kozłowski R. Polymeric Systems of Antimicrobial Peptides—Strategies and Potential Applications. Molecules. 2013;18:14122-37.

[170] Kazemzadeh-Narbat M, Lai BFL, Ding C, Kizhakkedathu JN, Hancock REW, Wang R. Multilayered coating on titanium for controlled release of antimicrobial peptides for the prevention of implant-associated infections. Biomaterials. 2013;34:5969-77.

[171] Shukla A, Fleming KE, Chuang HF, Chau TM, Loose CR, Stephanopoulos GN, et al. Controlling the release of peptide antimicrobial agents from surfaces. Biomaterials. 2010;31:2348-57.

[172] Cutter CN, Willett JL, Siragusa GR. Improved antimicrobial activity of nisin-incorporated polymer films by formulation change and addition of food grade chelator. Letters in Applied Microbiology. 2001;33:325-8.

[173] Ehtezazi T, Washington C. Controlled release of macromolecules from PLA microspheres: using porous structure topology. J Controlled Release. 2000;68:361-72.

[174] Appendini P, Hotchkiss JH. Review of antimicrobial food packaging. Innovative Food Science & Emerging Technologies. 2002;3:113-26.

[175] Fu K, Pack D, Klibanov A, Langer R. Visual Evidence of Acidic Environment Within Degrading Poly(lactic-co-glycolic acid) (PLGA) Microspheres. Pharm Res. 2000;17:100-6.

[176] Marr AK, Gooderham WJ, Hancock REW. Antibacterial peptides for therapeutic use: obstacles and realistic outlook. Curr Opin Pharmacol. 2006;6:468-72.

[177] Fox JL. Antimicrobial peptides stage a comeback. Nat Biotech. 2013;31:379-82.

[178] Fujiwara S, Imai J, Fujiwara M, Yaeshima T, Kawashima T, Kobayashi K. A potent antibacterial protein in royal jelly. Purification and determination of the primary structure of royalisin. J Biol Chem. 1990;265:11333-7.

[179] Fontana R, Mendes MA, Souza BMd, Konno K, César LIMM, Malaspina O, et al. Jelleines: a family of antimicrobial peptides from the Royal Jelly of honeybees (Apis mellifera). Peptides. 2004;25:919-28.

[180] Lim K, Chua RRY, Saravanan R, Basu A, Mishra B, Tambyah PA, et al. Immobilization Studies of an Engineered Arginine–Tryptophan-Rich Peptide on a Silicone Surface with Antimicrobial and Antibiofilm Activity. ACS Appl Mater Interfaces. 2013;5:6412-22.

[181] Pace CN, Vajdos F, Fee L, Grimsley G, Gray T. How to measure and predict the molar absorption coefficient of a protein. Protein Sci. 1995;4:2411-23.

[182] Wiegand I, Hilpert K, Hancock REW. Agar and broth dilution methods to determine the minimal inhibitory concentration (MIC) of antimicrobial substances. Nat Protocols. 2008;3:163-75.

[183] Hancock REW, Farmer SW, Li Z, Poole K. Interaction of aminoglycosides with the outer membranes and purified lipopolysaccharide and OmpF porin of Escherichia coli. Antimicrobial Agents and Chemotherapy. 1991;35:1309-14.

[184] Ivanov IE, Morrison AE, Cobb JE, Fahey CA, Camesano TA. Creating antibacterial surfaces with the peptide chrysophsin-1. ACS Applied Materials and Interfaces. 2012;4:5891-7.

[185] Vreuls C, Zocchi G, Thierry B, Garitte G, Griesser SS, Archambeau C, et al. Prevention of bacterial biofilms by covalent immobilization of peptides onto plasma polymer functionalized substrates. Journal of Materials Chemistry. 2010;20:8092-8.

[186] Oren Z, Shai Y. Selective Lysis of Bacteria but Not Mammalian Cells by Diastereomers of Melittin:‚Äâ Structure‚àíFunction Study‚Ä†. Biochemistry. 1997;36:1826-35.

[187] Fontana R, Mendes MA, De Souza BM, Konno K, C √©sar LMM, Malaspina O, et al. Jelleines: A family of antimicrobial peptides from the Royal Jelly of honeybees (Apis mellifera). Peptides. 2004;25:919-28.

[188] Yau WM, Wimley WC, Gawrisch K, White SH. The preference of tryptophan for membrane interfaces. Biochemistry. 1998;37:14713-8.

[189] Chan DI, Prenner EJ, Vogel HJ. Tryptophan- and arginine-rich antimicrobial peptides: Structures and mechanisms of action. Biochimica et Biophysica Acta (BBA) - Biomembranes. 2006;1758:1184-202.

[190] Aliste MP, MacCallum JL, Tieleman DP. Molecular Dynamics Simulations of Pentapeptides at Interfaces:,Äâ Salt Bridge and Cation,àíœÄ Interactions,Ä†. Biochemistry. 2003;42:8976-87.

[191] Peschel A, Jack RW, Otto M, Collins LV, Staubitz P, Nicholson G, et al. Staphylococcus aureus Resistance to Human Defensins and Evasion of Neutrophil Killing via the Novel Virulence Factor Mprf Is Based on Modification of Membrane Lipids with l-Lysine. The Journal of Experimental Medicine. 2001;193:1067-76.

[192] Goldman MJ, Anderson GM, Stolzenberg ED, Kari UP, Zasloff M, Wilson JM. Human ℂ≤-defensin-1 is a salt-sensitive antibiotic in lung that is inactivated in cystic fibrosis. Cell. 1997;88:553-60.

[193] Park IY, Cho JH, Kim KS, Kim Y-B, Kim MS, Kim SC. Helix Stability Confers Salt Resistance upon Helical Antimicrobial Peptides. Journal of Biological Chemistry. 2004;279:13896-901.

[194] Wiradharma N, Khoe U, Hauser CAE, Seow SV, Zhang S, Yang Y-Y. Synthetic cationic amphiphilic α-helical peptides as antimicrobial agents. Biomaterials. 2011;32:2204-12.

[195] La Rocca P, Biggin PC, Tieleman DP, Sansom MSP. Simulation studies of the interaction of antimicrobial peptides and lipid bilayers. Biochimica et Biophysica Acta (BBA) - Biomembranes. 1999;1462:185-200.

[196] Pérez-Payá E, Houghten RA, Blondelle SE. Determination of the secondary structure of selected melittin analogues with different haemolytic activities. Biochem J. 1994;299:587-91.

[197] Hancock REW, Wong PGW. Compounds which increase the permeability of the Pseudomonas aeruginosa outer membrane. Antimicrobial Agents and Chemotherapy. 1984;26:48-52.

[198] Mishra B, Leishangthem GD, Gill K, Singh AK, Das S, Singh K, et al. A novel antimicrobial peptide derived from modified N-terminal domain of bovine lactoferrin: Design, synthesis, activity against multidrug-resistant bacteria and Candida. Biochimica et Biophysica Acta (BBA) - Biomembranes. 2013;1828:677-86.

[199] Zhang L, Rozek A, Hancock REW. Interaction of Cationic Antimicrobial Peptides with Model Membranes. Journal of Biological Chemistry. 2001;276:35714-22.

[200] Trautner BW. Management of catheter-associated urinary tract infection. Current opinion in infectious diseases. 2010;23:76-82.

[201] Richards MJMF, Edwards JRMS, Culver DHP, Robert P. Gaynes MD, the, System NNIS. Nosocomial Infections in Combined Medical,ÄêSurgical Intensive Care Units in the United States¬†,Ä¢,ÄÇ. Infection Control and Hospital Epidemiology. 2000;21:510-5.

[202] Bernik DL. Silicon based materials for drug delivery devices and implants. Recent Patents on Nanotechnology. 2007;1:186-92.

[203] Pfleiderer B, Xu P, Ackerman JL, Garrido L. Study of aging of silicone rubber biomaterials with NMR. Journal of Biomedical Materials Research. 1995;29:1129-40.

[204] Gao G, Yu K, Kindrachuk J, Brooks DE, Hancock REW, Kizhakkedathu JN. Antibacterial Surfaces Based on Polymer Brushes: Investigation on the Influence of Brush Properties on Antimicrobial Peptide Immobilization and Antimicrobial Activity. Biomacromolecules. 2011;12:3715-27.

[205] Siow KS, Britcher L, Kumar S, Griesser HJ. Plasma Methods for the Generation of Chemically Reactive Surfaces for Biomolecule Immobilization and Cell Colonization - A Review. Plasma Processes and Polymers. 2006;3:392-418.

[206] Hirai T, Kawasaki K, Tanaka K. Interfacial kinetics of a model epoxy-amine addition reaction. Physical Chemistry Chemical Physics. 2012;14:13532-4.

[207] Han HJ, Kannan RM, Wang S, Mao G, Kusanovic JP, Romero R. Multifunctional dendrimer-templated antibody presentation on biosensor surfaces for improved biomarker detection. Advanced Functional Materials. 2010;20:409-21.

[208] Wong I, Ho CM. Surface molecular property modifications for poly(dimethylsiloxane) (PDMS) based microfluidic devices. Microfluidics and nanofluidics. 2009;7:291-306.

[209] Gao G, Lange D, Hilpert K, Kindrachuk J, Zou Y, Cheng JTJ, et al. The biocompatibility and biofilm resistance of implant coatings based on hydrophilic polymer brushes conjugated with antimicrobial peptides. Biomaterials. 2011;32:3899-909.

[210] Matsuda A, Kobayashi H, Itoh S, Kataoka K, Tanaka J. Immobilization of laminin peptide in molecularly aligned chitosan by covalent bonding. Biomaterials. 2005;26:2273-9.

[211] Gaur RK, Gupta KC. A spectrophotometric method for the estimation of amino groups on polymer supports. Analytical Biochemistry. 1989;180:253-8.

[212] Lu S. Immobilization of antimicrobial peptides onto titanium surfaces: University of British Columbia; 2009.

[213] Kowalczuk D, Ginalska Gy, Golus J. Characterization of the developed antimicrobial urological catheters. International Journal of Pharmaceutics. 2010;402:175-83.

[214] Stepanovi*ƒ*á S, Vukovi*ƒ*á D, Daki*ƒ*á I, Savi*ƒ*á B, ≈†vabi*ƒ*á-Vlahovi*ƒ*á M. A modified microtiter-plate test for quantification of staphylococcal biofilm formation. Journal of Microbiological Methods. 2000;40:175-9.

[215] Lawson MC, Hoth KC, DeForest CA, Bowman CN, Anseth KS. Inhibition of Staphylococcus epidermidis biofilms using polymerizable vancomycin derivatives. Clinical Orthopaedics and Related Research¬Æ. 2010;468:2081-91.

[216] Wise Sr JP, Goodale BC, Wise SS, Craig GA, Pongan AF, Walter RB, et al. Silver nanospheres are cytotoxic and genotoxic to fish cells. Aquatic Toxicology. 2010;97:34-41.

[217] Hancock REW, Sahl H-G. Antimicrobial and host-defense peptides as new anti-infective therapeutic strategies. Nat Biotech. 2006;24:1551-7.

[218] Zasloff M. Antimicrobial peptides of multicellular organisms. Nature. 2002;415:389-95.

[219] O'Toole GA. Microtiter Dish Biofilm Formation Assay. 2011:e2437.

[220] Ivanov IE, Morrison AE, Cobb JE, Fahey CA, Camesano TA. Creating Antibacterial Surfaces with the Peptide Chrysophsin-1. ACS Appl Mater Interfaces. 2012;4:5891-7.

[221] Oren Z, Shai Y. Selective Lysis of Bacteria but Not Mammalian Cells by Diastereomers of Melittin: Structure−Function Study†. Biochemistry. 1997;36:1826-35.

[222] Miller DJ, Araújo PA, Correia PB, Ramsey MM, Kruithof JC, van Loosdrecht MCM, et al. Short-term adhesion and long-term biofouling testing of polydopamine and poly(ethylene glycol) surface modifications of membranes and feed spacers for biofouling control. Water Res. 2012;46:3737-53.

[223] Low WC, Rujitanaroj P-O, Lee D-K, Messersmith PB, Stanton LW, Goh E, et al. Nanofibrous scaffold-mediated REST knockdown to enhance neuronal differentiation of stem cells. Biomaterials. 2013;34:3581-90.

[224] Zhu L-P, Jiang J-H, Zhu B-K, Xu Y-Y. Immobilization of bovine serum albumin onto porous polyethylene membranes using strongly attached polydopamine as a spacer. Colloids and Surfaces B: Biointerfaces. 2011;86:111-8.

[225] Ham HO, Liu Z, Lau K, Lee H, Messersmith PB. Facile DNA immobilization on surfaces through a catecholamine polymer. Angew Chem. 2011;123:758-62.

[226] Arena JT, McCloskey B, Freeman BD, McCutcheon JR. Surface modification of thin film composite membrane support layers with polydopamine: Enabling use of reverse osmosis membranes in pressure retarded osmosis. J Membr Sci. 2011;375:55-62.

[227] Hong S, Na YS, Choi S, Song IT, Kim WY, Lee H. Non-Covalent Self-Assembly and Covalent Polymerization Co-Contribute to Polydopamine Formation. Adv Funct Mater. 2012;22:4711-7.

[228] Lee H, Scherer NF, Messersmith PB. Single-molecule mechanics of mussel adhesion. Proceedings of the National Academy of Sciences. 2006;103:12999-3003.

[229] Xi Z-Y, Xu Y-Y, Zhu L-P, Wang Y, Zhu B-K. A facile method of surface modification for hydrophobic polymer membranes based on the adhesive behavior of poly(DOPA) and poly(dopamine). J Membr Sci. 2009;327:244-53.

[230] Bolton JL, Turnipseed SB, Thompson JA. Influence of quinone methide reactivity on the alkylation of thiol and amino groups in proteins: studies utilizing amino acid and peptide models. Chem-Biol Interact. 1997;107:185-200.

[231] Dellatore SM. Strategies for Immobilization of Cell Adhesion Molecule and Cytokine Receptor Ligands: Inspiration from the Cell Membrane and Marine Mussels: ProQuest; 2008.

[232] Anderson DGR. Oxidation and reactivity of 3, 4-dihydroxyphenylacetaldehyde, a reactive intermediate of dopamine metabolism. 2011.

[233] Yang J, Cohen Stuart MA, Kamperman M. Jack of all trades: versatile catechol crosslinking mechanisms. Chem Soc Rev. 2014.

[234] Mata A, Fleischman A, Roy S. Characterization of Polydimethylsiloxane (PDMS) Properties for Biomedical Micro/Nanosystems. Biomedical Microdevices. 2005;7:281-93.

[235] Kang SM, You I, Cho WK, Shon HK, Lee TG, Choi IS, et al. One-Step Modification of Superhydrophobic Surfaces by a Mussel-Inspired Polymer Coating. Angewandte Chemie International Edition. 2010;49:9401-4.

[236] Dietrich PM, Horlacher T, Girard-Lauriault P-L, Gross T, Lippitz A, Min H, et al. Adlayers of Dimannoside Thiols on Gold: Surface Chemical Analysis. Langmuir. 2011;27:4808-15.

[237] Lee H, Rho J, Messersmith PB. Facile Conjugation of Biomolecules onto Surfaces via Mussel Adhesive Protein Inspired Coatings. Adv Mater (Weinheim, Ger). 2009;21:431-4.

[238] Mishra B, Basu A, Saravanan R, Xiang L, Yang LK, Leong SSJ. Lasioglossin-III: antimicrobial characterization and feasibility study for immobilization applications. RSC Advances. 2013;3:9534-43.

[239] Gao G, Cheng John TJ, Kindrachuk J, Hancock Robert EW, Straus Suzana K, Kizhakkedathu Jayachandran N. Biomembrane Interactions Reveal the Mechanism of Action of Surface-Immobilized Host Defense IDR-1010 Peptide. Chem Biol. 2012;19:199-209.

[240] Guangliang C, Mingyan Z, Shihua C, Guohua L, Juming Y. Nanolayer biofilm coated on magnetic nanoparticles by using a dielectric barrier discharge glow plasma fluidized bed for immobilizing an antimicrobial peptide. Nanotechnology. 2009;20:465706.

[241] Appendini P, Hotchkiss JH. Surface modification of poly(styrene) by the attachment of an antimicrobial peptide. J Appl Polym Sci. 2001;81:609-16.

[242] McDonald TJ, Knight BA, Shields BM, Bowman P, Salzmann MB, Hattersley AT. Stability and reproducibility of a single-sample urinary C-peptide/creatinine ratio and its correlation with 24-h urinary C-peptide. Clinical chemistry. 2009;55:2035-9.

[243] Henkelman S, Rakhorst G, Blanton J, van Oeveren W. Standardization of incubation conditions for hemolysis testing of biomaterials. Materials Science and Engineering: C. 2009;29:1650-4.

[244] Vasilev K, Cook J, Griesser HJ. Antibacterial surfaces for biomedical devices. Expert Review of Medical Devices. 2009;6:553-67.

[245] Gao P, Nie X, Zou M, Shi Y, Cheng G. Recent advances in materials for extended-release antibiotic delivery system. J Antibiot. 2011;64:625-34.

[246] Ungaro F, d'Angelo I, Coletta C, d'Emmanuele di Villa Bianca R, Sorrentino R, Perfetto B, et al. Dry powders based on PLGA nanoparticles for pulmonary delivery of antibiotics: Modulation of encapsulation efficiency, release rate and lung deposition pattern by hydrophilic polymers. Journal of Controlled Release. 2012;157:149-59.

[247] Lan S-F, Kehinde T, Zhang X, Khajotia S, Schmidtke DW, Starly B. Controlled release of metronidazole from composite poly-ε-caprolactone/alginate (PCL/alginate) rings for dental implants. Dental Materials. 2013;29:656-65.

[248] Nair LS, Laurencin CT. Biodegradable polymers as biomaterials. Progress in Polymer Science. 2007;32:762-98.

[249] Woodruff MA, Hutmacher DW. The return of a forgotten polymer—Polycaprolactone in the 21st century. Progress in Polymer Science. 2010;35:1217-56.

[250] Chang HI, Perrie Y, Coombes AGA. Delivery of the antibiotic gentamicin sulphate from precipitation cast matrices of polycaprolactone. Journal of Controlled Release. 2006;110:414-21.

[251] Lin G, Cosimbescu L, Karin NJ, Gutowska A, Tarasevich BJ. Injectable and thermogelling hydrogels of PCL-g-PEG: mechanisms, rheological and enzymatic degradation properties. Journal of Materials Chemistry B. 2013;1:1249-55.

[252] Cherkasov A, Hilpert K, Jenssen H, Fjell CD, Waldbrook M, Mullaly SC, et al. Use of Artificial Intelligence in the Design of Small Peptide Antibiotics Effective against a Broad Spectrum of Highly Antibiotic-Resistant Superbugs. ACS Chem Biol. 2009;4:65-74.

[253] Nichols M, Kuljanin M, Nategholeslam M, Hoang T, Vafaei S, Tomberli B, et al. Dynamic Turn Conformation of a Short Tryptophan-Rich Cationic Antimicrobial Peptide and Its Interaction with Phospholipid Membranes. The Journal of Physical Chemistry B. 2013;117:14697-708.

[254] Chen J, Wang L, Shi L, Ren L, Wang Y. Local co-delivery and release of antimicrobial peptide and RGD using porous TiO2. RSC Advances. 2014;4:27630-3.

[255] Kazemzadeh-Narbat M, Noordin S, Masri BA, Garbuz DS, Duncan CP, Hancock REW, et al. Drug release and bone growth studies of antimicrobial

peptide-loaded calcium phosphate coating on titanium. Journal of Biomedical Materials Research Part B: Applied Biomaterials. 2012;100B:1344-52.

[256] Guiton PS, Cusumano CK, Kline KA, Dodson KW, Han Z, Janetka JW, et al. Combinatorial Small-Molecule Therapy Prevents Uropathogenic Escherichia coli Catheter-Associated Urinary Tract Infections in Mice. Antimicrob Agents Chemother. 2012;56:4738-45.

[257] Oren Z, Shai Y. Selective Lysis of Bacteria but Not Mammalian Cells by Diastereomers of Melittin: Structure−Function Study. Biochemistry. 1997;36:1826-35.

[258] Allen C, Yu Y, Maysinger D, Eisenberg A. Polycaprolactone-b-poly(ethylene Oxide) Block Copolymer Micelles as a Novel Drug Delivery Vehicle for Neurotrophic Agents FK506 and L-685,818. Bioconjugate Chem. 1998;9:564-72.

[259] Peyman GA, Yang D, Khoobehi B, Rahimy MH, Chin SY. In vitro evaluation of polymeric matrix and porous biodegradable reservoir devices for slow-release drug delivery. Ophthalmic surgery and lasers. 1996;27:384-91.

[260] Zhao J, Guo LY, Yang XB, Weng J. Preparation of bioactive porous HA/PCL composite scaffolds. Appl Surf Sci. 2008;255:2942-6.

[261] Luo P, Baldwin RL. Mechanism of Helix Induction by Trifluoroethanol: A Framework for Extrapolating the Helix-Forming Properties of Peptides from Trifluoroethanol/Water Mixtures Back to Water. Biochemistry. 1997;36:8413-21.

[262] Zhao J, Tamm LK. FTIR and Fluorescence Studies of Interactions of Synaptic Fusion Proteins in Polymer-Supported Bilayers†. Langmuir. 2002;19:1838-46.

[263] Koutsopoulos S, Unsworth LD, Nagai Y, Zhang S. Controlled release of functional proteins through designer self-assembling peptide nanofiber hydrogel scaffold. Proceedings of the National Academy of Sciences. 2009;106:4623-8.

[264] Gunatillake PA, Adhikari R. Biodegradable synthetic polymers for tissue engineering. Eur Cell Mater. 2003;5:1-16.

[265] Powers J-PS, Hancock REW. The relationship between peptide structure and antibacterial activity. Peptides. 2003;24:1681-91.

[266] Bi X, Wang C, Ma L, Sun Y, Shang D. Investigation of the role of tryptophan residues in cationic antimicrobial peptides to determine the mechanism of antimicrobial action. Journal of Applied Microbiology. 2013;115:663-72.

[267] Saravanan R, Li X, Lim K, Mohanram H, Peng L, Mishra B, et al. Design of short membrane selective antimicrobial peptides containing tryptophan and arginine residues for improved activity, salt-resistance, and biocompatibility. Biotechnol Bioeng. 2014;111:37-49.

[268] Schibli DJ, Hwang PM, Vogel HJ. Structure of the Antimicrobial Peptide Tritrpticin Bound to Micelles: A Distinct Membrane-Bound Peptide Fold. Biochemistry. 1999;38:16749-55.

[269] Lu H, Wang J, Bai Y, Lang JW, Liu S, Lin Y, et al. Ionic polypeptides with unusual helical stability. Nat Commun. 2011;2:206.

[270] Gollwitzer H, Ibrahim K, Meyer H, Mittelmeier W, Busch R, Stemberger A. Antibacterial poly(d,l-lactic acid) coating of medical implants using a biodegradable drug delivery technology. J Antimicrob Chemother. 2003;51:585-91.

[271] Bastari K, Arshath M, Ng Z, Chia J, Yow Z, Sana B, et al. A controlled release of antibiotics from calcium phosphate-coated poly(lactic-co-glycolic acid) particles and their in vitro efficacy against Staphylococcus aureus biofilm. J Mater Sci: Mater Med. 2014;25:747-57.

[272] Cherkasov A, Hilpert K, Jenssen H, Fjell CD, Waldbrook M, Mullaly SC, et al. Use of Artificial Intelligence in the Design of Small Peptide Antibiotics Effective against a Broad Spectrum of Highly Antibiotic-Resistant Superbugs. ACS Chemical Biology. 2008;4:65-74.

[273] Chen F, Yin G, Liao X, Yang Y, Huang Z, Gu J, et al. Preparation, characterization and in vitro release properties of morphine-loaded PLLA-PEG-PLLA microparticles via solution enhanced dispersion by supercritical fluids. J Mater Sci: Mater Med. 2013;24:1693-705.

[274] Wang R, Neoh KG, Kang E-T, Tambyah PA, Chiong E. Antifouling coating with controllable and sustained silver release for long-term inhibition of infection and encrustation in urinary catheters. Journal of Biomedical Materials Research Part B: Applied Biomaterials. 2015;103:519-28.

Appendix

Table A.1. MICs of variant peptides after 1st round of peptide engineering

Peptide	Sequence	Net Charge	Hydrophilicity	MIC (μM)
Jelleine I	PFKISIHL	1.1	-0.6	2.6
J1	PFKIISHL	1.1	-0.6	25
J2	IFKIISHL	1.1	-0.9	12.5
J3	PFKRISHL	2.1	0	12.5
J4	WFKIISHL	1.1	-1.1	12.5
J5	PFKIWSHL	1.1	-0.8	12.5
J6	PFKWWSHL	1.1	-1	12.5
J7	PFKWWSHW	1.1	-1.2	12.5
J8	PFKIIRHL	2.1	-0.3	50
J9	PFIKILHR	2.1	-0.3	50
J10	PFRKILHR	3.1	0.3	25
J11	WFWKWWRR	3	-0.9	10.6
J12	IFIKIIRR	0.3	-0.1	25
J13	RFWKWWRR	0.4	-0.1	12.5

Table A.2. MICs of variant peptides after 2nd round of peptide engineering

Peptide	Sequence	Net Charge	Hydrophilicity	MIC (μM)
J11a1	WFWKWWRRR	+4	-0.9	7.5
J11a2	WFWKWWRRRR	+5	-0.9	5
J11a3	WFWKWWRRRRR	+6	-0.9	3.8

Table A.3. MICs of CWR11 against E. coli in the presence of different salt concentration.

	Minimum Inhibitory Concentration (μM)		
	No NaCl	150 mM NaCl	300 mM NaCl
E.coli	5.2 ± 0.5	7.3 ± 0.0	12.5 ± 0.0